Data Fusion of Nonlinear Measurement Data in the Presence of Correlated Sensor-to-Sensor Errors.

By

MANSOUR MOHAMAD AL-SAMARA (BSC)

This thesis is submitted as the fulfilment of requirement for the award of Master of Engineering (M.ENG) by research to:

DUBLIN CITY UNIVERSITY

Supervisor: Dr.Hugh MC Cabe

School of Electronic Engineering

SEPTEMBER 1993.

LIBRARY
DUBLIN CITY
UNIVERSITY

DECLARATION

I hereby certify that this material, which I now submit for assessment on the program of study leading to the award of Master of Engineering (M.ENG) is entirely my own work and has not been taken from the work of others save and to the extent that such work has been cited and acknowledged within the text of my work.

Signed: MANSOUR AL-SAMARA Date: 27/09/1993

Date: 27/09/1993

ACKNOWLEDGMENTS

I would like to express my gratitude to my advisor Dr Hugh Mc Cabe, for his excellence, advise, moral support, encouragement, and guidance in the process of my work. I would like to thank Professor C McCorkell the Dean of School Engineering for his support.

My special thanks go to my wife, Bariaa, for her understanding and patience and my sons, Nizar and Manaf, for the source of pleasure.

TABLE OF CONTENTS

ABSTRACT

Data Fusion of Nonlinear Measurement Data in the Presence of Correlated Sensor-to-Sensor Errors.

By

MANSOUR MOHAMAD AL-SAMARA

Data fusion of nonlinear measurement data in the presence of correlated sensor-to-sensor errors is examined. The scenario involves three spatially distributed sensors making three noisy angle-of-arrival measurements on a signal emitted by a source whose position is to be estimated. The noisy angle-of-arrival measurements from two of the sensors are triangulated to form a noisy position measurement in two dimensions. A second pair of sensor noisy angle-of-arrival measurements are also triangulated to form a second noisy position measurement. Both of these noisy position measurements are nonlinear functions of the noisy angle-of-arrival measurements.

Since there are three sensors S1, S2, and S3, sensor S2 is common to both triangulation process, causing a non-zero cross-correlation across both noisy nonlinear position measurements. Since the position measurements are nonlinear functions of the angle-of-arrival measurements, we must use a first-order approximation to the covariance matrix for each measurement vector.

The statistics governing the errors on these angle measurements come from a variety of distributions,

namely the uniform, sawtooth, and triangular distributions.

The optimum fusion algorithm applied to the distributed measurements forms a linear operation on the measurement vectors. Since the measurements are nonlinear functions of the parameters, an exact calculation of the covariance matrix in closed form is not possible because of the intractable nature of the mathematics involved. Consequently, these conditions give sub-optimum conditions for the algorithm. However it is found that the trace of the error covariance matrix of the fused measurement is less than the trace of the error covariance matrix associated with each individual measurement vector. Finally, a mathematical high-order approximation to the covariance matrix is performed. The impact of these high-order terms is examined through simulations.

CHAPTER I

CENTRALIZED VERSUS DECENTRALIZED DATA FUSION

1.1 Introduction

Traditional surveillance and communication systems use a single sensor such as radar or sonar for estimating the position of an object. In these systems, complete sensor observations are made at a central location and classical testing procedures are employed for signal processing. There is an increasing interest now in distributed sensor systems where several sensing techniques, such as sonic, microwave, infrared, x-ray sensors, and radar etc, generate data for subsequent fusion.

The basic goal of multiple sensor systems is to improve system performance, for example, reliability and speed. This can be achieved by properly combining the information obtained from the various sensors and sending them to the fusion centre which processes the measurements formed by each sensor. The object is to extract from these measurements an estimate which is statistically superior to the individual measurements themselves.

There are two major options for signal processing with multiple sensors. There are generally described as centralized and decentralized fusion. We discuss each one separately.

1.2 Centralized Data Fusion

In centralized data fusion measurements from distributed sensors are transmitted to the fusion centre. This requires transmission of sensor information without delay and with large communication bandwidth. The structure of a centralized fusion system is illustrated in Fig(1.1).

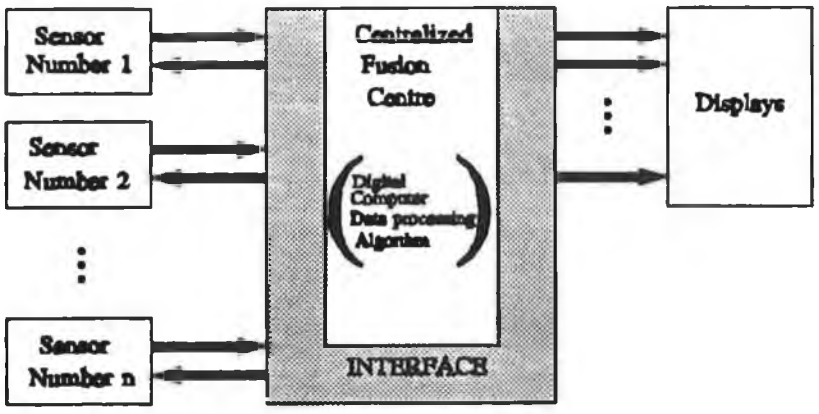

Figure(1.1) Centralized data fusion.

1.3 Distributed Data Fusion

The second option for data fusion is to have signal processing carried out at the local sensor level. The results are available locally and partial results are transmitted to the fusion centre for further processing. Global results are then available at the data fusion centre. This type of system is called

decentralized data fusion.

Many benefits may be derived from the use of multiple sensors in a target surveillance systems, such as accurate angular position and range rate information for radar systems to provide improved tracking. The major purpose of multi-sensor fusion is to complement the data from one sensor with that from another sensor. In this way it is possible to obtain better information and to make a more accurate estimate than is possible with a single sensor system.

The fusion algorithm analyzed here is based on the centralized fusion approach.

Chapter II discuses the nature of the data fusion problem to be solved. It is shown there that the measurements are nonlinear functions of the parameters to be estimated. Consequently first-order approximations to the covariance matrix for each measurement vector must be computed. There are developed in chapter III.

Chapter IV discuses the optimum fusion algorithm to be applied to the distributed measurements. It is shown there that the algorithm is optimum only for measurements which are linear functions of the parameter vector to be estimated. As noted previously,

since the measurements are nonlinear functions of the parameters, we must use a first-order approximation to the covariance matrix of the measurement vectors. An exact calculation of the covariance matrix in closed form is not possible because of the intractable nature of the mathematics involved. Consequently, these conditions provide an interesting test of the optimal fusion algorithm when applied under sub-optimum conditions.

Chapter V discusses simulation results for scenario number 1, and scenario number 2, in low-noise case, and high-noise case.

Chapter VI investigates the impact of high-order terms in the approximation to the error covariance matrix and discusses simulation results for the covariance matrices using second-order terms.

Chapter VII discusses conclusions based on the results.

CHAPTER II

DESCRIPTION OF DATA FUSION PROBLEM

2.1 Introduction

The scenario defining the data fusion problem to be analyzed is shown in figure (2.1). S1, S2, and S3 are three sensors located at known coordinates (x_1,y_1), (x_2,y_2) and (x_3,y_3), respectively. The object at point P which has coordinates (x,y) emits a signal whose angle-of-arrival θ is measured by each sensor. The location of the object (x,y) is to be estimated from these angle-of-arrival measurements.

Each sensor makes a measurement of the angle-of-arrival with respect to the horizontal axis X as shown in figure (2.1). θ_{i_m} represents the measurement made by sensor i, i = 1,2,3. The object coordinates are determined by triangulation on two angle-of-arrival measurements as shown in the next section.

2.2 Triangulation Using True Angle-Of-Arrival Measurements

In figure (2.1) the object at point P (x,y) is observed by three spatially distributed sensors.

The angle-of-arrival measurements from two of the sensors are triangulated to form a position measurement of the source. A second pair of sensor angle-of-arrival measurements is also triangulated to form a second position measurement. Since, there are only three sensors, one sensor is common to both triangulation processes. Define the following

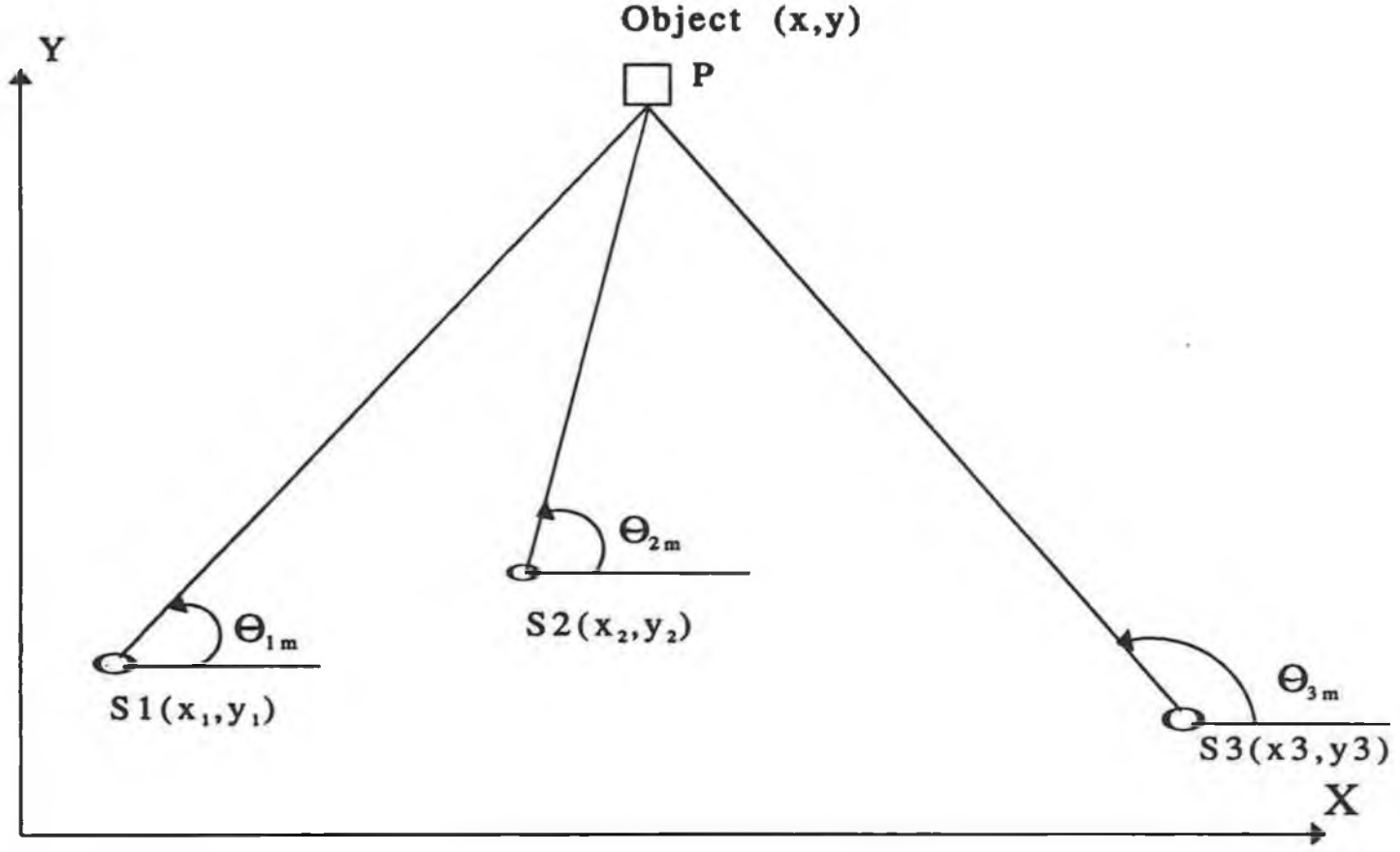

Figure (2.1) Geometrical configuration of object and sensors in two dimensions.

quantities:

(x,y): coordinates of the object to be estimated.

(x_1,y_1): location of sensor S1, (known)

(x_2,y_2): location of sensor S2, (known)

(x_3,y_3): location of sensor S3. (known)

The angle θ_1 made by sensor S1 is such that:

$$\tan\theta_1 = \left(\frac{y-y_1}{x-x_1}\right) \tag{2.1}$$

A similar equation holds for the measurement from sensor S2:

$$\tan\theta_2 = \left(\frac{y-y_2}{x-x_2}\right) \tag{2.2}$$

Therefore,

$$(y-y_1) = (x-x_1)\tan\theta_1 \tag{2.3}$$

and

$$(y-y_2) = (x-x_2)\tan\theta_2 \tag{2.4}$$

From (2.3), $y = (x-x_1)\tan\theta_1 + y_1$ (2.5)

From (2.4), $y = (x-x_2)\tan\theta_2 + y_2$ (2.6)

Since equation (2.5) = (2.6) $(y = y)$

$$(x-x_1)\tan\theta_1+y_1 = (x-x_2)\tan\theta_2+y_2$$

$$x\tan\theta_1-x_1\tan\theta_1+y_1 = x\tan\theta_2-x_2\tan\theta_2+y_2$$

$\therefore$

$$x = \frac{x_1\tan\theta_1-x_2\tan\theta_2+y_2-y_1}{\tan\theta_1-\tan\theta_2} \qquad (2.7)$$

Equation (2.7) gives the x coordinate of the object in terms of the known quantities x_1, x_2, θ_1, θ_2, y_1, and y_2. Knowing x, the y coordinate of the object is obtained from equation (2.5)

$$y = (x-x_1)\tan\theta_1+y_1 \qquad (2.8)$$

Let x_{12},y_{12} denote the measured object position by triangulation between sensor S1 and sensor S2. Therefore

$$x_{12} = \frac{x_1\tan\theta_1-x_2\tan\theta_2+y_2-y_1}{\tan\theta_1-\tan\theta_2} \qquad (2.9)$$

and

$$y_{12} = (x_{12}-x_1)\tan\theta_1+y_1 \qquad (2.10)$$

We define the position vector z_{12} for the sensor pair S1/S2 as follows:

$$z_{12} = [x_{12}, y_{12}]^T$$

A similar set of equations holds for triangulation between sensor S2, and sensor S3. Using these two sensors, the measurements x_{23}, and y_{23} are given by:

$$x_{23} = \frac{x_2 \tan\theta_2 - x_3 \tan\theta_3 + y_3 - y_2}{\tan\theta_2 - \tan\theta_3} \qquad (2.11)$$

and

$$y_{23} = (x_{23} - x_2)\tan\theta_2 + y_2 \qquad (2.12)$$

We define the position vector z_{23} for the sensor pair S2/S3 as follows:

$$z_{23} = [x_{23}\ y_{23}]^T$$

We have assumed up to now that the angle-of-arrival measurements θ_1, θ_2 and θ_3 are perfect (have no errors). Of course this is never true in practice and consequently the errors in the angle-of-arrival measurements feed forward into errors in the measured position vectors z_{12}, and z_{23}. These errors in the measured position vectors z_{12} and z_{23} must in turn be quantified in the form of a measurement error covariance matrix associated with each of the vectors z_{12}, and z_{23}. This is pursued further in chapter III. The fusion algorithm applied to the noisy measurement vectors must reduce the errors in the individual

sensor measurements and in the process produce a fused measurement which is statistically superior to the individual input measurements themselves. The criterion of optimality is minimum trace of the covariance matrix associated with the fused measurement. The results presented later show that even under sub-optimum conditions of nonlinear measurements and first-order approximations to the measurement covariance matrices, the trace of the fused covariance matrix is less than the trace of the individual measurement error covariance matrices.

We observe that the measured angle θ_2 appears in equation (2.9) in connection with x_{12} measurement and also in equation (2.11) in connection with x_{23} measurement. Therefore non zero cross-covariance matrix exists between measurement vectors z_{12} and z_{23}. Equations (2.9), (2.10), (2.11), and (2.12) show that calculation of closed form expression for the elements in the covariance matrix is impossible because of the intractable nature of the mathematics involved.

In the next chapter we derive the first-order approximation to the covariance matrices for the measurement vectors z_{12} and z_{23}.

CHAPTER III

DERIVATION OF MEASUREMENT COVARIANCE MATRIX AND CROSS-COVARIANCE MATRIX

3.1 Errors In Sensor Measurements

Equations (2.9), and (2.10) give the triangulated coordinates of the object P in terms of the known quantities x_1, y_1, x_2, y_2, θ_1, and θ_2, where

(x_1,y_1) = location of sensor S1

(x_2,y_2) = location of sensor S2

θ_1 = angle-of-arrival measurement at S1

θ_2 = angle-of-arrival measurement at S2

$$x_{12} = \frac{x_1\tan\theta_1 - x_2\tan\theta_2 + y_2 - y_1}{\tan\theta_1 - \tan\theta_2} \qquad (2.9)$$

$$y_{12} = (x_{12} - x_1)\tan\theta_1 + y_1 \qquad (2.10)$$

These equations are exact provided there are no errors in the measured values θ_{1m} and θ_{2m}. Let

θ_{1t} = the true value of θ_1

θ_{2t} = the true value of θ_2

$\Delta\theta_1$ = the error in θ_1

$\Delta\theta_2$ = the error in θ_2

Then the noisy measured angles θ_{1m}, and θ_{2m} are given by:

$$\theta_{1m} = \theta_{1t} + \Delta\theta_1$$

$$\theta_{2m} = \theta_{2t} + \Delta\theta_2$$

The errors in the angle-of-arrival measurements feed

forward into errors in the measured positions x and y of the object. Denote the relationship between x_{12} and the parameters θ_1, θ_2, x_1, x_2, y_1, and y_2 as follows:

$$x_{12} = f_1(\theta_2, \theta_1, x_2, x_1, y_2, y_1),$$

Likewise

$$y_{12} = f_2(\theta_2, \theta_1, x_2, x_1, y_2, y_1),$$

We now derive how, to a first-order approximation, errors in θ_1, and θ_2 map into errors in x_{12}, and y_{12}. To accomplished this, we take the following partial derivatives:

$$\Delta x_{12} = \frac{\partial f_1}{\partial \theta_1}(\theta_1, \theta_2)\Delta\theta_1 + \frac{\partial f_1}{\partial \theta_2}(\theta_1, \theta_2)\Delta\theta_2 \qquad (3.1)$$

$$\Delta y_{12} = \frac{\partial f_2}{\partial \theta 1}(\theta_1, \theta_2)\Delta\theta_1 + \frac{\partial f_2}{\partial \theta_2}(\theta_1, \theta_2)\Delta\theta_2 \qquad (3.2)$$

Δx_{12} and Δy_{12} represent the errors in the object triangulated position using sensors S1 and S2.

From (3.1) and (3.2) we see that

$$\Delta z_{12} = \begin{bmatrix} \Delta x_{12} \\ \Delta y_{12} \end{bmatrix} = \begin{bmatrix} \frac{\partial x_{12}}{\partial \theta_1} & \frac{\partial x_{12}}{\partial \theta_2} \\ \frac{\partial y_{12}}{\partial \theta_1} & \frac{\partial y_{12}}{\partial \theta_2} \end{bmatrix} \begin{bmatrix} \Delta\theta_1 \\ \Delta\theta_2 \end{bmatrix} \qquad (3.3)$$

where Δz_{12} represents the error vector in the object triangulated position measured by sensors S1 and S2.

Let

$$A_{12} = \begin{bmatrix} a_{11} & a_{12} \\ a_{21} & a_{22} \end{bmatrix}_{12} = \begin{bmatrix} \frac{\partial x_{12}}{\partial \theta_1} & \frac{\partial x_{12}}{\partial \theta_2} \\ \frac{\partial y_{12}}{\partial \theta_1} & \frac{\partial y_{12}}{\partial \theta_2} \end{bmatrix} \qquad (3.4)$$

and

$$\Delta\theta_{12} = \begin{bmatrix} \Delta\theta_1 \\ \Delta\theta_2 \end{bmatrix} \qquad (3.5)$$

From (3.3), and (3.4),

$$\Delta z_{12} = A_{12}\ \Delta\theta_{12} \qquad (3.6)$$

We now formulate each of the elements in the matrix A_{12}.

3.2 Calculation Of Elements in Matrix A_{12}

3.2.1 Calculation of a_{11}

From the equation (2.9)

$$a_{11} = \frac{\partial x_{12}}{\partial \theta_1} = \frac{\partial}{\partial \theta_1}\left[\frac{x_1\tan\theta_1 - x_2\tan\theta_2 + y_2 - y_1}{\tan\theta_1 - \tan\theta_2}\right]$$

$$= \frac{x_1\sec^2\theta_1(\tan\theta_1 - \tan\theta_2) - \sec^2\theta_1(x_1\tan\theta_1 - x_2\tan\theta_2 + y_2 - y_1)}{(\tan\theta_1 - \tan\theta_2)^2}$$

$$= \frac{-x_1\sec^2\theta_1\tan\theta_2 + x_2\sec^2\theta_1\tan\theta_2 + \sec^2\theta_1(y_1 - y_2)}{(\tan\theta_1 - \tan\theta_2)^2}$$

$$a_{11} = \frac{\partial x_{12}}{\partial \theta_1} = \frac{\sec^2\theta_1 [(x_2 - x_1)\tan\theta_2 + (y_1 - y_2)]}{(\tan\theta_1 - \tan\theta_2)^2} \qquad (3.7)$$

3.2.2 Calculation of a_{12}

From the equation (2.9)

$$a_{12} = \frac{\partial x_{12}}{\partial \theta_2} = \frac{\partial}{\partial \theta_2}\left[\frac{x_1\tan\theta_1 - x_2\tan\theta_2 + y_2 - y_1}{\tan\theta_1 - \tan\theta_2}\right]$$

$$= \frac{-x_2\sec^2\theta_2(\tan\theta_1 - \tan\theta_2) + \sec^2\theta_2(x_1\tan\theta_1 - x_2\tan\theta_2 + y_2 - y_1)}{(\tan\theta_1 - \tan\theta_2)^2}$$

$$= \frac{\sec^2\theta_2\tan\theta_1(x_1 - x_2) + \sec^2\theta_2(y_2 - y_1)}{(\tan\theta_1 - \tan\theta_2)^2}$$

$$a_{12} = \frac{\partial x_{12}}{\partial \theta_2} = \frac{\sec^2\theta_2 [(x_1 - x_2)\tan\theta_1 + (y_2 - y_1)]}{(\tan\theta_1 - \tan\theta_2)^2} \qquad (3.8)$$

3.2.3 Calculation of a_{21}

From the equation (2.10)

$$a_{21} = \frac{\partial y_{12}}{\partial \theta_1} = \frac{\partial}{\partial \theta_1}[(x_{12} - x_1)\tan\theta_1 + y_1]$$

$$= \frac{\partial}{\partial\theta_1}[x_{12}\tan\theta_1 - x_1\tan\theta_1 + y_1]$$

$$= \left(\frac{\partial x_{12}}{\partial\theta_1}\right)\tan\theta_1 + x_{12}\sec^2\theta_1 - x_1\sec^2\theta_1$$

$$a_{21} = a_{11}\tan\theta_1 + \sec^2\theta_1(x_{12} - x_1) \qquad (3.9)$$

3.2.4 Calculation of a_{22}

From the equation (2.10)

$$a_{22} = \frac{\partial y_{12}}{\partial\theta_2} = \frac{\partial}{\partial\theta_2}[(x_{12} - x_1)\tan\theta_1 + y_1]$$

$$= \left(\frac{\partial x_{12}}{\partial\theta_2}\right)\tan\theta_1$$

$$a_{22} = a_{12}\tan\theta_1 \qquad (3.10)$$

3.3 Calculation of Elements In A_{23} matrix

A similar equation (3.3) holds to calculate the error vector (Δz_{23}) in the object triangulated position measured by sensors S2 and S3.

$$\Delta z_{23} = \begin{bmatrix} \Delta x_{23} \\ \Delta y_{23} \end{bmatrix} = \begin{bmatrix} \frac{\partial x_{23}}{\partial \theta_2} & \frac{\partial x_{23}}{\partial \theta_3} \\ \frac{\partial y_{23}}{\partial \theta_2} & \frac{\partial y_{23}}{\partial \theta_3} \end{bmatrix} \begin{bmatrix} \Delta \theta_2 \\ \Delta \theta_3 \end{bmatrix} \qquad (3.11)$$

Let

$$A_{23} = \begin{bmatrix} a_{11} & a_{12} \\ a_{21} & a_{22} \end{bmatrix}_{23} = \begin{bmatrix} \frac{\partial x_{23}}{\partial \theta_2} & \frac{\partial x_{23}}{\partial \theta_3} \\ \frac{\partial y_{23}}{\partial \theta_2} & \frac{\partial y_{23}}{\partial \theta_3} \end{bmatrix} \qquad (3.12)$$

and

$$\Delta \theta_{23} = \begin{bmatrix} \Delta \theta_2 \\ \Delta \theta_3 \end{bmatrix} \qquad (3.13)$$

From (3.12) and (3.13),

$$\Delta z_{23} = A_{23} \, \Delta \theta_{23}$$

It is not necessary to rederive the expressions for matrix A_{23}. The equations derived for matrix A_{12} may be used to fill in the entries of matrix A_{23}. This is accomplished by replacing $\theta_1, x_1, \theta_2, x_2, y_1, y_2$, and x_{12} in equations (3.7), (3.8), (3.9), and (3.10) with $\theta_2, x_2, \theta_3, x_3, y_2, y_3$, and x_{23} respectively. The resulting equations are as follows;

$$a_{11} = \frac{\partial x_{23}}{\partial \theta_2} = \frac{\sec^2\theta_2 [\tan\theta_3 (x_3 - x_2) + (y_2 - y_3)]}{(\tan\theta_2 - \tan\theta_3)^2} \qquad (3.14)$$

$$a_{12} = \frac{\partial x_{23}}{\partial \theta_3} = \frac{\sec^2\theta_3 [\tan\theta_2 (x_2 - x_3) + (y_3 - y_2)]}{(\tan\theta_2 - \tan\theta_3)^2} \qquad (3.15)$$

$$a_{21} = \frac{\partial y_{23}}{\partial \theta_2} = a_{11}\tan\theta_2 + \sec^2\theta_2 (x_{23} - x_2) \qquad (3.16)$$

and

$$a_{22} = \frac{\partial y_{23}}{\partial \theta_3} = a_{12}\tan\theta_2 \qquad (3.17)$$

In the next section we give a brief review of the covariance matrix and it's properties.

Then we derive the covariance matrix associated with the error in the measured position. The covariance matrix will be a function of the variance of the measured angles.

3.4 Definition and Properties of a General Covariance Matrix P

We define the error $\tilde{X}$ in the estimate of a state vector X to be the difference between the estimated value $\hat{X}$ and the actual value X:

$$\tilde{X} = \hat{X} - X$$

The covariance matrix P associated with X is defined as

$$P \equiv E[\tilde{X}\tilde{X}^T] \qquad (3.18)$$

The covariance matrix provides a statistical measure of the uncertainty in the estimate of the elements in vector X.

Suppose vector X has two components as follows:

$$X = \begin{bmatrix} x_1 \\ x_2 \end{bmatrix}$$

If the mean value of X is

$$E\{X\} = \bar{X} = \begin{bmatrix} \overline{x_1} \\ \overline{x_2} \end{bmatrix}$$

then the covariance matrix of X is:

$$P = E\left\{ \begin{bmatrix} (x_1-\overline{x_1}) \\ (x_2-\overline{x_2}) \end{bmatrix} [(x_1-\overline{x_1})\ (x_2-\overline{x_2})] \right\}$$

$$= \begin{bmatrix} E\{(x_1-\overline{x_1})^2\} & E\{(x_1-\overline{x_1})\ (x_2-\overline{x_2})\} \\ E\{(x_2-\overline{x_2})\ (x_1-\overline{x_1})\} & E\{(x_2-\overline{x_2})^2\} \end{bmatrix}$$

Note the covariance matrix of an n-state vector is an nxn symmetric matrix whose diagonal entries are the variance of the estimates of the corresponding elements. The off-diagonal terms of P are indicators of the cross-correlation between the elements of X. They are related to the linear correlation coefficient

$\rho(x_1, x_2)$ between x_1 and x_2 by

$$\rho(x_1, x_2) = \frac{E\{ [(x_1-\overline{x_1})(x_2-\overline{x_2})] \}}{\sigma_{x_1}\sigma_{x_2}} \qquad (3.19)$$

where σ indicates the standard deviation.

A covariance matrix is at least positive semi-definite and is usually positive definite.

P is positive semi-definite if for all vectors $z \neq 0$

$$z^T P z \geq 0$$

or

$$E\{(z^T \tilde{x})(\tilde{x}^T z)\} \geq 0$$

or

$$E\{(\tilde{x}^T z)^T(\tilde{x}^T z)\} \geq 0$$

Therefore P is at least positive semi-definite.

We now derive the first-order approximation to covariance matrix P_{z12}

3.5 First-Order Approximation to Covariance Matrix P_{z12} for Measurement Vector z_{12}

In our scenario for the measurement noise associated with the object position measurements there are two covariance matrices P_{z12}, P_{z23}, and cross-covariance matrix P_{z1223}.

P_{z12} is the covariance matrix for the errors in the measurement vector z_{12} obtained by triangulation between sensor S1 and sensor S2.

P_{z23} is the covariance matrix for the errors in the measurement vector z_{23} obtained by

triangulation between sensor S2 and sensor S3.

p_{z1223} is the cross-covariance matrix between the errors in the measurement vectors z_{12} and z_{23} and is not zero because sensor S2 is the common sensor between measurements z_{12} and sensor z_{23}

From the equation (3.6)

$$\Delta z_{12} = A_{12}\ \Delta\theta_{12}$$

where Δz_{12} is the error vector in the measured object position using sensors S1 and S2 and

$$\Delta z_{12} = \begin{bmatrix} \Delta x_{12} \\ \Delta y_{12} \end{bmatrix} \qquad \textit{and} \qquad \Delta\theta_{12} = \begin{bmatrix} \Delta\theta_1 \\ \Delta\theta_2 \end{bmatrix}$$

Since we assume $\overline{\Delta\theta_i} = E(\Delta\theta_i) = 0$ i.e the sensor makes an unbiased measurement, (i = 1, 2, 3, ..) (sensor errors are zero mean)

$$\overline{\Delta z_{12}} = E[\Delta z_{12}] = E\ [A_{12}\ \Delta\theta_{12}]$$
$$= A_{12}\ E[\Delta\theta_{12}]$$
$$= A_{12}\overline{\Delta\theta_{12}} = 0$$

Therefore the error covariance matrix for the error in measurement vector z_{12} is:

$$P_{z12} = E\{[\Delta z_{12}\ \Delta z_{12}^T]\}$$
$$= E\ \{[A_{12}\Delta\theta_{12}\ \Delta\theta_{12}^T A_{12}^T]\}$$
$$= A_{12}E\left\{\begin{bmatrix} \Delta\theta_1 \\ \Delta\theta_2 \end{bmatrix}[\ \Delta\theta_1\ \ \Delta\theta_2\ ]\,A_{12}^T\right\}$$

Since the angle errors have zero mean,

$$= A_{12}\, E\left\{ \begin{bmatrix} (\Delta\theta_1)^2 & \Delta\theta_1\Delta\theta_2 \\ \Delta\theta_2\Delta\theta_1 & (\Delta\theta_2)^2 \end{bmatrix} A_{12}^T \right\}$$

$$\sigma_{\theta 1}^2 = E(\Delta\theta_1)^2$$

$$\sigma_{\theta 2}^2 = E(\Delta\theta_2)^2$$

where $\sigma_{\theta 1}$, and $\sigma_{\theta 2}$ are the standard deviation of the errors in θ_1 and θ_2 respectively. Therefore

$$P_{z12} = A_{12} \begin{bmatrix} \sigma_{\theta_1}^2 & E\{ (\Delta\theta_1\Delta\theta_2) \} \\ E\{ (\Delta\theta_1\Delta\theta 2) \} & \sigma_{\theta_2}^2 \end{bmatrix} A_{12}^T$$

Since $\Delta\theta_1$, and $\Delta\theta_2$ are assumed to be statistically independent,

$$E[\Delta\theta_1\Delta\theta_2] = E(\Delta\theta_1)E(\Delta\theta_2) = 0$$

Therefore

$$P_{z12} = A_{12} \begin{bmatrix} \sigma_{\theta_1}^2 & 0 \\ 0 & \sigma_{\theta_2}^2 \end{bmatrix} A_{12}^T \qquad (3.20)$$

P_{z12} the error covariance matrix for triangulation between sensor S1, and sensor S2 is equal to:

$$P_{z12} = A_{12} P_{\theta 12} A_{12}^T \qquad (3.21)$$

where A_{12} is the derivative matrix given by the equations (3.7), (3.8), (3.9), (3.10), and $P_{\theta 12}$ is equal to:

$$P_{\theta_{12}} = \begin{bmatrix} \sigma_{\theta_1}^2 & 0 \\ 0 & \sigma_{\theta_2}^2 \end{bmatrix} \qquad (3.22)$$

$$P_{x12} = \begin{bmatrix} a_{11} & a_{12} \\ a_{21} & a_{22} \end{bmatrix}_{12} \begin{bmatrix} \sigma_{\theta_1}^2 & 0 \\ 0 & \sigma_{\theta_2}^2 \end{bmatrix} \begin{bmatrix} a_{11} & a_{21} \\ a_{12} & a_{22} \end{bmatrix}_{12} \qquad (3.23)$$

$$= \begin{bmatrix} a_{11}^2\sigma_{\theta_1}^2 + a_{12}^2\sigma_{\theta_2}^2 & a_{21}a_{11}\sigma_{\theta_1}^2 + a_{12}a_{22}\sigma_{\theta_2}^2 \\ a_{21}a_{11}\sigma_{\theta_1}^2 + a_{12}a_{22}\sigma_{\theta_2}^2 & a_{21}^2\sigma_{\theta_1}^2 + a_{22}^2\sigma_{\theta_2}^2 \end{bmatrix}$$

$$= \begin{bmatrix} \sigma_{x_{12}}^2 & [\rho_{xy}]_{12}\sigma_{x_{12}y_{12}} \\ [\rho_{xy}]_{12}\sigma_{x_{12}y_{12}} & \sigma_{y_{12}}^2 \end{bmatrix} \qquad (3.24)$$

where

$$\sigma_{x_{12}}^2 = (a_{11}^2)_{12}(\sigma_{\theta_1})^2 + (a_{12}^2)_{12}(\sigma_{\theta_2})^2$$

$$\sigma_{y_{12}}^2 = (a_{21}^2)_{12}(\sigma_{\theta_1})^2 + (a_{22}^2)_{12}(\sigma_{\theta_2})^2 \qquad \text{and}$$

$$[\rho_{xy}]_{12} = \frac{a_{21}a_{11}\sigma_{\theta_1}^2 + a_{12}a_{22}\sigma_{\theta_2}^2}{\sigma_{x_{12}}\sigma_{y_{12}}}$$

where ρ is the correlation coefficient and has a value: $-1 \leq \rho \leq 1$

3.6 First-Order Approximation to Covariance Matrix P_{z23} for Measurement Vector z_{23}

P_{z23} is the covariance matrix for the errors in the

measurement vector z_{23} and it is not necessary to rederive separately the equations for that because they are similar to P_{z12} equations. The equations (3.19), (3.20), (3.21), (3.22), (3.23), and (3.24) may be used to calculate P_{z23}. This is accomplished by replacing Δz_{12} in equation (3.6) with Δz_{23}; replacing A_{12} in equation (3.20) with A_{23}, where the entries for the matrix A_{23} are given by the equations (3.14), (3.15), (3.16), and (3.17) and replace $\sigma_{\theta 1}^2$, and $\sigma_{\theta 2}^2$ in equation (3.20) with $\sigma_{\theta 2}^2$ and $\sigma_{\theta 3}^2$ respectively. Therefore the equations defining the matrix P_{z23} are as follows:

$$P_{z23} = E\{[\Delta z_{23}\ \Delta z_{23}^T]\} \tag{3.25}$$

where Δz_{23} the error vector in the object triangulated position measured by sensor S2 and S3.

$$P_{z23} = A_{23}\begin{bmatrix}\sigma_{\theta 2}^2 & 0\\ 0 & \sigma_{\theta 3}^2\end{bmatrix}A_{23}^T \tag{3.26}$$

$$P_{z23} = A_{23}P_{\theta 23}A_{23}^T \tag{3.27}$$

$$P_{\theta_{23}} = \begin{bmatrix}\sigma_{\theta 2}^2 & 0\\ 0 & \sigma_{\theta 3}^2\end{bmatrix} \tag{3.28}$$

$$P_{z23} = \begin{bmatrix}a_{11} & a_{12}\\ a_{21} & a_{22}\end{bmatrix}_{23}\begin{bmatrix}\sigma_{\theta 2}^2 & 0\\ 0 & \sigma_{\theta 3}^2\end{bmatrix}\begin{bmatrix}a_{11} & a_{21}\\ a_{12} & a_{22}\end{bmatrix}_{23} \tag{3.29}$$

$$= \begin{bmatrix} a_{11}^2\sigma_{\theta 2}^2 + a_{12}^2\sigma_{\theta 3}^2 & a_{21}a_{11}\sigma_{\theta 2}^2 + a_{12}a_{22}\sigma_{\theta 3}^2 \\ a_{21}a_{11}\sigma_{\theta 2}^2 + a_{12}a_{22}\sigma_{\theta 3}^2 & a_{21}^2\sigma_{\theta 2}^2 + a_{22}^2\sigma_{\theta 3}^2 \end{bmatrix}$$

$$= \begin{bmatrix} \sigma_{x_{23}}^2 & [\rho_{xy}]_{23}\sigma_{x_{23}y_{23}} \\ [\rho_{xy}]_{23}\sigma_{x_{23}y_{23}} & \sigma_{y_{23}}^2 \end{bmatrix} \qquad (3.30)$$

where

$$\sigma_{x_{23}}^2 = (a_{11}^2)_{23}(\sigma_{\theta_2})^2 + (a_{12}^2)_{23}(\sigma_{\theta_3})^2$$

$$\sigma_{y_{23}}^2 = (a_{21}^2)_{23}(\sigma_{\theta_2})^2 + (a_{22}^2)_{23}(\sigma_{\theta_3})^2 \qquad \text{and}$$

$$[\rho_{xy}]_{23} = \frac{a_{21}a_{11}\sigma_{\theta 2}^2 + a_{12}a_{22}\sigma_{\theta 3}^2}{\sigma_{x_{23}}\sigma_{y_{23}}}$$

where ρ is the correlation coefficient and has a value: $-1 \leq \rho \leq 1$

3.7 The Cross-Covariance Matrix P_{z1223}

The cross-covariance matrix between the measurements z_{12}, and z_{23} is not zero because sensor S2 is the common sensor. By definition

$$P_{z1223} = E\{[\Delta z_{12}\ \Delta z_{23}^T]\} \qquad (3.31)$$

$$= E\{\ [A_{12}\Delta\theta_{12}]\ \ [A_{23}\Delta\theta_{23}]^T\}$$

$$= E\{\ [A_{12}\begin{bmatrix}\Delta\theta_1\\ \Delta\theta_2\end{bmatrix}]\ \ [A_{23}\begin{bmatrix}\Delta\theta_2\\ \Delta\theta_3\end{bmatrix}]^T\}$$

$$= A_{12}\ E\{\begin{vmatrix}\Delta\theta_1\\ \Delta\theta_2\end{vmatrix}[\Delta\theta_2\ \ \Delta\theta_3]\ A_{23}^T\}$$

$$= A_{12}\ E\{\begin{bmatrix}(\Delta\theta_1\Delta\theta_2) & (\Delta\theta_1\Delta\theta_3)\\ (\Delta\theta_2)^2 & (\Delta\theta_2\Delta\theta_3)\end{bmatrix}A_{23}^T\}$$

$$= A_{12}\begin{bmatrix}E(\Delta\theta_1\Delta\theta_2) & E(\Delta\theta_1\Delta\theta_3)\\ E(\Delta\theta_2)^2 & E(\Delta\theta_2\Delta\theta_3)\end{bmatrix}A_{23}^T$$

$\Delta\theta_1$, $\Delta\theta_2$ are statistically independent, therefore

$$E(\Delta\theta_1\ \Delta\theta_2) = E(\Delta\theta_1)\ E(\Delta\theta_2) = 0$$

Also $\Delta\theta_2$ and $\Delta\theta_3$ are statistically independent, therefore

$$E(\Delta\theta_2\ \Delta\theta_3) = E(\Delta\theta_2)\ E(\Delta\theta_3) = 0$$

$$\sigma_{\theta 2}^2 = E(\Delta\theta_2)^2$$

Therefore the cross-covariance matrix is equal to:

$$P_{z1223} = A_{12}\begin{bmatrix}0 & 0\\ \sigma_{\theta_2}^2 & 0\end{bmatrix}A_{23}^T \qquad (3.32)$$

From the equation (3.31) we see the cross-covariance matrix is equal to:

$$P_{z1223} = E\left\{ \begin{vmatrix} (x_{12}-\overline{x_{12}}) \\ (y_{12}-\overline{y_{12}}) \end{vmatrix} [\,(x_{23}-\overline{x_{23}})\,(y_{23}-\overline{y_{23}})\,] \right\}$$

$$P_{z1223} = E\left\{ \begin{vmatrix} (x_{12}-\overline{x_{12}})(x_{23}-\overline{x_{23}}) & (x_{12}-\overline{x_{12}})(y_{23}-\overline{y_{23}}) \\ (y_{12}-\overline{y_{12}})(x_{23}-\overline{x_{23}}) & (y_{12}-\overline{y_{12}})(y_{23}-\overline{y_{23}}) \end{vmatrix} \right\}$$

$$= \begin{bmatrix} \rho_{x_{12}x_{23}}\sigma_{x_{12}}\sigma_{x_{23}} & \rho_{x_{12}y_{23}}\sigma_{x_{12}}\sigma_{y_{23}} \\ \rho_{y_{12}x_{23}}\sigma_{y_{12}}\sigma_{x_{23}} & \rho_{y_{12}y_{23}}\sigma_{y_{12}}\sigma_{y_{23}} \end{bmatrix}$$

where

$$\rho_{x_{12}x_{23}}\ ,\ \rho_{x_{12}y_{23}}\ ,\ \rho_{y_{12}x_{23}}\ ,\ \textit{and}\ \ \rho_{y_{12}y_{23}}$$

represent the correlation coefficient elements of the cross-covariance matrix. By definition

$$\rho_{x_{12}x_{23}} = \frac{E[\,(x_{12}-\overline{x_{12}})\,(x_{23}-\overline{x_{23}})\,]}{\sigma_{x_{12}}\sigma_{x_{23}}}$$

$$\rho_{x_{12}x_{23}} = \frac{p_{z1223}(1,1)}{\sqrt{p_{z12}(1,1)}\sqrt{p_{z23}(1,1)}} \qquad (3.33)$$

$$\rho_{x_{12}y_{23}} = \frac{E[\,(x_{12}-\overline{x_{12}})\,(y_{23}-\overline{y_{23}})\,]}{\sigma_{x_{12}}\sigma_{y_{23}}}$$

$$= \frac{p_{z1223}(1,2)}{\sqrt{p_{z12}(1,1)}\sqrt{p_{z23}(2,2)}} \qquad (3.34)$$

$$\rho_{y_{12}x_{23}} = \frac{E[(y_{12}-\overline{y_{12}})(x_{23}-\overline{x_{23}})]}{\sigma_{y_{12}}\sigma_{x_{23}}}$$

$$= \frac{p_{z1223}(2,1)}{\sqrt{p_{z12}(2,2)}\sqrt{p_{z23}(1,1)}} \qquad (3.35)$$

and

$$\rho_{y_{12}y_{23}} = \frac{E[(y_{12}-\overline{y_{12}})(y_{23}-\overline{y_{23}})]}{\sigma_{y_{12}}\sigma_{y_{23}}}$$

$$= \frac{p_{z1223}(2,2)}{\sqrt{p_{z12}(2,2)}\sqrt{p_{z23}(2,2)}} \qquad (3.36)$$

This completes the derivation of the covariance matrices.

Chapter IV discusses the optimum fusion algorithm to be applied to the correlated, distributed measurements.

CHAPTER IV

SUMMARY OF OPTIMAL DATA FUSION ALGORITHM FOR N DISTRIBUTED SENSORS IN THE PRESENCE OF ARBITRARILY CORRELATED SENSOR-TO-SENSOR ERRORS

4.1 Introduction

The optimal data fusion algorithm used here was originally presented in reference [8]. Consequently, only a summary of the derivation is presented in this chapter.

The fusion algorithm is designed to optimally fuse measurements from N distributed sensors. The measurement vector from each sensor is assumed to be full-state and unbiased (zero mean error). The errors in each measurement vector are assumed to be arbitrarily correlated with the errors from the other (N-1) measurement vectors. It is assumed that all measurements and covariance matrices have been coordinate transformed to a common frame of reference. The optimization criterion is minimum trace of the error covariance matrix of the fused measurement. This means that the trace of the error covariance matrix of the fused measurement must be less than the trace of the error covariance matrix associated with each of the N measurement vectors. Gradient matrix techniques are employed to derive the necessary and sufficient

conditions for minimization of the trace the optimum covariance matrix.

4.2 Summary of Derivation of Optimal Fusion Algorithm

Suppose we have N distributed sensors each making an unbiased full-state measurement on some evolving process. The process is characterized by a vector X of length M. All measurements are full-state contemporaneous and transformed to a common frame of reference. The error in the measurement from the i-th sensor is characterized by an MxM error covariance matrix P_{ii}. In addition, the errors from measurement i have an arbitrary correlation with the errors from the other (N-1) measurements. Therefore, each measurement $\hat{X}$ is characterized by a covariance matrix P_{ii} and (N-1) cross-covariance matrices P_{ij}, i = 1,2,...N, j = 1,2,...N, i≠j. No specific assumptions are made concerning the probability density function governing these errors. However it is assumed that the errors are zero mean.

The fused measurement $\hat{X}$ is defined to be a linear weighted sum of the individual measurement vectors $\hat{X}_i$, as follows:

$$\hat{X} = \sum_{i=1}^{N} A_i \hat{X}_i \qquad (4.1)$$

We require the fused measurement $\hat{X}$ to be unbiased. Therefore

$$E\{\hat{X}\} = \sum_{i=1}^{N} A_i E\{\hat{X}_i\} = \sum_{i=1}^{N} A_i \bar{X} = \bar{X}$$

$$\sum_{i=1}^{N} A_i = I$$

This provides the first constraint on the coefficient matrices A_i. Solving for A_N and substituting back into (4.1)

$$\hat{X} = \sum_{i=1}^{N-1} A_i \hat{X}_i + [I - \sum_{i=1}^{N-1} A_i] \hat{X}_N$$

The error in the estimate is

$$\tilde{X} = \sum_{i=1}^{N-1} A_i (\hat{X} - \bar{X}) + [I - A_i] (\hat{X} - \bar{X})$$

This shows that the error is a weighted sum of the error in each measurement vector.

The error covariance matrix P, associated with $\hat{X}$ is

$$P = E\{\tilde{X}\tilde{X}\}$$

$$P = E\{ [\sum_{i=1}^{N-1} A_i (X_i-\bar{X}) + [I-\sum_{i=1}^{N-1} A_i] (X_N-\bar{X})] \times$$

$$[\sum_{j=1}^{N-1} (X_j-\bar{X})^T A_j^T + (X_N-\bar{X})^T [I-\sum_{j=1}^{N-1} A_j]^T] \}$$

$$P = \sum_{i=1}^{N-1}\sum_{j=1}^{N-1} A_i P_{ij} A_j^T + [I-\sum_{i=1}^{N-1} A_i] \sum_{j=1}^{N-1} P_{Nj} A_j^T + \sum_{i=1}^{N-1} A_i P_{iN} [I-\sum_{j=1}^{N-1} A_j]^T +$$

$$[I-\sum_{i=1}^{N-1} A_i] P_{NN} [I-\sum_{j=1}^{N-1} A_j]^T \qquad (4.2)$$

The criterion of the optimal algorithm is minimization of the trace of the optimal covariance matrix P. Using gradient matrix identities derived in [8], it is shown that

$$\frac{\partial}{\partial A_k} Tr(P) = 2\sum_{i=1}^{N-1} A_i P_{ik} + 2P_{Nk} - 2\sum_{i=1}^{N-1} A_i (P_{iN}+P_{Nk}) - 2[I-\sum_{i=1}^{N-1} A_i] P_{NN}$$

$$= 2\sum_{i=1}^{N-1} A_i \{ P_{ik}-P_{iN}-P_{Nk}+P_{NN} \} + 2P_{Nk} - 2P_{NN} \qquad (4.3)$$

By setting this gradient equation to zero

$$\sum_{i=1}^{N-1} A_i \{ P_{ik} - P_{iN} - P_{Nk} + P_{NN} \} = (P_{NN} - P_{Nk}) \qquad (4.4)$$

where

$$k = 1,2,3,\ldots,(N-1)$$

Equation (4.4) represents (N-1) equations involving the (N-1) unknown matrices A_1, A_2, ..., A_{N-1}

Define

$$P'_{ik} = P_{ik} - P_{iN} - P_{Nk} + P_{NN} ,$$

$$i = 1,2,3, \ldots,(N-1)$$

$$k = 1,2,3,\ldots,(N-1)$$

and

$$P'_{Nk} = (P_{NN} - P_{NK}) \quad , \qquad k = 1,2,3,\ldots,(N-1)$$

Then the (N-1) equations (4.4) can be written in the following matrix form

$$[A_1 A_2 \ldots A_{N-1}] \begin{bmatrix} P'_{11} & P'_{12} & P'_{13} & \cdot\cdot & P'_{1,N-1} \\ P'_{21} & P'_{22} & P'_{23} & \cdot\cdot & P'_{2,N-1} \\ P'_{31} & P'_{32} & P'_{33} & \cdots & P'_{3,N-1} \\ \cdots & & & & \\ P'_{N-1,1} & P'_{N-1,2} & P'_{N-1,3} & \cdots & P'_{N-1,N-1} \end{bmatrix}$$

$$= [P'_{N1} \quad P'_{N2} \quad P'_{N3} \quad \ldots \quad P'_{N,N-1}]$$

The solution for the gain matrices is

$$[A_1\ A_2\ A_3\ \ .....\ \ A_{N-1}]$$

$$= [P'_{N1}\ P'_{N2}\ P'_{N3}\ ....P'_{N,N-1}] \times$$

$$\begin{bmatrix} P'_{11} & P'_{12} & P'_{13} & \cdots & P'_{1,N-1} \\ P'_{21} & P'_{22} & P'_{23} & \cdots & P'_{2,N-1} \\ \cdots\cdots\cdots & & & & \\ P'_{N-1,1} & P'_{N-1,2} & P'_{N-1,3} & \cdots & P'_{N-1,N-1} \end{bmatrix}^{-1}$$

$$= [P'_{N1}\ P'_{N2}\ P_{N3}\ ....P'_{N,N-1}]\,[P']^{-1} \qquad (4.5)$$

Equation (4.5) is the necessary condition for minimization of the trace of the fused covariance matrix P. However it is not the sufficient condition for minimization of the trace.

We now summarize the sufficent condition for minimization. Further details are available in reference [8]

4.3 Sufficient Conditions for Minimization of Trace

$$d^2\{Tr(P)\} = Tr\{\sum_{m=1}^{N-1} \frac{\partial}{\partial A_m}[dTr(P)]\,dA_m^T\}$$

$$d^2\{Tr(P)\} = Tr\{[dA_1\ dA_2 \ldots dA_{N-1} - \sum_{k=1}^{N-1} dA_k] \times$$

$$\begin{bmatrix} P_{11} & P_{12} & \cdots & P_{1,N-1} & P_{1,N} \\ P_{21} & P_{22} & \cdots & P_{2,N-1} & P_{2,N} \\ \cdots\cdots & & & & \\ \cdots\cdots & & & & \\ P_{N-1,1} & P_{N-1,2} & \cdots & P_{N-1,N-1} & P_{N-1,N} \\ P_{N,1} & P_{N,2} & \cdots & P_{N,N-1} & P_{N,N} \end{bmatrix} \begin{bmatrix} dA_1^T \\ dA_2^T \\ \cdot \\ \cdot \\ dA_{N-1}^T \\ -\sum_{k=1}^{N-1} dA_m^T \end{bmatrix} \}$$

$$= Tr\{\mathcal{F}\ \mathcal{P}\ \mathcal{F}\} = Tr\{\ \mathcal{E}\ \mathcal{E}^T\ \} > 0$$

Therefore $d^2\{Tr(P)\} \geq 0$ if and only if the partitioned error covariance matrix $\mathcal{P}$ is positive definite. Under this condition, therefore, the gain matrices (4.5) establish a minimum of the cost functional Tr(P).

We now present the final form for the optimum covariance matrix P.

4.4 Optimum Error Covariance Matrix P

It is shown in [8] that the optimum covariance matrix P is given by:

$$P = P_{NN} - [P'_{N1}\ P'_{N2} \ldots P'_{N,N-1}]\ [P']^{-1} \begin{bmatrix} (P'_{N1})^T \\ (P'_{N2})^T \\ \cdots \\ (P'_{N,N-1})^T \end{bmatrix} \quad (4.6)$$

Equation (4.6) gives the (symmetric) error covariance matrix corresponding to the fused measurement (4.1). The diagonal elements of P are less than the corresponding diagonal elements of each of the individual error covariance matrices P_{ii}, i = 1,2,3,...,N. Consequently, the trace of the optimum covariance matrix P must be less than the trace of each measurement covariance matrix P_{ii}, i = 1,2,3,...,N.

The second term on the right in (4.6) represents the net reduction in uncertainty brought about by the fusion process.

This completes summary of optimal fusion algorithm. Since it will be applied to the special case N = 2 distributed measurements, we now look at the special form of the algorithm in this case.

4.5 Optimum Fusion Algorithm for Special Case of N = 2 Measurements

In our scenario there are three sensors generating uncorrelated angle-of-arrival measurements θ_i, i = 1,2,3. These three angle-of-arrival measurements are used to form two separate distributed measurement

vectors z_{12}, and z_{23} of the position of an object in two-dimensional space as shown in chapter III. Measurement z_{12} has a covariance matrix P_{z12}. Measurement z_{23} has a covariance matrix P_{z23}. Measurements z_{12}, and z_{23} have a non zero cross-covariance matrix P_{z1223}. This is because S2 is the common sensor to both measurements.

Therefore, in terms of the matrices in the optimum fusion algorithm, we have:

$$P_{11} = P_{z12}$$

$$P_{22} = P_{z23}$$

$$P_{12} = P_{z1223}$$

$$P_{21} = (P_{z1223})^T$$

From the definition

$$P'_{ik} = P_{ik} - P_{iN} - P_{Nk} + P_{NN}$$

we get

$$P'_{11} = P_{z12} - P_{z1223} - (P_{z1223})^T + P_{z23} \qquad (4.7)$$

From equation (4.5), we get

$$P' = P'_{11}$$

From the definition

$$P'_{Nk} = P_{NN} - P_{Nk}$$

we get

$$P'_{21} = P_{z23} - (P_{z1223})^T$$

From equation (4.5) we see the gain matrix A_1 given by

$$A_1 = P'_{21}(P'_{11})^{-1}$$

$$= [P_{z23} - (P_{z1223})^T][P_{z12} - P_{z1223} - (P_{z1223})^T + P_{z23}]^{-1}$$

and

$$A_2 = I - A_1$$

The optimum error covariance matrix P_o is obtained from equation (4.6) as follows

$$P_o = P_{22} - P'_{21}\,[P'_{11}]^{-1}\,(P'_{21})^T$$

$$= P_{z23} - [P_{z23} - P_{z1223}{}^T][P_{z12} - P_{z1223} - P_{z1223}{}^T + P_{z23}]^{-1} \times [P_{z23}{}^T - P_{z1223}] \qquad (4.8)$$

In the next chapter we discuss simulation results for the scenario given in figure (2.1).

CHAPTER V

SIMULATION RESULTS

5.1 Introduction

In this chapter we describe two simulation examples (scenario no1, and scenario no2) in two-dimensions. Two cases are examined for each scenario a low-noise case and a high-noise case to illustrate the improvement in the estimation in the fusion centre by using the fusion algorithm and for demonstrating the basic principles presented previously.

5.2 Basic Concept of the Simulation Flow Diagram

Figure (5.1) shows the simulation flow diagram of the data generation and fusion algorithm.

As we see from figure (5.1) the algorithm is simulated for three spatially distributed sensors S1, S2, and S3 with known locations $(x_1,y1)$, (x_2,y_2), and (x_3,y_3) respectively and we specify the coordinates of (x,y) of the object's position.

Knowing the position of the three sensors and of the object we compute the true angle-of-arrival values θ_{1t}, θ_{2t}, and θ_{3t} respectively. The next step is to generate errors in the angle-of-arrival measurements. The statistics governing the errors on these angle measurements come from a variety of distributions, namely the uniform, sawtooth, and triangular

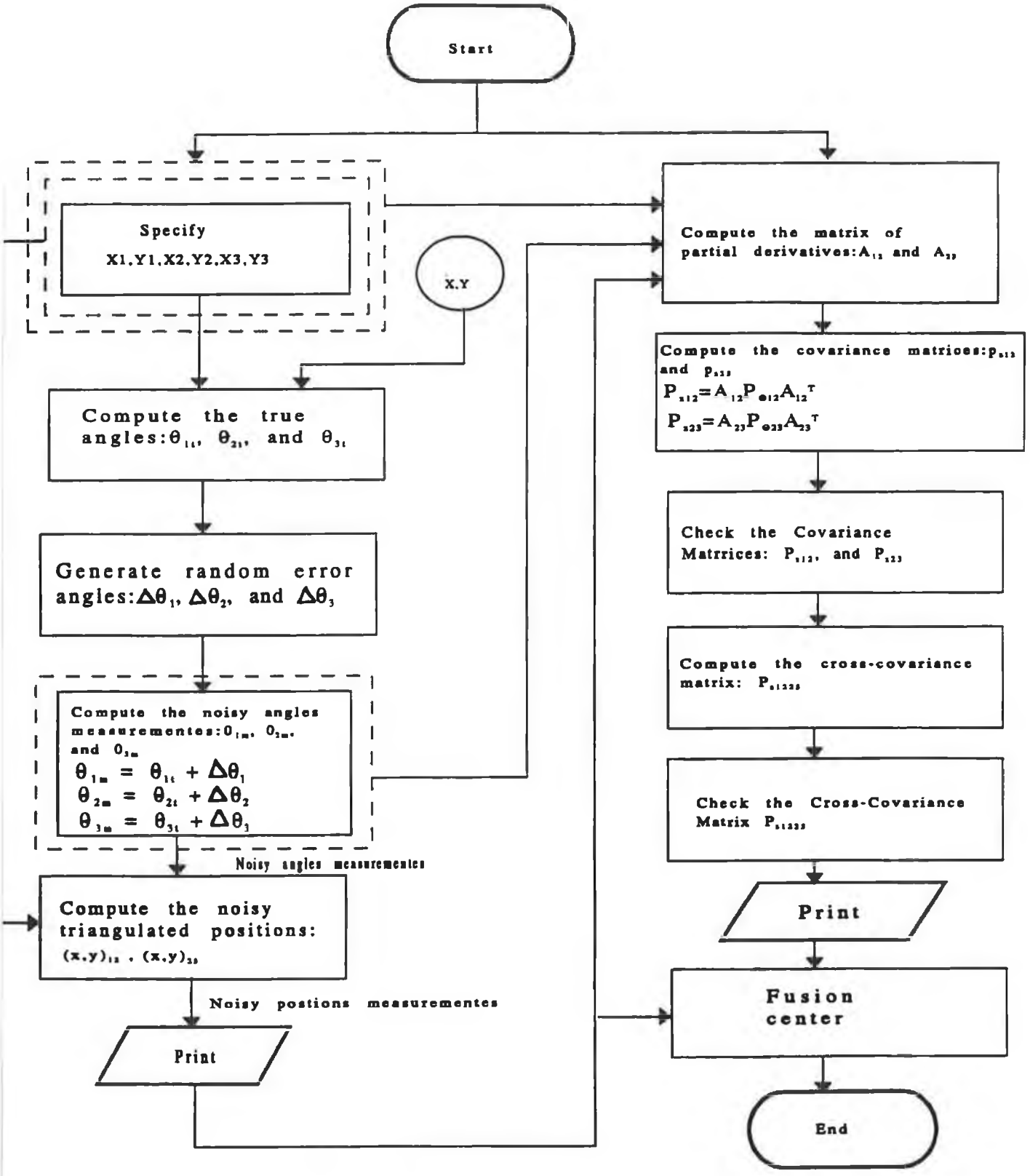

Figure (5.1) Simulation Flow Diagram

distributions. These several different distributions are used to test the fusion algorithm in a rigorous manner.

5.2.1 Errors on sensor S1:

We assume sensor S1 errors have a uniform pdf as shown in figure (5.2) on page 46. A random number y with pdf U(0,1) is generated. That number is substituted into the right side of the equation (A-6) in appendix A. That produces the random number with pdf $U(-\delta_u, \delta_u)$. Equation (A-6) is used to generate random angle-of-arrival errors in S1 measurement ($\Delta\theta_1$). This value is added to the true angle θ_{1t} to produce the measured angle θ_{1m}.

$$\theta_{1m} = \theta_{1t} + \Delta\theta_1$$

5.2.2 Errors on Sensor S2:

We assume sensor S2 errors have a sawtooth pdf as shown in figure (5.2). A random number y with pdf U(0,1) is generated. That number is substituted into the right side of the equation (B-8), or (B-9) depending on whether $0 \leq y \leq 0.5$, or $0.5 \leq y \leq 1$ (see appendix B). That produces the random number with a sawtooth pdf $(-\delta_s, \delta_s)$. Equations (B-8), and (B-9) are used to generate random angle-of-arrival errors in S2 measurement data ($\Delta\theta_2$). This value is added to the true angle θ_{2t} to produce θ_{2m}.

$$\theta_{2m} = \theta_{2t} + \Delta\theta_2$$

5.2.3 Errors on Sensor S3

We assume sensor S3 errors have a triangle pdf as shown in figure (5.2). A random number y with pdf U(0,1) is generated. That number is substituted into the right side of the equations (C-8) or (C-9) depending on whether $0 \leq y \leq 0.5$, or $0.5 \leq y \leq 1$ (see appendix C). That produces a random number with a triangle pdf $(-\delta_t, \delta_t)$. Equation (C-8), and (C-9) are used to generate random angle-of-arrival errors in sensor S3 measurement data $(\Delta\theta_3)$. This value is added to the true angle θ_{3t} to produce θ_{3m}.

$$\theta_{3m} = \theta_{3t} + \Delta\theta_3$$

From the noisy angle measurements θ_{1m}, θ_{2m}, and θ_{3m} we compute the noisy position measurements (x_{12}, y_{12}), and (x_{23}, y_{23}) using equations(2.9),(2.10), (2.11), and (2,12). We now have two noisy triangulated position vectors z_{12}, and z_{23} as defined in chapter II.

5.2.4 First-Order Approximation Covariance Matrix

The next step is to compute the first order-approximation to the covariance matrices of the two position vectors z_{12} and z_{23}. We do this by first computing the matrix of partial derivatives A_{12} defined by the equation (3.4). The elements of A_{12} are defined by the equations (3,7), (3,8), (3,9), and (3,10). The matrix of partial derivatives A_{23} is define by equation (3.12). The elements of A_{23} are

defined by the equations (3.14), (3,15), (3,16), and (3,17). As we see from these equations we need the noisy angle-of-arrival measurements to compute the partial derivative matrices A_{12}, and A_{23}. From these equations we see that θ_1, and θ_2 appear directly in matrix A_{12}, and θ_2, θ_3 appear directly in the matrix A_{23}. We use the noisy angle-of-arrival measurements because we do not have the true angles θ_{1t}, θ_{2t}, and θ_{3t}. Therefore the partial derivative matrices are at best only noisy approximations to the true values. We also need the noisy position measurements as we see in equations (3.9) and (3.16) to compute the partial derivative matrices. These noisy position measurements are not accurate and also increase the error in the partial derivative matrices. For these reasons the covariance matrix is an approximation to the true covariance matrix. The covariance matrix of the noisy angle measurement $P_{\theta 12}$ is calculated by the equation (3.22). The variance of the angle errors for sensor S1, $\sigma_{\theta 1}^2$, is given by the equation (A-3). The variance of the angle errors for sensor S2, $\sigma_{\theta 2}^2$, is given by equation (B-3). When the matrix of partial derivatives A_{12}, has been computed, the covariance matrix P_{z12} is computed using equation (3.21). The covariance matrix P_{z23} is computed in a like manner using equation (3.27), where the covariance matrix of the noisy angle measurement $P_{\theta 23}$ is given by the equation (3.28). The variance of the angle errors for

sensor S3, $\sigma_{\theta_3}^2$, is given by the equation (C-3).

When the covariance matrices have been computed we next check that these are symmetric and that the correlation coefficients have a magnitude less than one.

5.2.5 Cross-Covariance Matrix

When this is complete, we then compute the cross-covariance matrix P_{z1223} by using the equation (3.32). When P_{z1223} is computed, we check the correlation coefficient elements of the cross-covariance matrix. These correlation coefficients also should have a magnitude less than unity.

At this point we have two noisy measurement vectors z_{12}, and z_{23}. We have the covariance matrices associated with these vectors, namely P_{z12} , and P_{z23}. We also have the cross-covariance matrix between these two vectors, namely P_{z1223}. The data is now ready to be fused using the optimal fusion algorithm discussion in chapter IV.

We compute the optimum covariance matrix P_o using equation (4.8). When P_o is computed we then check the trace of the optimum matrix P_o and compare it with the trace of the individual covariance matrices P_{z12} and P_{z23}. The fusion algorithm attempts to produce an optimum covariance matrix P_o with a trace which is less than that of P_{z12} and of P_{z23} individually. The

optimum fusion algorithm assumes that the covariance matrix is correct for each of the input measurement vectors. We have seen that the covariance matrix is only a first-order approximation to the true covariance matrix. In addition, the pdf's governing the errors on the sensors are quite different from each other. These conditions provide an interesting test for the optimum fusion algorithm under sub-optimum conditions.

5.2.6 Solution of Nonlinear Estimation Problem Using Linear Estimation Techniques

It should also be pointed out here that what is basically a nonlinear estimation problem is being addressed using linear estimation techniques.

Our measurement data consists of noisy angles-of-arrival. We are interested in the position of the object. From equation (2.9) and (2.10) we see that the position of the object is a nonlinear function of the data. Normally we would resort to nonlinear estimation techniques to estimate the object's position from the data. However we are not doing that here. Instead, we invert the measurements and use the first-order approximation to the covariance matrices of the noisy position measurments. We then use a linear fusion technique to estimate the object location from the noisy inverted data. The distribution governing the noisy position data is

unknown. However, the fusion algorithm dose not need this information. All it needs is the covariance matrix of the position measurements for which we provide a first-order approximation. One of the aims of this research is to see how well this works.

The next section discusses simulation example for scenario no1, low-noise case.

The simulations were carried using MATLAB on a 386 PC

5.3 Scenario Number 1 (no1), Low-Noise Case.

Figure (5.2) shows the configuration of the object and sensors for scenario no1 in two dimensions.

---- represents the noisy angle-of-arrival measurements data.

_____ represents the true angle value.

As we see from figure (5.2) sensor S1 has a uniform pdf $U(-\delta_u, \delta_u)$, sensor S2 has a sawtooth pdf and sensor S3 has a triangle pdf.

The values used in the low noise simulation are:

Object true position p (x = 6, y = 7)

S1 location ($x_1 = 2$, $y_1 = 3$),

S2 location ($x_2 = 5$, $y_2 = 4$),

S3 location ($x_3 = 9$, $y_3 = 3$),

Each sensor calculates the true object angle-of-arrival. These are:

$\theta_{1t} = 45° = 0.7854$ radians

$\theta_{2t} = 71° = 1.25$ radians

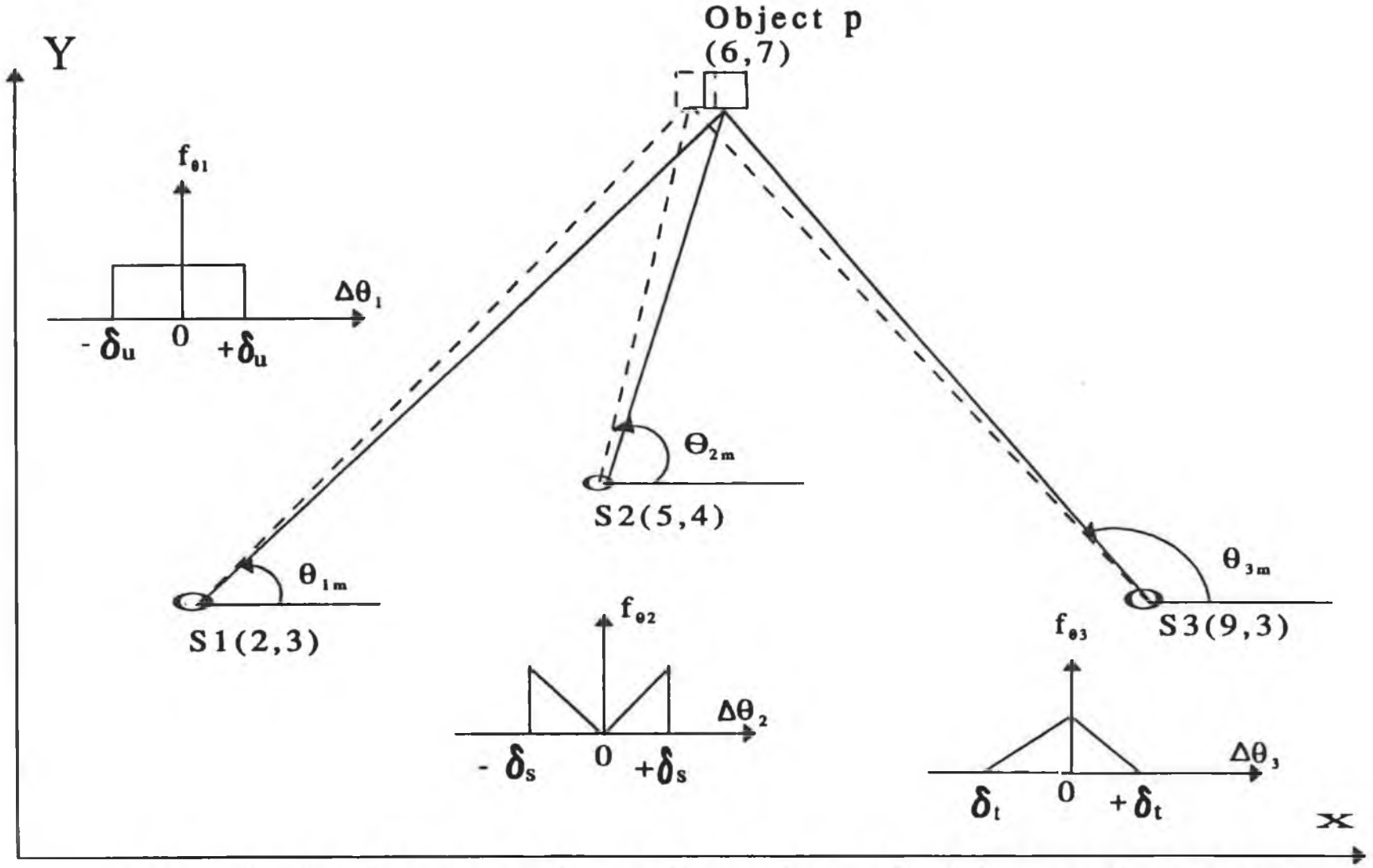

Figure (5.2) Geometrical configuration of object and sensors for scenario no1

θ_{3t} = 126.87° = 2.2143 radians

Noise pdf in the three sensors S1, S2, and S3 are:

δ_u = 2 degrees = 0.0349 radians

σ_u = 1.15 degrees = 0.0202 radians

δ_s = 2 degrees = 0.0349 radians

σ_s = 1.41 degrees = 0.0247 radians

δ_t = 2 degrees = 0.0349 radians

σ_t = 0.8193 degrees = 0.0143 radians

From the equation (A-3) we compute the noisy standard deviation for a uniform random variable σ_u

From the equation (B-3) we compute the noisy standard deviation for a sawtooth random variable σ_s

From the equation (C-3) we compute the noisy standard deviation for a triangle random variable σ_t.

As we see the standard deviation of the errors are small compared to the true values of the angles. Therefore, this is a low-noise case. The covariance matrix should be very close to the true covariance matrix.

As mentioned earlier it is impossible to determine the pdf governing the measurement vectors z_{12}, and z_{23} because of the nonlinear function of the angles θ_1, θ_2, and θ_3. However the fusion algorithm can be applied because it does not need to know the pdf, just the covariance matrices.

5.3.1 Discussion of Simulation Results, Scenario no1, Low-Noise Case

The computer simulation was run 50 times and the results are plotted and discussed in the next several pages.

Figure (5.3) shows the actual error in the noisy measured position x_{12} obtained by triangulation between sensors S1, and S2. The dotted line represents the actual errors in the noisy measurements x_{12}, and the solid line represents the square root of $P_{z12}(1,1)$. The solid line is the theoretical standard deviation of the errors according to the covariance matrix. The numeric mean value of the errors in noisy measurement x_{12} in figure (5.3) is Mx12_err = (0.0039). The numeric standard deviation is Sx12_err = (0.1484). This compares favourably with the theoretical standard deviation given by the solid line in the figure.

Figure (5.4) shows the actual errors in the noisy measurements position x_{23} obtained by triangulation between sensors S2, and S3. The dotted line represents the actual errors in noisy measurements x_{23}, and the solid line represents the square root of $P_{z23}(1,1)$. The solid line is the theoretical standard deviation of the errors according to the covariance matrix. The numeric mean value of the errors in x_{23} noisy measurements in figure (5.4) is Mx23_err=

(0.0067). The numeric standard deviation is Sx23_err = 0.0594. This also compares favourably with the theoretical standard deviation given by the solid line in the figure.

Figure (5.6) shows the errors in the fused estimate in x position obtained by fusion of the noisy measurements x_{12}, and x_{23}. The dotted line represents the errors in the fused estimate and the solid line represents the square root of $P_o(1,1)$. The numeric mean value of the errors in the fused estimate in figure (5.6) in x dimension is Xfuse_err = (0.0037). The numeric standard deviation of the errors in the fused estimate is Sxfuse_err = (0.0654).

Figure (5.7) shows the actual errors in the measured noisy position y_{12} obtained by triangulation between sensors S1, and S2. The dotted line represents the actual errors in the noisy measurements y_{12}, and the solid line represents the square root of $P_{z12}(2,2)$. The numeric mean value of the errors in the figure is My12_err = (-0.0048). The numeric standard deviation is Sy12_err = (0.2707).

Figure (5.8) shows the actual errors in the measured noisy position y_{23} obtained by triangulation between sensors S2, and S3. The dotted line represents the actual errors in the noisy measurements y_{23}, and the

solid line represents the square root of $P_{z23}(2,2)$. The numeric mean value of the errors in the figure is My23_err = (0.0198). The numeric standard deviation is Sy23_err = (0.1168).

Figure (5.10) shows the errors in the fused estimate in y position obtained by fusion the noisy measurements y_{12}, and y_{23}. The dotted line represents the errors in the fused estimate in y position and the solid line represents the square root of $P_o(2,2)$. The numeric mean value of the errors in the fused estimate in figure (5.10) is Yfuse_err = (0.0094). The numeric standard deviation of the errors in the fused estimate is Syfuse_err = (0.1008).

Figure (5.3) shows the actual errors in the noisy measurements x_{12} and the theoretical standard deviation of the errors in low-noise case in scenario no1 in x postion.

We can see from figure (5.3) that the errors change between negative and positive values. Also we see the theoretical standard deviation increasing and decreasing in according with the magnitude of the errors. The statistics are changing with time. Between n = 5 and n = 6 we see the magnitude of the error increases from 0.12 to 0.275. We also note the theoretical standard deviation increase from 0.12 to 0.18 (the same value of 0.12 here is coincidence). We

also see the same thing between n = 10 and n = 11 the magnitude of the error increases from 0.11 to 0.185. We also note that the theoretical standard deviation increases from 0.15 to 0.185. Between n = 30 and n = 33 , we see the magnitude of the error increases from 0.17 to 0.32. The theoretical standard deviation increases from 0.15 to 0.2. Between n = 34 and n = 37, as the magnitude of the error increases and decreases, the theoretical standard deviation increases and decreases in a like manner.

In general, the standard deviation tracks the magnitude of the errors.

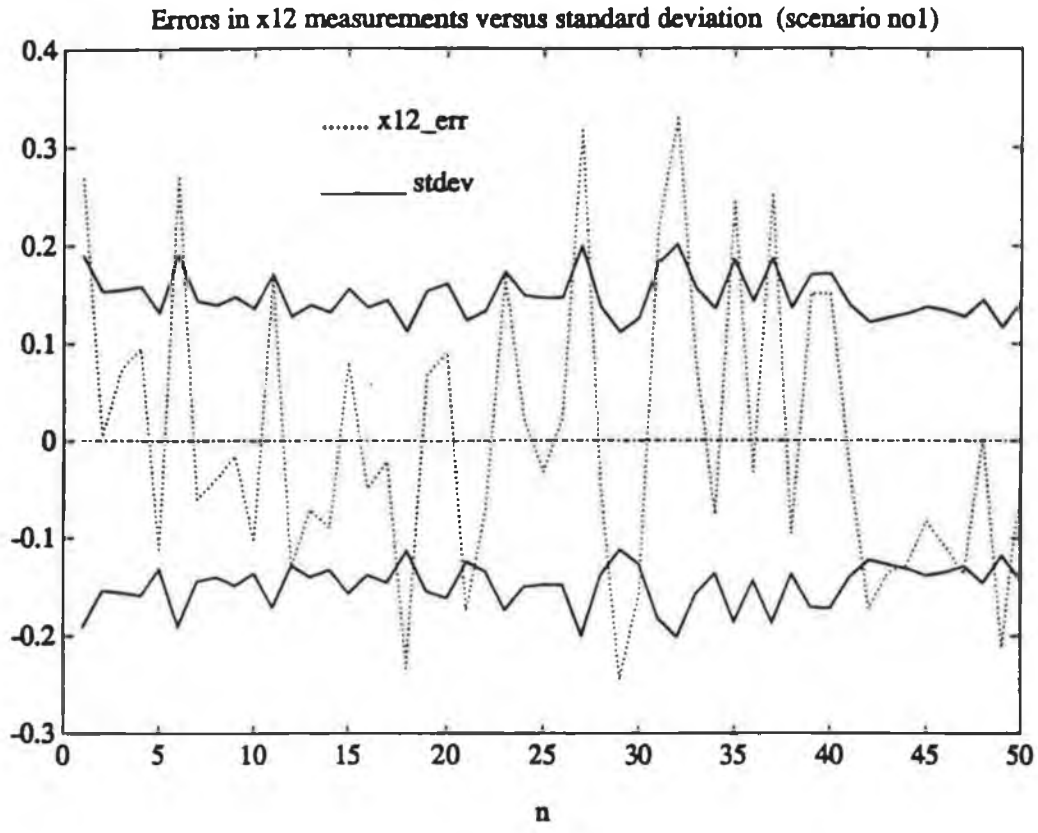

Figure (5.3)

....x12_err represents the actual errors in the noisy measurements x_{12} in low-noise case in x position.

_____ stdev represents the square root of $P_{z12}(1,1)$, the theoretical standard deviation of the errors according to the first-order approximation to the covariance matrix.

Figure (5.4) shows the actual errors in the noisy measurements x_{23} and the theoretical standard deviation of the errors in low-noise case in scenario no1 in x position.

We can see from figure (5.4) that x_{23} noisy measurements are higher quality measurements than the x_{12} noisy measurements because the standard deviation of x_{23} measurements is smaller than the standard deviation of x_{12} measurements. Also we can see from this figure most of the errors are less than 0.1, and are smaller than the errors in the noisy measurements x_{12}. The theoretical standard deviation of 0.06 is close to the numeric one. We see from figure (5.4) the standard deviation is approximately constant for all values of n.

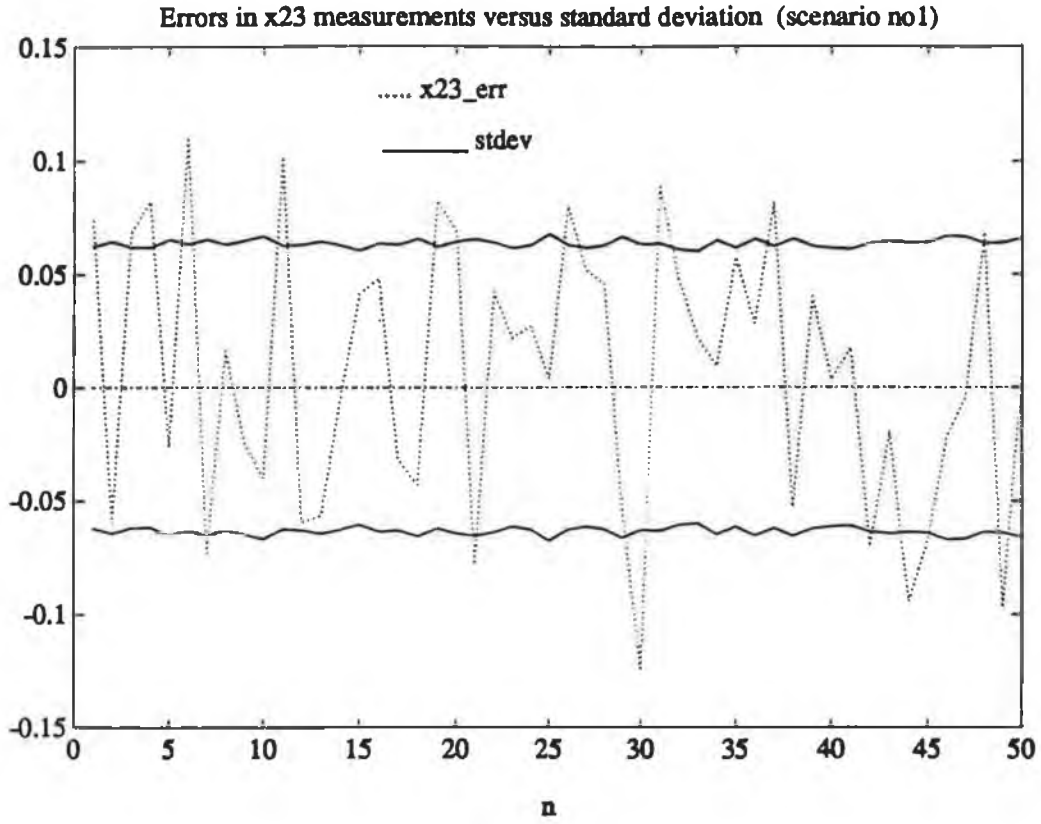

Figure (5.4)

... x23_err represents the actual errors in the noisy measurements x_{23} in low-noise case in scenario no1.

_____ stdev represents the square root of $P_{z23}(1,1)$, the theoretical standard deviation of the errors according to the first-order approximation to the covariance matrix.

Figure (5.5) shows the percentage errors in the fused estimate in low-noise case in scenario no1 in x position.

We immediately observe that the fused estimate (solid line) clips the peak errors in the measurements. Also in this figure we can see the improved performance that is obtained by fusion of the error in the two measurements x_{12} and x_{23}. For example at n = 6 we see the fused measurement clips the large error in x_{12}, and remains close to the higher accuracy measurement x_{23}. We also observe the same effect at n = 27. The error in x_{12}, and x_{23} are both positive, and the fused estimate error is closer to that of x_{23}. Under these conditions (where both measurement errors are of like sign), the fusion algorithm cannot in general produce an error which is less than the smaller one. In order to reduce errors, the fusion algorithm relies on opposite sign errors to cancel each other out. With errors of the same sign, this cancellation is not generally possible. We see the same effect at n = 22, 32, and between n = 37 and 50. But when the errors in the x_{12}, and x_{23} are of opposite algebraic signs, the fusion algorithm produces a smaller error than the smallest measurement error. For example at n = 16 where the error in x_{12} measurements is negative and the error in x_{23} measurements is positive we see the error in the fused estimate is less than the smaller error individually. We see the same effect at n = 23,

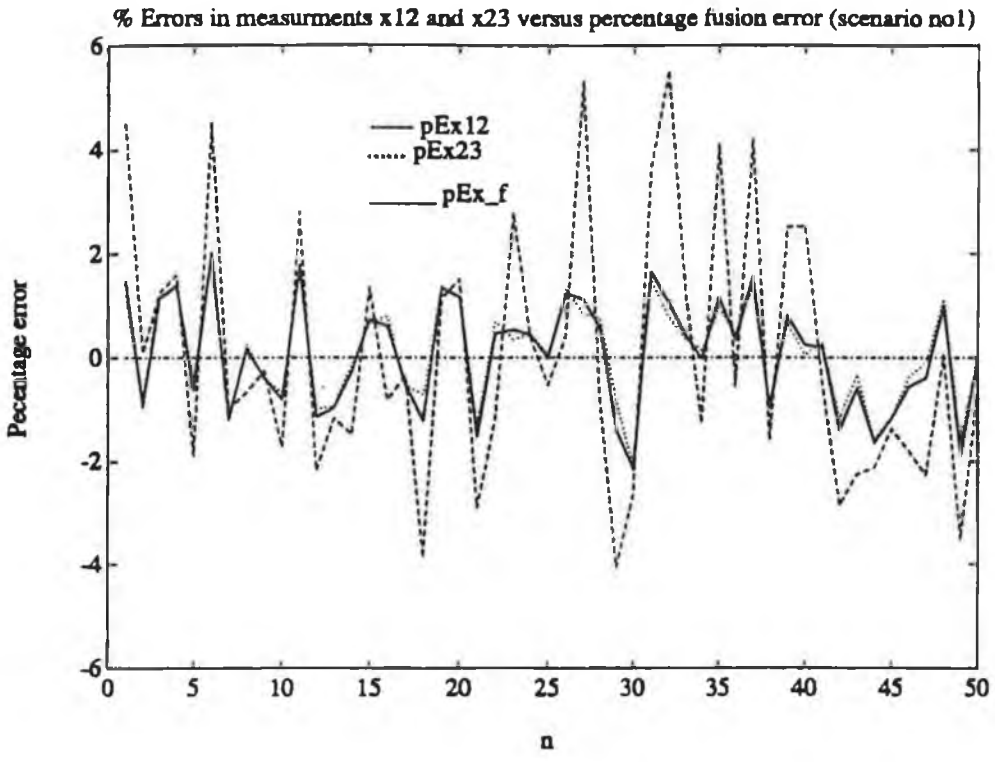

Fig (5.5)

---- (pEx12) represents the percentage error in the noisy measurements x_{12} in low-noise case in scenario no1 in x position.

.... (pEx23) represents the percentage error in the noisy measurements x_{23} in low-noise case in scenario no1 in x position.

____ (pEx_f) represents the percentage error in the fused estimate for low-noise case in scenario no1 in x position.

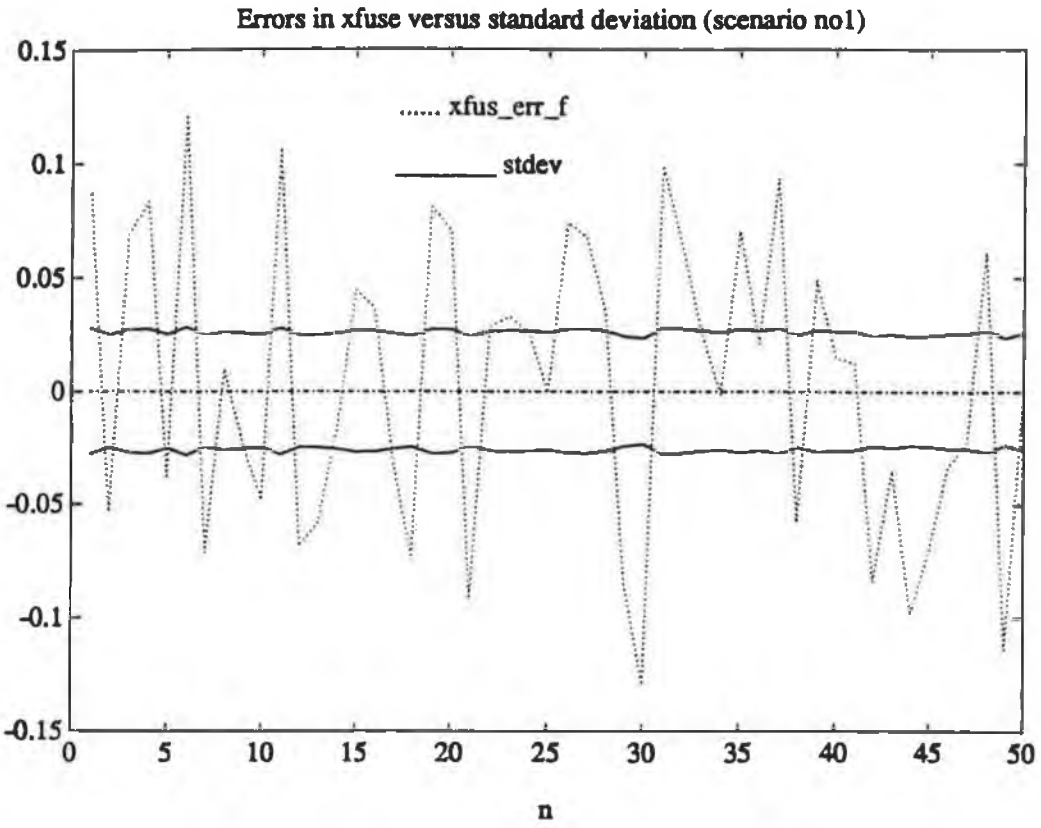

Figure (5.6)

.... xfuse_err_f represents the errors in the fused estimate in low-noise case in scenario no1 in x position.

____ stdev represents the square root of $P_o(1,1)$, the theoretical standard deviation of the errors in the fused estimate in low-noise case in scenario no1 in x position.

25, and n = 34.

Figure (5.7) shows the actual errors in the noisy measurements y_{12} and the theoretical standard deviation of the errors in low-noise case in scenario no1 in y position.

We see from figure (5.7) between n = 5 and n = 6, the magnitude of the error increases from 0.18 to 0.5. We also note the standard deviation increases from 0.29 to 0.36.

In general, we can see from this figure the theoretical standard deviation tracks the magnitude of the errors with a few exception at n = 18, for example.

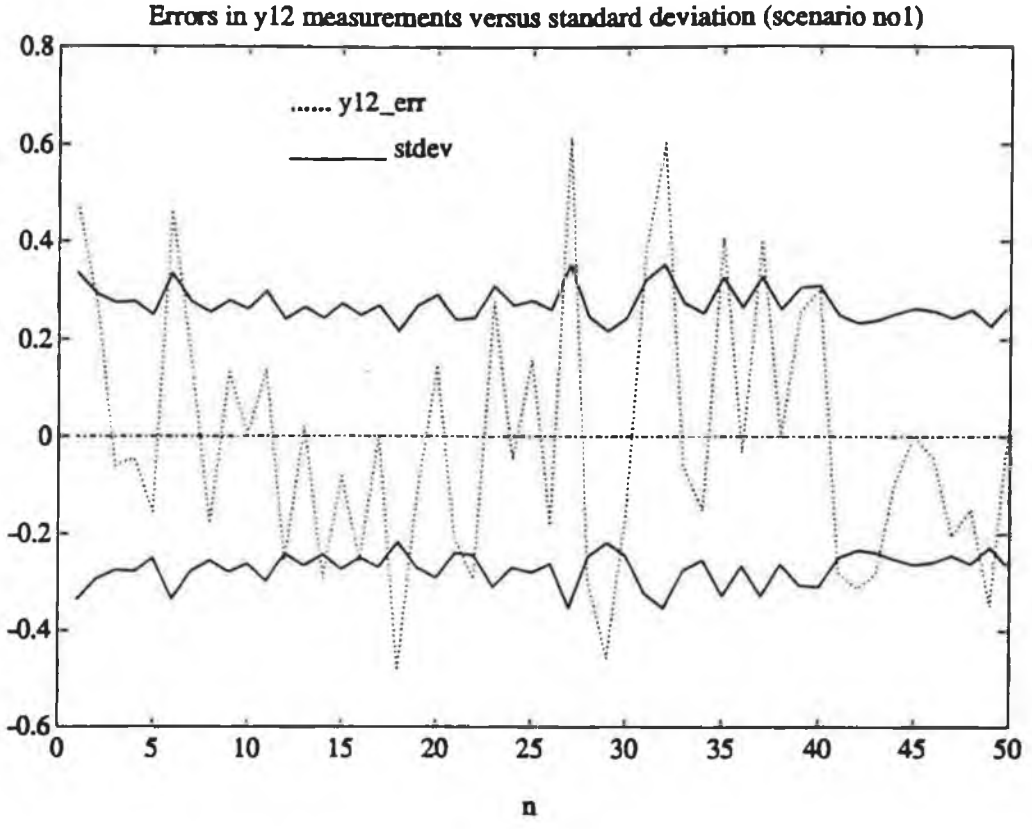

Figure (5.7)

.... y12_err represents the actual errors in the noisy measurements y_{12} in low-noise case in scenario no.

_____ stdev represents square root of $P_{z12}(2,2)$, the theoretical standard deviation of the errors according to that first-order approximation to the covariance matrix.

Figure (5.8) shows the actual errors in the noisy measurements y_{23} and the theoretical standard deviation of the errors in low-noise case in scenario no1 in y postion.

We can see from figure (5.8) that y_{23} noisy measurements are more accurate than y_{12} noisy measurements. Also we can see that most of the errors are less than 0.11 and the standard deviation of 0.11 is close to the numeric one. We see from figure (5.8) the standard deviation is approximately constant for all values of n.

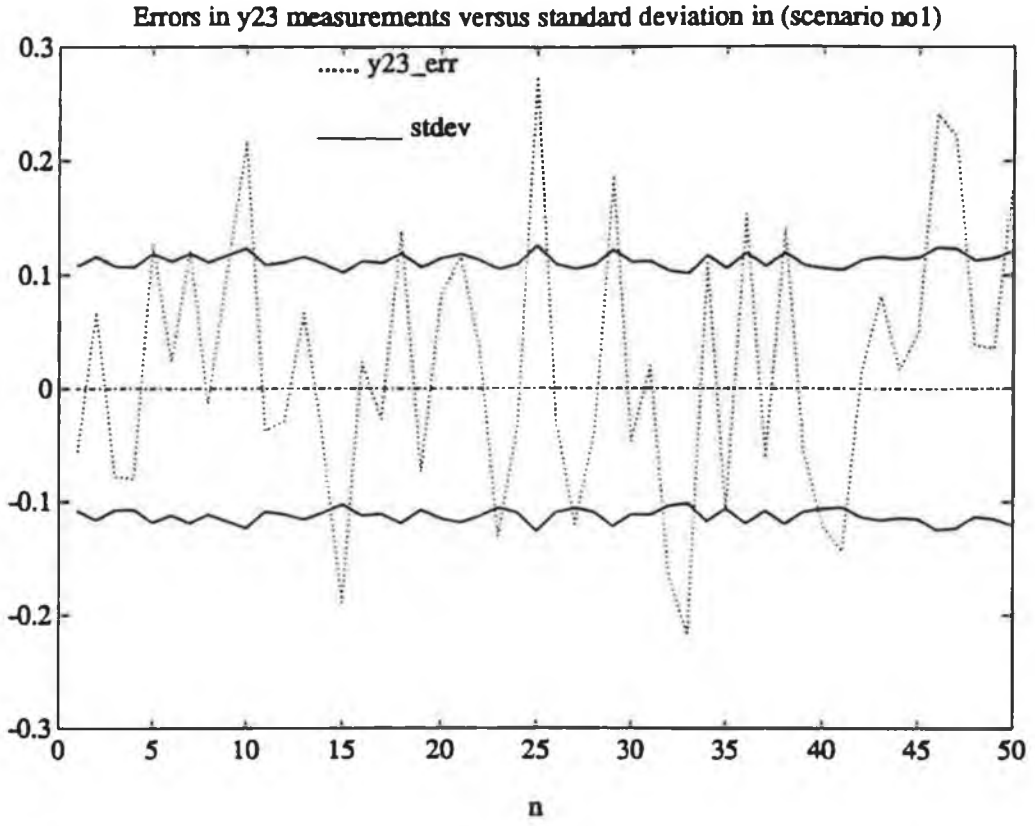

Figure (5.8)

.... y23_err represents the actual errors in the noisy measurements y_{23} in low-noise case in scenario no1 in y position.

_____ stdev represents the square root of $P_{z23}(2,2)$, the theoretical standard deviation of the errors according to that first-order approximation to the covariance matrix in low-noise case in scenario no1 in y position.

Figure (5.9) shows the percentage errors in the fused estimate in low-noise case in scenario no1 in the y position.

We can see that the noisy measurements y_{23} are more accurate than the y_{12} noisy measurements. The improvement offered by the fusion algorithm is obvious from the figure. The fused estimate clips the peak errors in both y_{12}, and y_{23}. For example at n = 28 the error in y_{12} is positive and in y_{23} is negative. We see the error in the fused estimate is smaller than the smallest magnitude error which is the error in y_{23}. At n = 29 the same effect is obvious. The error in y_{12} is negative and the error in y_{23} is positive. We see the error in the fused estimate is smaller than the smallest magnitude error which is the error in y_{23}. We observe the same effect at n = 18, 21, 22, 23, and between n = 42 to n = 50 (the errors in y_{12}, and y_{23} are of opposite algebric signs). The fusion algorithm produces an error which is smaller than the smallest one. But we see when the errors in the measurements y_{12}, and y_{23} are of the same algebraic sign, the error in the fused estimate is not less than the smallest measurement error but clips the peak error and remains close to the smaller one. We see that at n = 6, both the errors in y_{12}, and y_{23} are positive, and the fused estimate clips the big error in y_{12} and is close to y_{23}. We observe the same effect at n = 12, 13, 20, and n = 41.

Overall, the figure shows that the fused estimate is generally better than the individual measurements.

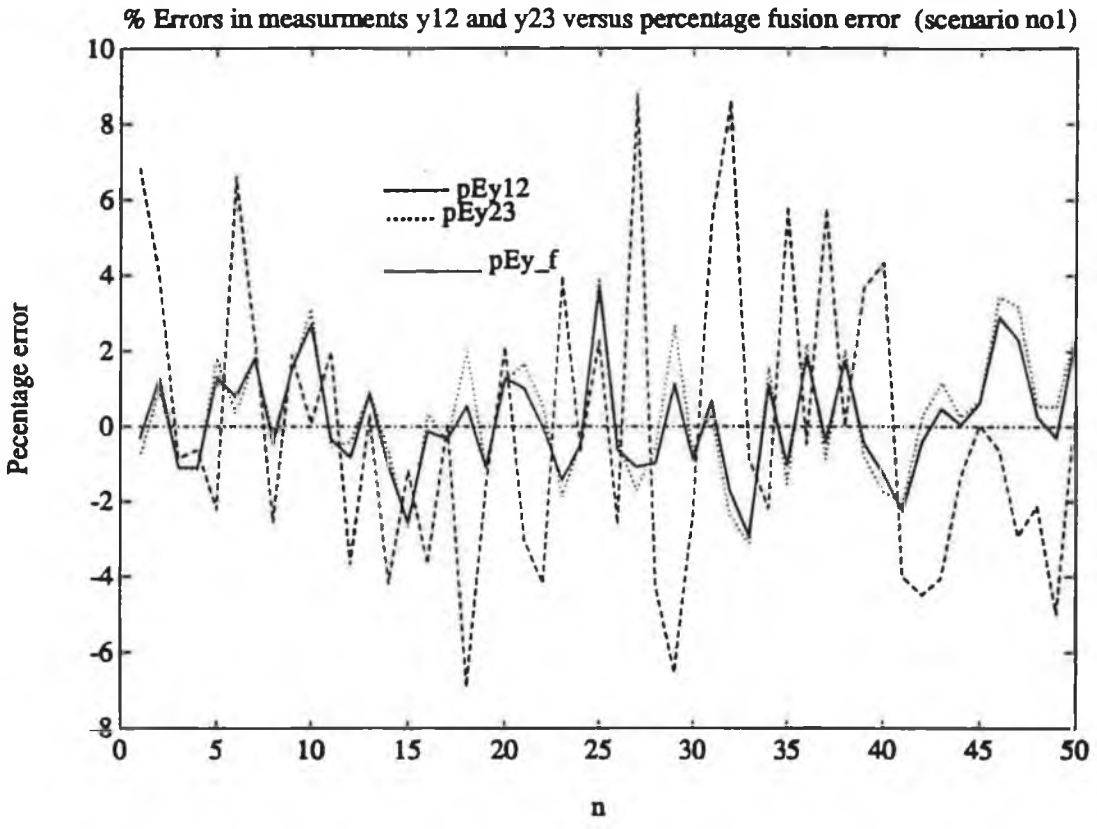

Figure (5.9)

---- pEy12 represents the percentage error in the noisy measurement y_{12} in low-noise case in scenario no1 in y position.

.... pEy23 represents the percentage error in the noisy measurement y_{23} in low-noise case in scenario no1 in y position.

____ pEy_f represents the percentage error in the fused estimate in low-noise case in scenario no1 in y position.

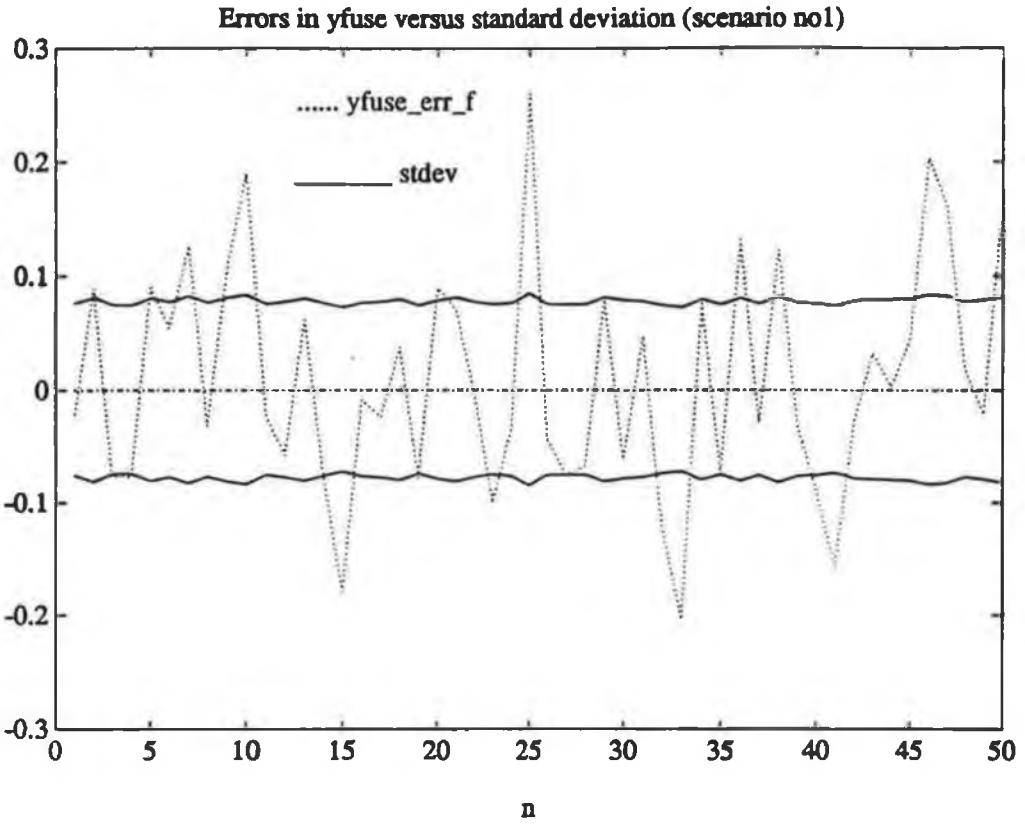

Figure (5.10)

.... yfuse_err represents the errors in the fused estiamte in low-noise case in scenario no1 in y position.

_____ stdev represents the square root of $P_0(2,2)$, the theoretical standard deviation of the errors in the fused estimate in y noisy position in low-noise case in scenario no1.

5.3.1.1 Trace of Covariance Matrices

The fusion algorithm is not designed to minimize the error in the fused measurements, although it achieves this many times.

It is the criterion of the fusion algorithm to produce the optimum covariance matrix having a trace which is less than the trace of the individual error covariance matrices.

Figure (5.11) shows the trace of the error covariance matrices in low-noise case in scenario no1.

From figure (5.11) we can see that the trace of the optimum error covariance matrix is less than the trace of the individual error covariance matrices p_{z12}, and P_{z23}.

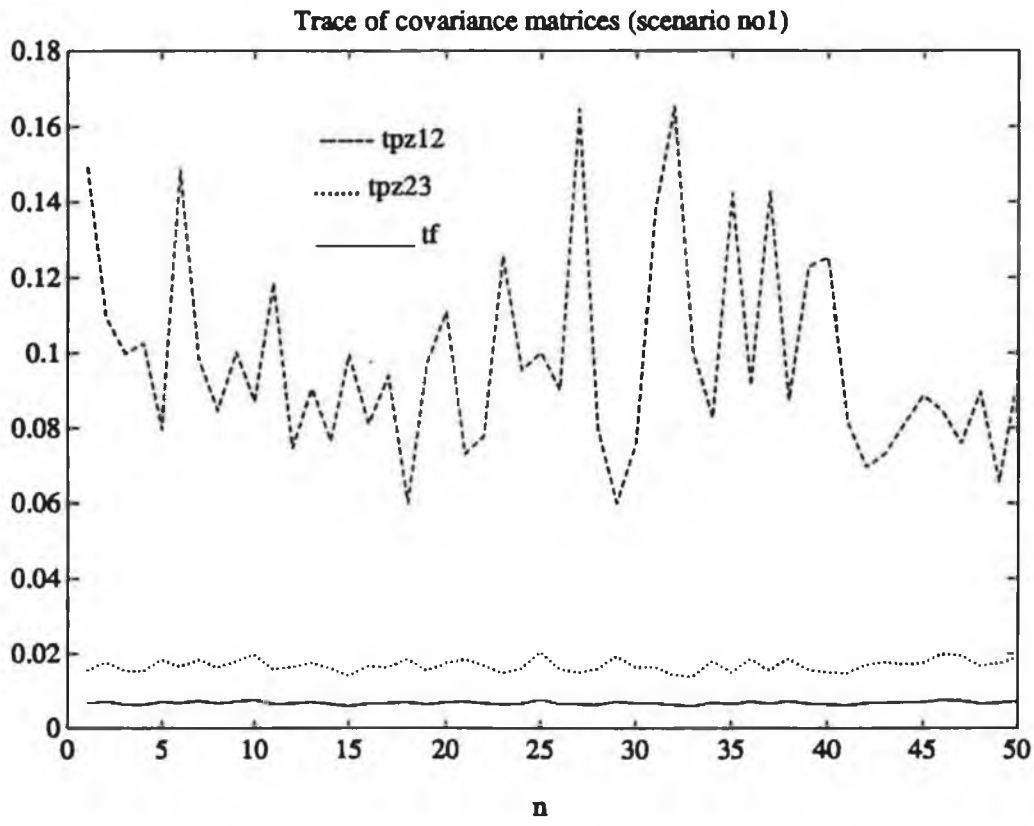

Figure (5.11)

--- tpz12 represents the trace of the error covariance matrix between sensor S1, and sensor S2 in low-noise case in scenario no1.

.... tpz23 represents the trace of the error covariance matrix between sensors S2, and S3 in low-noise case in scenario no1.

____ tf represents the trace of the optimum error covariance matrix in low-noise case in scenario no1.

Figure (5.12) shows the correlation coefficient elements for the cross-covariance matrix P_{z1223} which are calculated by the equations:

ρ_{x12x23} = rho11 is calculated by the equation (3.33),

ρ_{x12y23} = rho12 is calculated by the equation (3.34),

ρ_{y12x23} = rho21 is calculated by the equation (3.35), and

ρ_{y12y23} = rho22 is calculated by the equation (3.36).

From figure (5.12) we see all the correlation coefficients have magnitude less than one. The figure also shows that there is a strong correlation between the components of the two vectors z_{12} and z_{23}.

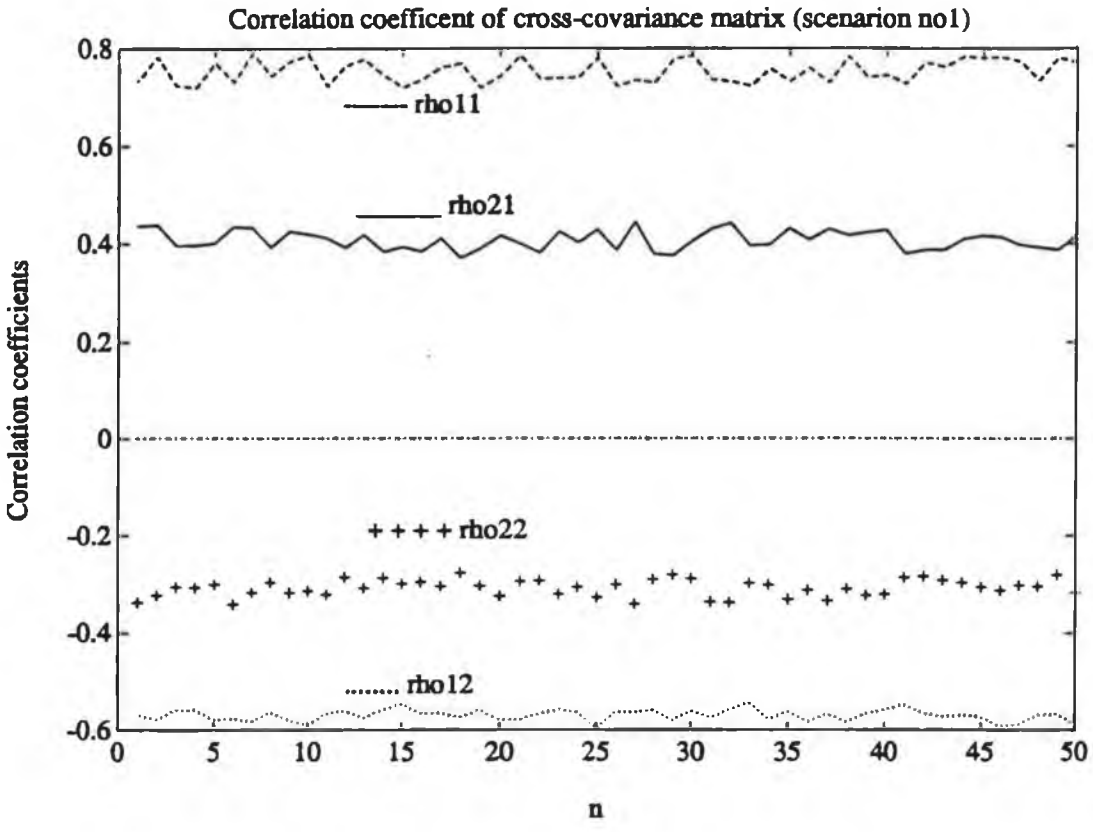

Figure (5.12)

---- rho11 = ρ_{x12x23} represents the correlation between the noisy measurements x_{12}, and the noisy measurement x_{23} in low-noise case in scenario no1.

.... rho12 = ρ_{x12y23} represents the correlation between the noisy measurements x_{12}, and the noisy measurements y_{23} in low-noise case in scenario no1.

____ rho21 = ρ_{y12x23} represents the correlation between the noisy measurements y_{12}, and the noisy measurements x_{23} in low-noise case in scenario no1.

++++ rho22 = ρ_{y12y23} represents the correlation between the noisy measurements y_{12}, and the noisy measurements y_{23} in low-noise case in scenario no1.

The next section discussion the simulation results for high-noise case in scenario no1.

5.4 Scenario no1, High-Noise Case

In this section we describe some simulation results for high-noise case.

The high-noise case has the same geometrical configuration as the low-noise case. The sensors have the same pdfs as the low-noise case. The differnce between the low-noise case and the high-noise case is in the measurement noise variances.

Each sensor calculates the true object angle-of-arrival. These are:

$$\theta_{1t} = 45° = 0.7854 \text{ radians}$$

$$\theta_{2t} = 71° = 1.25 \text{ radians}$$

$$\theta_{3t} = 126.87° = 2.2143 \text{ radians}$$

Noise pdfs in the three sensors S1, S2, and S3 are as follows:

$$\delta_u = 5 \text{ degrees} = 0.0873 \text{ radians}$$

$$\sigma_u = 2.88 \text{ degrees} = 0.0504 \text{ radians}$$

$$\delta_s = 4 \text{ degrees} = 0.0698 \text{ radians}$$

$$\sigma_s = 2.83 \text{ degrees} = 0.0494 \text{ radians}$$

$$\delta_t = 6 \text{ degrees} = 0.1047 \text{ radians}$$

$$\sigma_t = 2.45 \text{ degrees} = 0.0428 \text{ radians}$$

The same equations as used in the low-noise case are used to compute the standard deviations above.

As we see the standard deviation of the errors are larger than in the low-noise case.

5.4.1 Discussion of Simulation Results, Scenario no1, High-Noise Case

The computer simulation was run 50 times and the results are plotted and discussed in the next several pages.

Figure (5.13) shows the actual errors in the noisy measurements x_{12} from triangulation between sensors S1, and S2. The dotted line represents the actual error in the noisy measurements x_{12}, and the solid line represents the square root of $P_{z12}(1,1)$ in high-noise case in scenario no1 in x position. The solid line is the theoretical standard deviation of the errors according to the first-order approximation to the covariance matrix. The numeric mean value of the errors in the noisy measurements x_{12} in figure (5.13) is Mx12_err = - 0.0010. The numeric standard deviation is Sx12_err = 0.3505. This compares favourably with the theoretical standard deviation by the solid line in the figure. Comparing this figure with figure (5.3), we see that the errors are now much larger.

Figure (5.14) shows the actual errors in the noisy measurements x_{23} obtained by triangulation between sensors S2, and S3. The dotted line represents the actual errors in noisy measurements x_{23}, and the solid line represent the square root of $P_{z23}(1,1)$ in high-noise case in scenario no1. The solid line is the theoretical standard deviation of the errors according

to the covariance matrix. The numeric mean value of the errors in the noisy measurements x_{23} in figure (5.14) is Mx23_err = -0.0170. The numeric standard deviation is Sx23_err = 0.1378. This also compares favourably with the theoretical standard deviation given by the solid line in the figure.

Figure (5.16) shows the errors in the fused estimate obtained by fusion of the noisy measurements x_{12}, and x_{23}. The dotted line represents the errors in the fused estimate, and solid line represents the square root of $P_o(1,1)$. The numeric mean value of the errors in the fused estimate in figure (5.16) in x dimension is xfuse_err = -0.0343. The numeric standard deviation of the errors in the fused estimate is Sxfuse_err = 0.1583.

Figure (5.17) shows the actual errors in the noisy measurements y_{12} obtained by triangulation between sensors S1, and S2. The dotted line represents the actual errors in the noisy measurements y_{12}, and the solid line represents the square root of $P_{z12}(2,2)$, the theoretical standard deviation of the errors according to the first-order approximation to the covariance matrix. The numeric mean value of the errors in the figure is My12_err = 0.0188. The numeric standard deviation is Sy12_err = 0.7153.

Figure (5.18) shows the actual errors in the noisy measurements y_{23} from triangulation between sensors S2, and S3. The dotted line represents the actual errors in the noisy measurements y_{23}, and the solid line represents the square root of $P_{z23}(2,2)$, the theoretical standard deviation for the errors according to the first-order approximation to the covariance matrix. The mean value of the errors in the figure is My23_err = 0.0480. The numeric standard deviation is Sy23_err = 0.2682.

Figure (5.20) shows the errors in the fused estimate obtained by fusing the noisy measurements y_{12}, and y_{23}. The dotted line represents the errors in the fused estimate in y position, and the solid line reprsenents the square root of $P_o(2,2)$. The numeric mean value of the errors in the fused estimate in figure (5.20) is yfuse_err = -0.0186. The numeric standard deviation of the errors in the fused estimate is sxfuse_err = 0.2303.

The results of the simulations of scenario no1 for high-noise case are discussed in the next several pages.

Figure (5.13) shows the actual errors in the noisy measurements x_{12} (Mx12_err) and the numeric standard deviation of the errors in high-noise case in scenario no1 in x position.

We can see from figure (5.13) that the errors in the noisy measurements x_{12} have a magnitude bigger than the magnitude of the errors in the x_{12} noisy measurements in low-noise case figure (5.3). From figure (5.13) we see the errors change between negative and positive values and increase and decrease. Also we see the theoretical standard deviation increases and decreases in according with the magnitude of the errors. For example between n = 21, and n = 22 we see the magnitude of the errors increases from 0.6 to 0.8. We also note the theoretical standard deviation increases from 0.5 to 0.65. We also see the same thing between n = 33 and n = 34 the magnitude of the error decreases from 0.8 to 0.2. We also note the theoretical standard deviation decreases from 0.62 to 0.3. Between n = 37, and n = 43, we see the magnitude of the error increases and decreases, the theoretical standard deviation increases and decreases in a like manner. In general, the standard deviation tracks the magnitude of the errors.

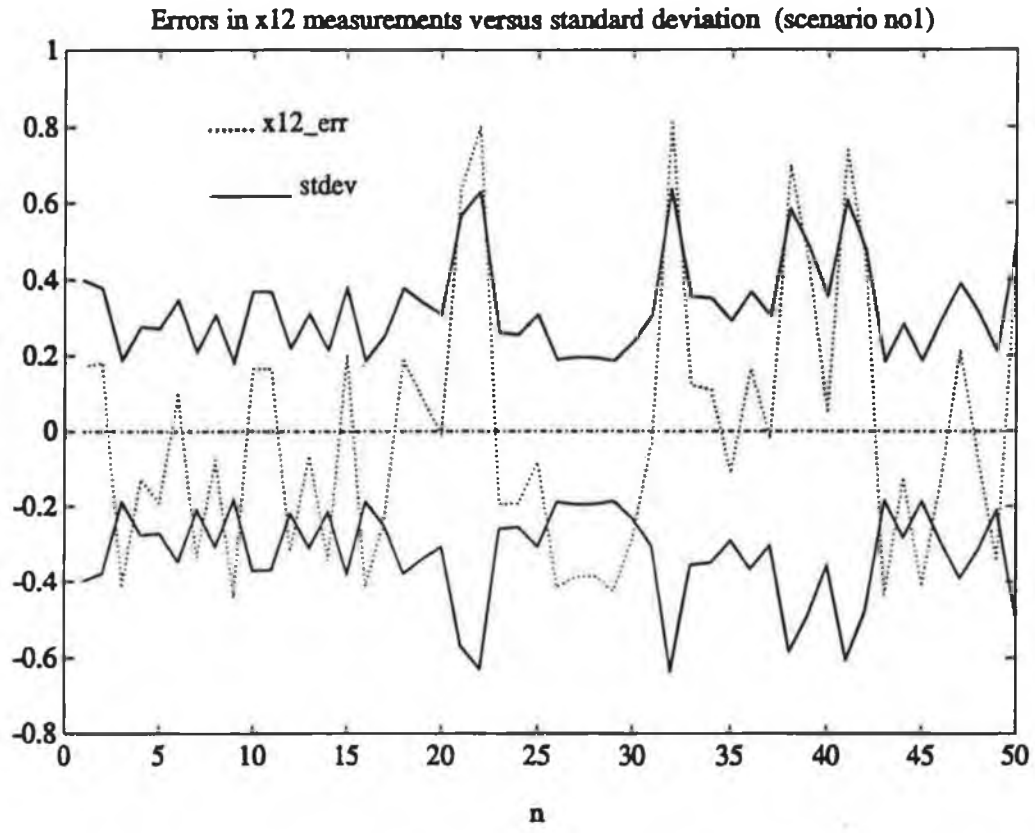

Figure (5.13)

....x12_err represents the actual errors in the noisy measurements x_{12} in scenario no1 high-noise case.

_____ stdev represents the square root of $P_{z12}(1,1)$, the theoratical standard deviation of the errors according to that first-order approximation to the covariance matrix.

Figure (5.14) shows the actual errors in the noisy measurements x_{23} and the the theoretical standard deviation of the errors in high-noise case in scenario no1 in x position.

We can see from the figure that x_{23} noisy measurements are higher quality measurements than the x_{12} noisy measurements because the standard deviation of the errors in x_{23} noisy measurements is smaller than the stndard deviation of the errors in x_{12} noisy measurements also, the actual errors seen to be smaller too. Also we can see from this figure the theoretical standard deviation tracks the magnitude of the errors and is close to the numeric one. We see from figure (5.14) the standard deviation is approximately constant for all values of n.

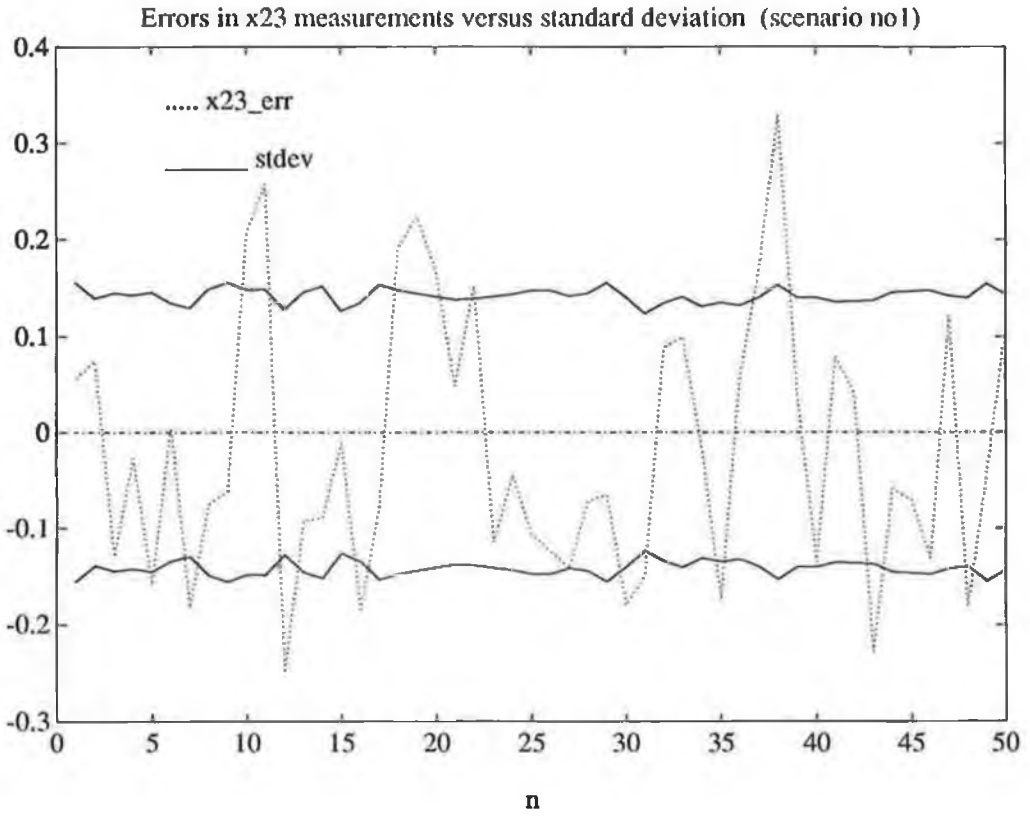

Figure (5.14)

..... x23_err represents the actual errors in the noisy measurements x_{23} in a high-noise case in scenario no1 in x position.

_____ stdev represents the square root of P_{z23} (1,1), the theoretical standard deviation of that the errors according to the first-order approximation to the covariance matrix in a high-noise case in scenario no1 in x position.

Figure (5.15) shows the percentage errors in the fused estimate in high-noise case in scenario no1 in x postion.

From the figure we can see the improvement offered by the fusion algorithm. It is, immediatly seen that the fused estimate (the solid line) clips the peak errors in the noisy measurements. For example at n = 21, we see the fused measurement clips the large error in the noisy measurement x_{12} and remains close to the higher accuracy noisy measurement x_{23}. We also observe the same effect at n = 32, 36, 37, 38 and 42 and several other places. As we noted before when the errors are of like sign, the fusion algorithm cannot in general produce an error which is less than the smaller one. In order to reduce the errors, the fusion algorithm relies on opposite sign errors to cancel each other out. With errors of the same sign, this cancellation is not generally possible. For example at n = 38 where the both of the errors in the noisy measurements x_{12}, and x_{23} are positive we see the fused measurement clips the large error which is in the noisy measurement x_{12}, and and remains close to the higher accuracy noisy measurement x_{23}. We see the same effect several times between n = 35 to n = 50.

But when the error in the x_{12}, and x_{23} are of opposite algebraic sign, the fusion algorithm produces a smaller error than the smallest measurement error. For example at n = 40 where the error in the x_{12} noisy

measurement is positive and the error in the noisy measurement x_{23} is negative, we see the error in the fused estimate is less than the smaller error individually. We also see the same effect at n = 33, and at n = 34.

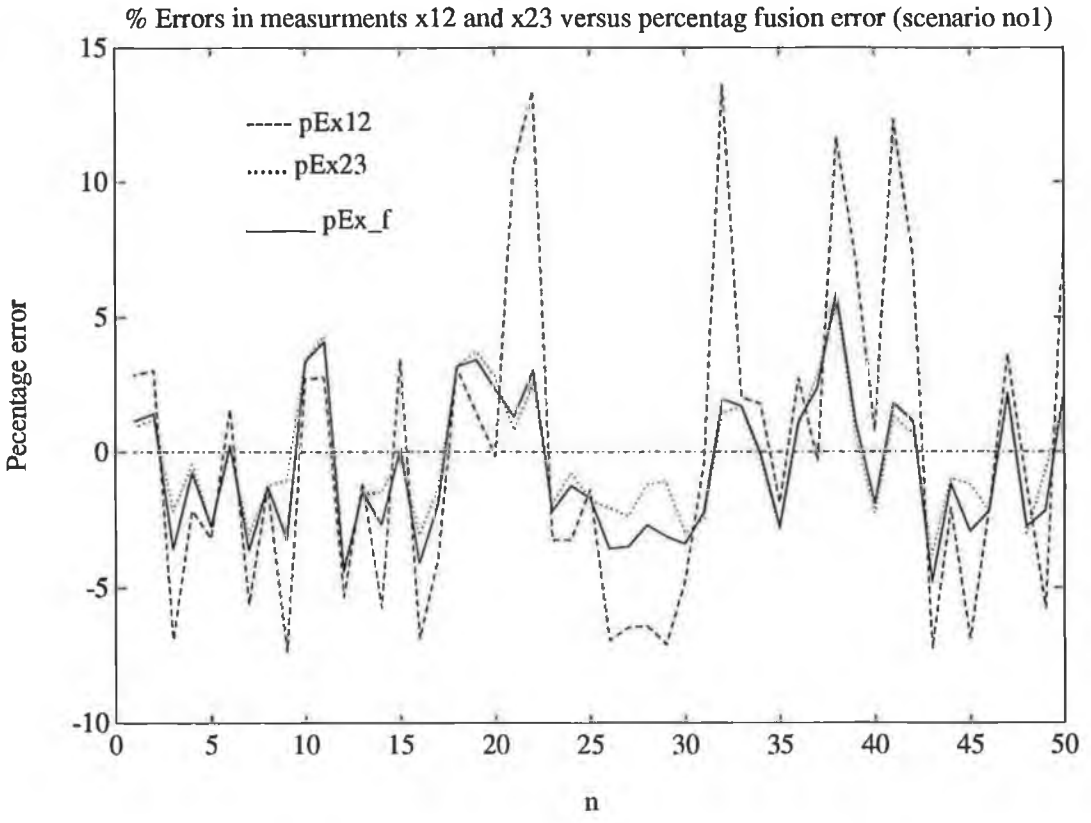

Fig (5.15)

---- (pEx12) represents the percentage error in the noisy measurements x_{12} in high-noise case in scenario no1 in x position.

.... (pEx23) represents the error in the noisy measurements x_{23} in high-noise case in scenario no1 in x position.

___ pEx_f represents the percentage error in the fused esimate in high-noise case in scenario no1 in x position.

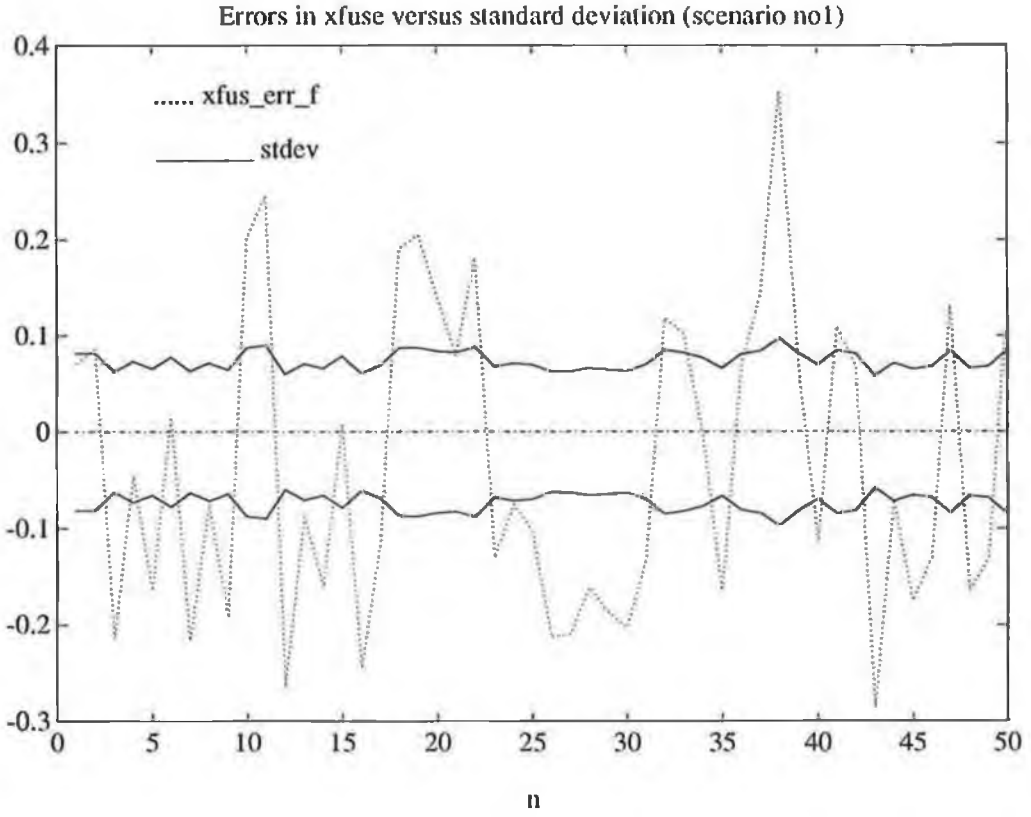

Figure (5.16)

..... xfuse_err represents the errors in fused estimate in high-noise case in scenario no1 in **x** position.

_____ stdev represents the square root of P_o (1,1), the standard deviation of the errors in the fused estimate in high-noise case in scenario no1 in **x** position.

Figure (5.17) shows the actual errors in the noisy measurements y_{12}, and the theoretical standard deviation of the errors in high-noise case in scenario no1 in y position.

We see from figure (5.17) between n = 20 and n = 21, the magnitude of the error increases from 0.5 to 1.45. We also note the theoretical standard deviation increases from 0.6 to 1.2.

In general we can see from figure (5.17) the theoretical standard deviation tracks the magnitude of the errors.

Figure (5.18) shows the actual errors in the noisy measurements y_{23} and the theoretical standard deviation of the errors in high-noise case in scenario no1 in y position.

We can see from figure (5.18) that y_{23} measurements are more accurate than y_{12} measurements. The standard deviation in figure (5.18) is approximately one-half that of figure (5.17) and the actual errors in both figures also show this trend.

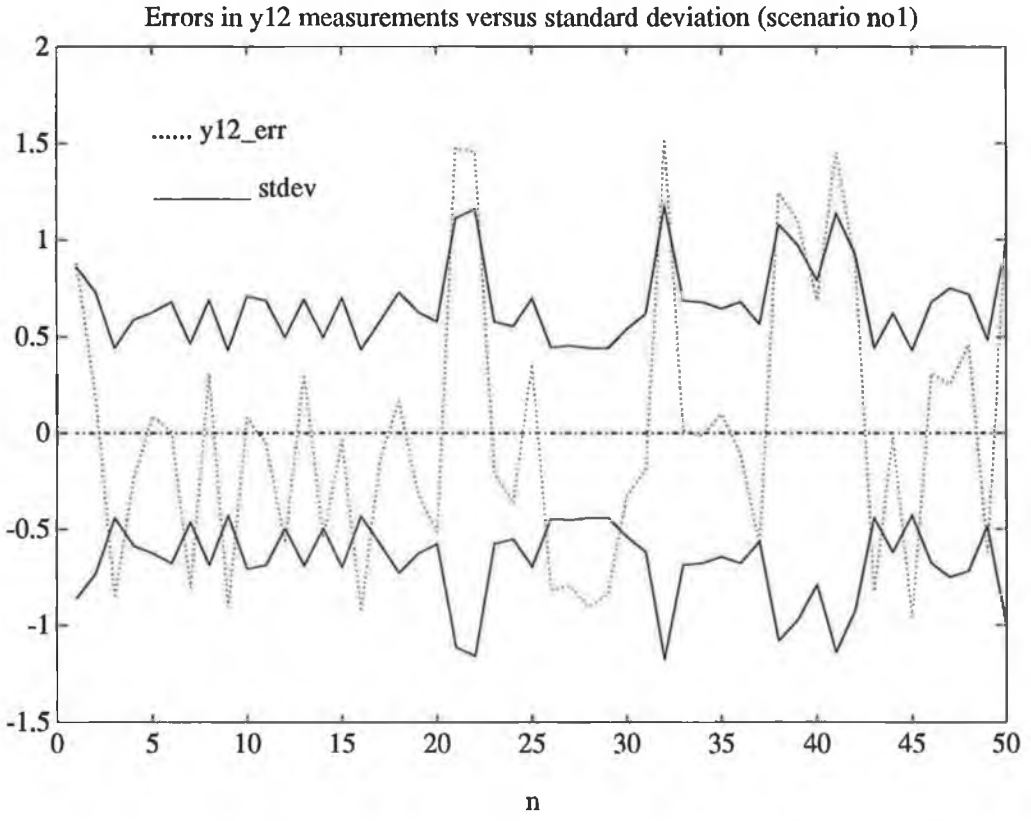

Figure (5.17)

.... y12_err represents the actual errors in the noisy measurements y_{12} in high-noise case in scenario no1 in y position.

____ stdev represents the square root of P_{z12} (2,2), the theoretical standard deviation of the errors according to that first-order approximation to the covarince matrix.

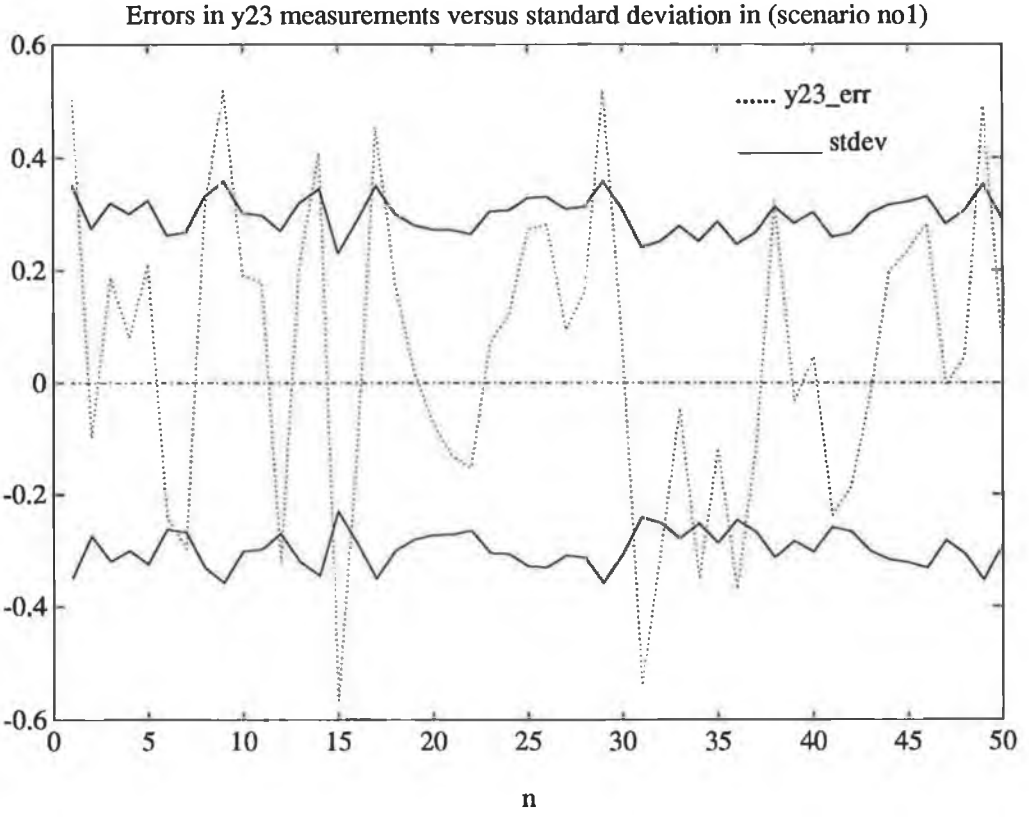

Figure (5.18)

..... y23_err represents the actual errors in the noisy measurements y_{23} in high-noise case in scenario no1 in y position.

_____ stdev represent the square root of $P_{z23}(2,2)$, the theoretical standard deviation of the errors according to the first-order approximation to the covariance matrix in high-noise case in scenario no1 in y position.

Figure (5.19) shows the percentage errors in the fused estimate in y position in high-noise case in scenario no1.

From figure (5.19) we can see the improvement offered by the fusion algorithm. The fused estimate clips the peak error in both noisy measurements y_{12}, and y_{23}. For example at n = 21, the error in the noisy measurements y_{12} is positive and large and in y_{23} is negative and small, we see that the error in the fused estimate is smaller than the smallest magnitude error which is in y_{23}. We see the same effect at n = 32. The error in y_{12} is positive and the error in y_{23} is negative. We see the error in the fused estimate is smaller than the smallest magnitude error which is the error in y_{23}. We observe the same effect at n = 3, 7, 9, 12, 17, 18, 19, and between n = 39 to n = 46. In there cases the errors in y_{12}, and y_{23} are of opposite algebraic signs and the fusion algorithm produces an error which is smaller than the smallest one. But we see when the errors in the noisy measurements y_{12}, and y_{23} are of the same algebraic sign, the fused error is not less than the smallest measurement error. Instead, it clips the peak error and remains close to the smaller one. For example at n = 38, both the errors in y_{12}, and y_{23} are positive; we see the fused estimate is close to y_{23}. We observe the same effect at n = 47, and n = 48.

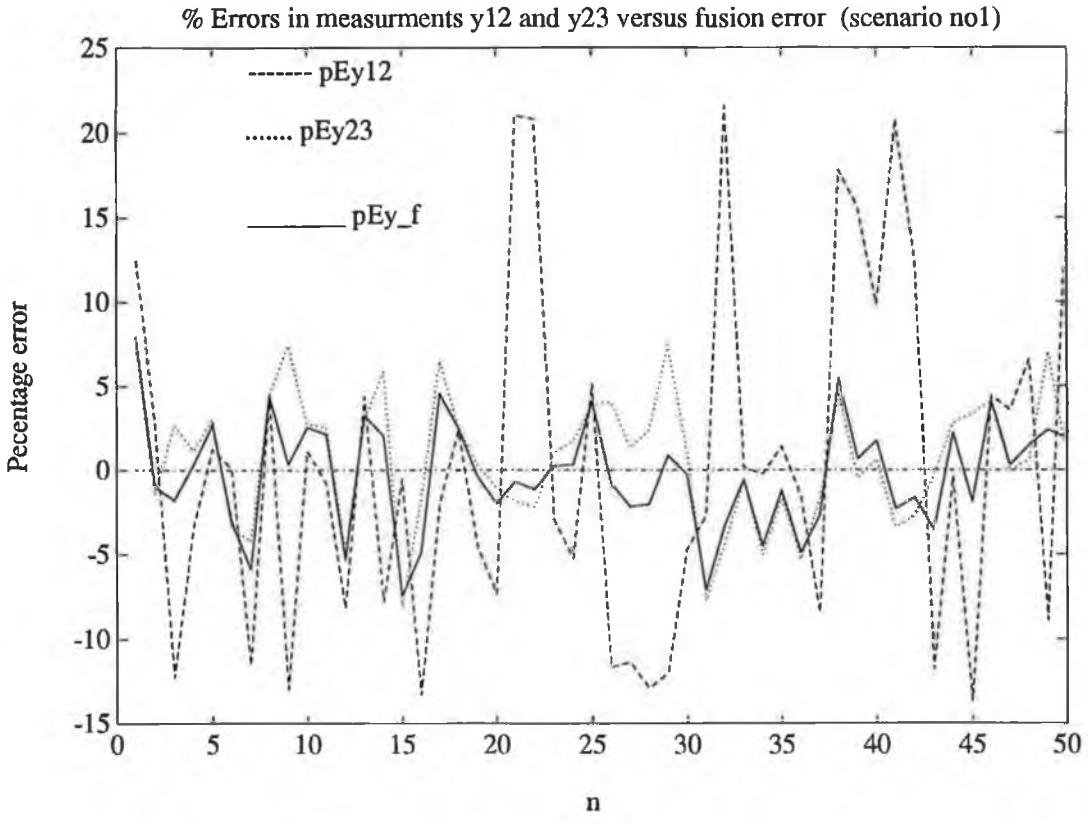

Fig (5.19)

----- (pEy12) represents the percentage error in the noisy measurement y_{12} in high-noise case in scenario no1 in y position.

..... (pEy23) represents the percentage error in the noisy measurement y_{23} in high-noise case in scenario no1 in y position.

_____ (pEy_f) represents the percentage error in the fused estimate in high-noise case in scenario no1 in y position.

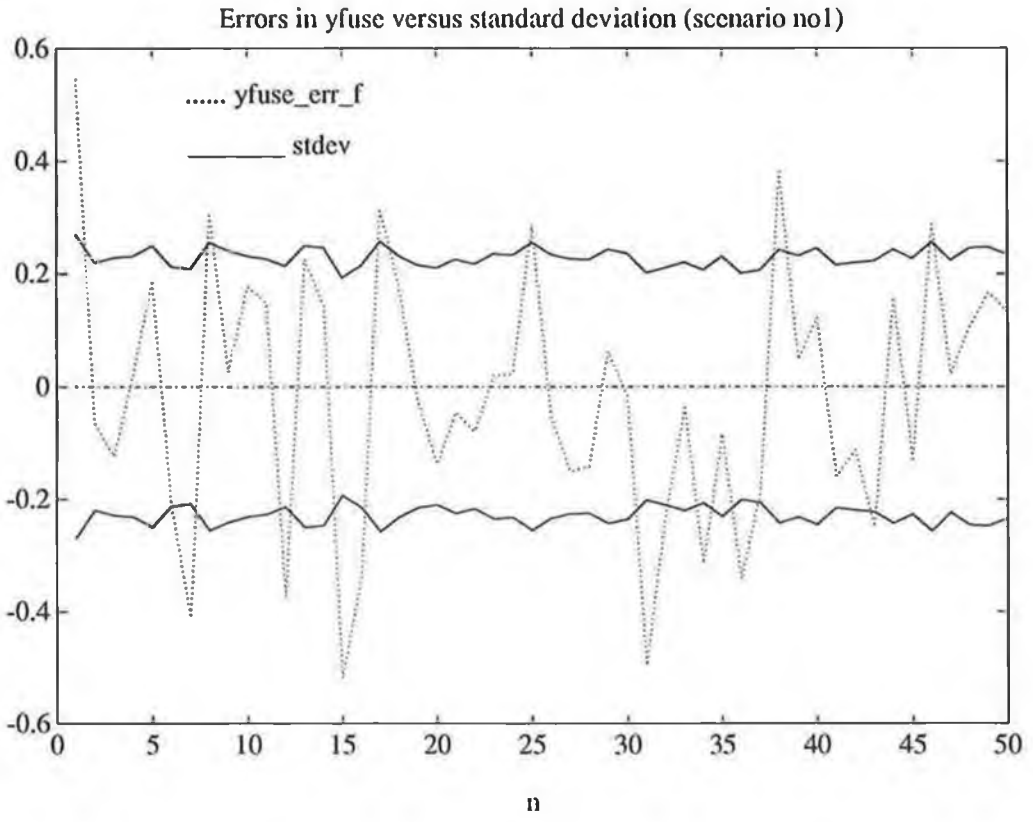

Figure (5.20)

.... yfuse_err_f represents the errors in the fused estimate in high-noise case in scenario no1 in y position.

_____ stdev reprents the square root of $P_o(2,2)$, the theoretical standard deviation of the errors in the fused estimate in high-noise case in scenario no1 in y position.

5.4.1.1 Trace of Covariance Matrices

Figure (5.21) shows the trace of the error covariance matrices in high-noise case in scenario no1.

From figure (5.21) we can see that the trace of the optimum error covariance matrix is less than the trace of the individual error covariance matrices P_{z12}, and P_{z23}. This is the criterion of the fusion algorithm to produce the optimum covariance matrix having a trace which is less than the trace of the individual error covariance matrices.

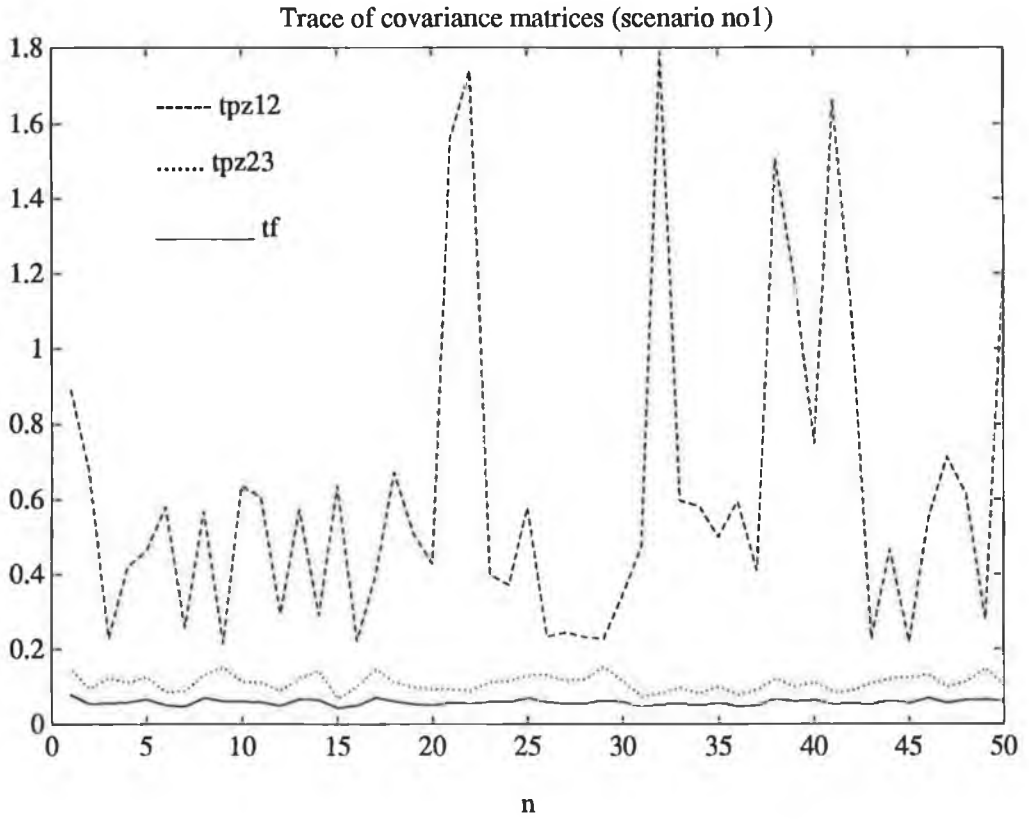

Figure (5.21)

---- tpz12 represents the trace of the error covariance matrix between sensor S1, and sensor S2 in high-noise case in scenario no1.

.... tpz23 represents the trace of the error covariance matrix between sensor S2, and sensor S3 in high-noise case in scenario no1.

____ tf represents the trace of the optimum error covariance matrix in high-noise case in scenario no1.

Figure (5.22) shows the correlation coefficent elements for the cross-covariance matrix p_{z1223}.
From figure (5.22) we see all the correlation coefficents have magnitude less than one. The figure also shows that there is a strong correlation between the components of the two vectors z_{12}, and z_{23}

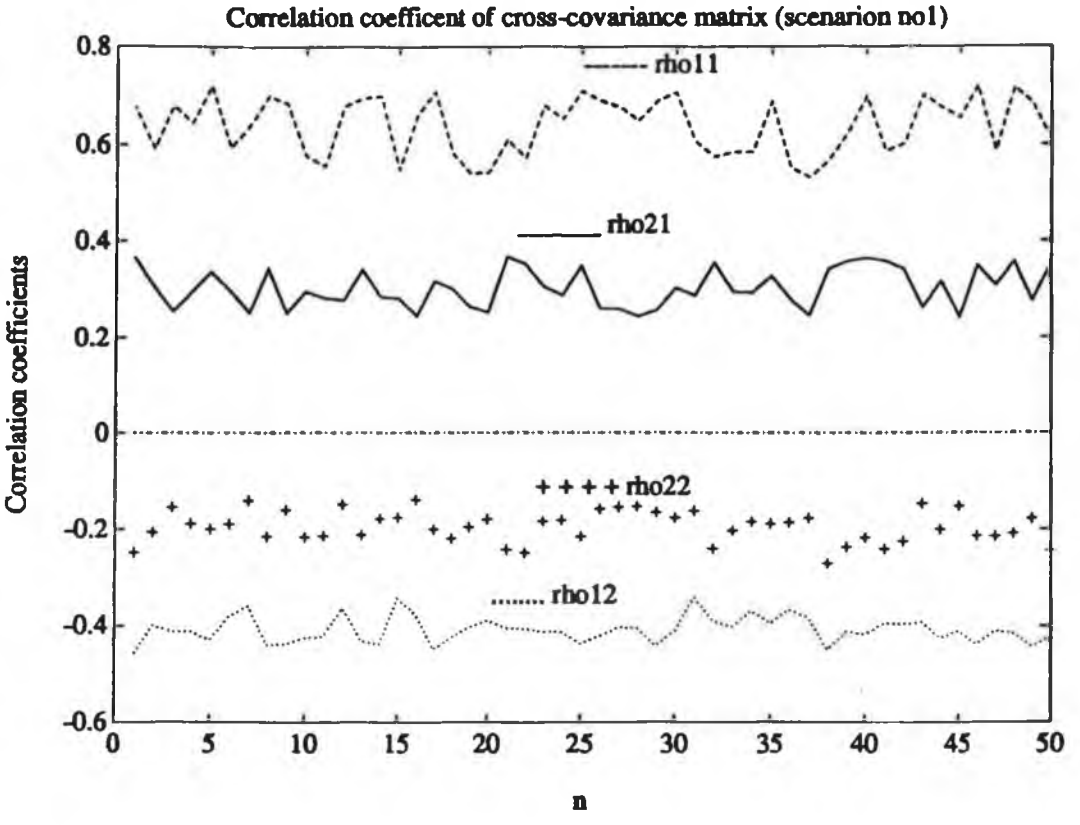

Figure (5.22)

--- rho11 = ρ_{x1223} represents the correlation between the noisy measurements x_{12} and the noisy measurements x_{23} in high-noise case in scenario no1.

... rho12 = ρ_{x12y23} represents the correlation between the noisy measurements x_{12}, and the noisy measurements y_{23} in high-noise case in scenario no1.

____ rho21 = ρ_{y12x23} represents the correlation between the noisy measurements y_{12}, and the noisy measurements x_{23} in high-noise case in scenario no1.

+ + rho22 = ρ_{y12y23} represents the correlation between the noisy measurements y_{12}, and the noisy measurements y_{23} in high-noise case in scenario no1.

The next section discusses scenario no2 which is less favourable for triangulation.

5.5 Scenario Number 2 (no2), Low-Noise Case

Figure (5.23) shows the configuration of the object and sensors for scenario no2 in two dimensions.

--- represents the noisy angle-of-arrival measurements data.

___ represents the true angle value.

Scenario no2 was chosen to give very slant angles for θ_{1t}, θ_{2t}, and θ_{3t}. This tests the fusion algorithm in a situation when even small errors in angle-of-arrival measurements can cause large measurement errors in the object position.

As we see from figure (5.23) the sensors have the same pdfs as in scenario no1. The values used in scenario no2 in the low-noise simulation are:

object true position p ($x = 8$, $y = 7$)

S1 location ($x_1 = 2$, $y_1 = 4$)

S2 location ($x_2 = 4$, $y_2 = 3$) and

S3 location ($x_3 = 5$, $y_3 = 3$)

Each sensor calculates the true object angle-of-arrival. These are:

$\theta_{1t} = 26.56° = 0.4636$ radians

$\theta_{2t} = 44.99° = 0.7854$ radians

$\theta_{3t} = 53.12° = 0.9273$ radians

Noise pdfs in three sensors S1, S2, and S3 in scenario no2 low-noise case are the same as in the scenario no1 low-noise case these are:

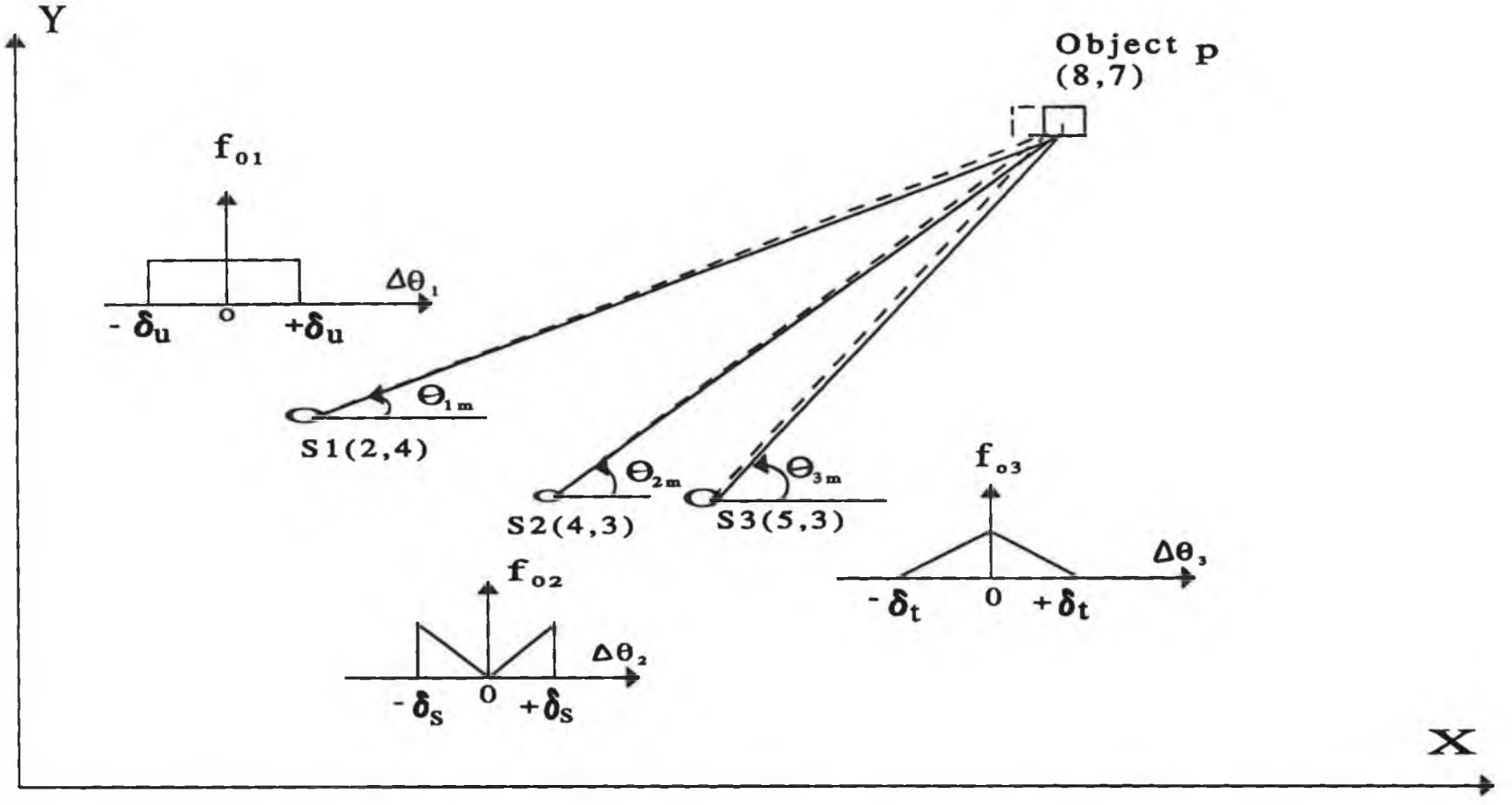

Figure (5.23) Geometrical configuration of object and sensors for scenario no2.

δ_u = 2 degrees = 0.0349 radians

σ_u = 1.15 degrees = 0.0202 radians

δ_s = 2 degrees = 0.0349 radians

σ_s = 1.41 degrees = 0.0247 radians

δ_t = 2 degrees = 0.0349 radians

σ_s = 0.8193 degrees = 0.0143 radians

The same equations as used in scenario no1 are used to compute the standard deviations above.

As we see, δ_s, and δ_t are individually one quarter of the difference in the slant angles between sensors S2 and S3.

5.5.1 Discussion of Simulation Results, Scenario no2, Low-Noise Case

The computer simulation was run 50 times and the results are plotted and discussed in the next pages.

Figure (5.24) shows the actual errors in the noisy measurements x_{12} from triangulation between sensors S1, and S2. The dotted line represents the actual error in the noisy measurements x_{12}, and the solid line represents the square root of $P_{z12}(1,1)$ in scenario no2 low-noise case in x position. The solid line is the theoretical standard deviation of the errors according to the first-order approximation to the covariance matrix. The numeric mean value of the errors in the noisy measurements x_{12} in figure (5.24) in x dimensional is Mx12_err = 0.0284. The numeric

standard deviation is Sx12_err = 0.4581.

Figure (5.25) shows the actual errors in the noisy measurements x_{23} obtained by triangulation between sensors S2, and S3. The dotted line represents the actual errors in the noisy measurements x_{23}, and the solid line represents the square root of $P_{z23}(1,1)$. The solid line is the theoretical standard deviation of the errors according to the first-order approximation to the covariance matrix. The numeric mean value of the errors in the noisy measurements x_{23} in figure (5.25) is Mx23_err = 0.1791. The numeric standard deviation Sx23_err = 0.7075.

Figure (5.27) shows the errors in the fused estimate obtained by fusion of the noisy measurements x_{12}, and x_{23}. The dotted line represents the errors in the fused, and the solid line represents the square root of $P_o(1,1)$. The numeric mean value of the errors in the fused estimate in figure (5.27) in x dimension is Mxfuse_err = -0.1230. The numeric standard deviation of the errors is Sxfuse_err = 0.2589.

Figure (5.28) shows the actual errors in the noisy measurements y_{12} obtained by triangulation between sensors S1, and S2. The dotted line represents the actual errors in the noisy measurements y_{12}, and the solid line represents the square root of $P_{z12}(2,2)$, the

theoretical standard deviation of the errors according to the covariance matrix. The numeric mean value of the errors in the figure is My12_err = 0.0263. The numeric standard deviation is Sy12_err = 0.3334.

Figure (5.29) shows the actual errors in the noisy measurements y_{23} obtained by triangulation between sensors S2, and S3. The dotted line represents the actual errors in the noisy measurements y_{23}, and the solid line represents the square root of $P_{z23}(2,2)$, the theoretical standard deviation of the errors according to the covariance matrix. The mean value of the errors in the figure is My23_err = 0.2220. The numeric standard deviation is Sy23_err = 0.8934.

Figure (5.31) shows the errors in the fused estimate obtained by the fusion of the noisy measurements y_{12}, and y_{23}. The dotted line represents the errors in the fused estimate, and the solid line represents the square root of $P_o(2,2)$. The numeric mean value of the errors in the fused estimate in the figure is Myfuse_err = 0.1093. The numeric standard deviation of the errors is Syfuse_err = 0.3198.

The results of the simulations of scenario no2 for low-noise case are discussed in the next several pages.

Figure (5.24) shows the actual errors in the noisy measurements x_{12} (Mx12_err) and the theoretical standard deviation of the errors in scenario no2 in low-noise case in x position.

We can see from the figure that the errors in the noisy measurements x12 in scenario no2 are larger than the errors in the noisy measurements x_{12} in scenario no1. In general we see the theoretical standard deviation tracks the magnitude of the errors.

Figure (5.25) shows the actual errors in the noisy measurements x_{23}, and the theoretical standard deviation of the errors in low-noise case in scenario no2 in x position.

We can see from the figure that the noisy measurements x_{23} are less accuracte than the noisy measurements x_{12} because the errors and that the standard deviation of the x_{23} noisy measurements are bigger than the errors and the standard deviation of the noisy measurements x_{12}. We see from the figure that the standard deviation tracks the magnitude of the errors.

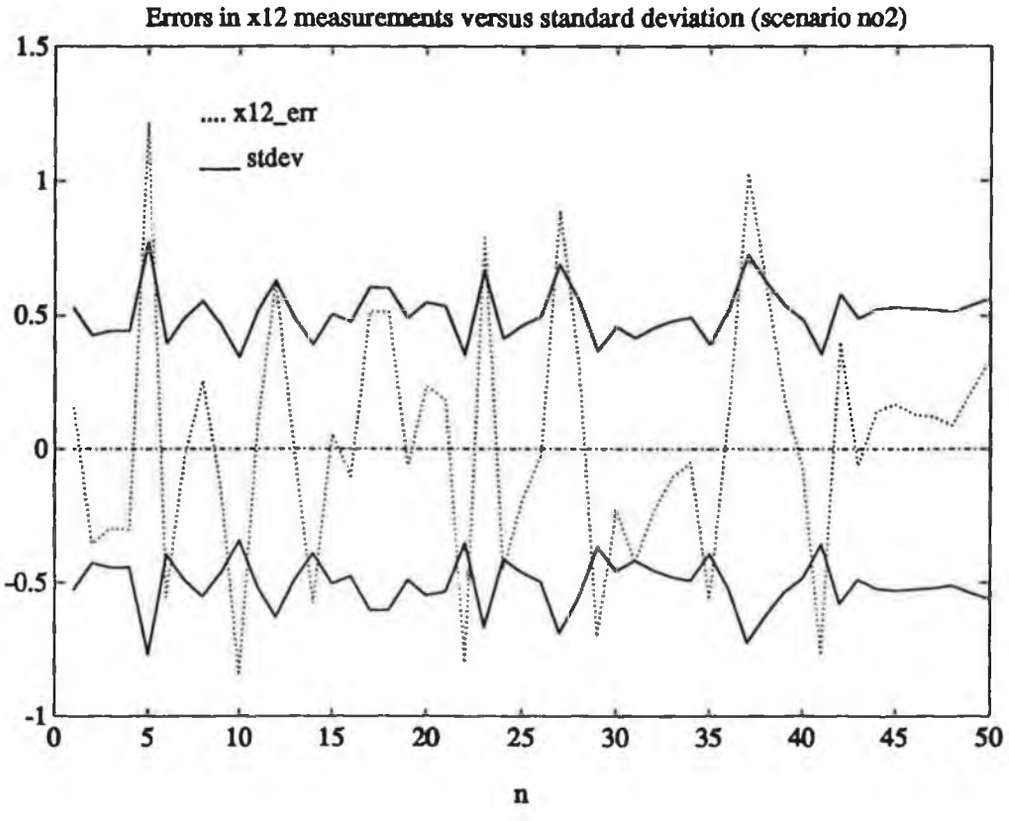

Figure (5.24)

.... x12_err represents the actual errors in the noisy measurements x12 in low-noise case in scenario no2 in x position.

____ stdev represents the square root of $P_{z12}(1,1)$, the theoretical standard deviation of the errors according to the first-order approximation to the covariance.

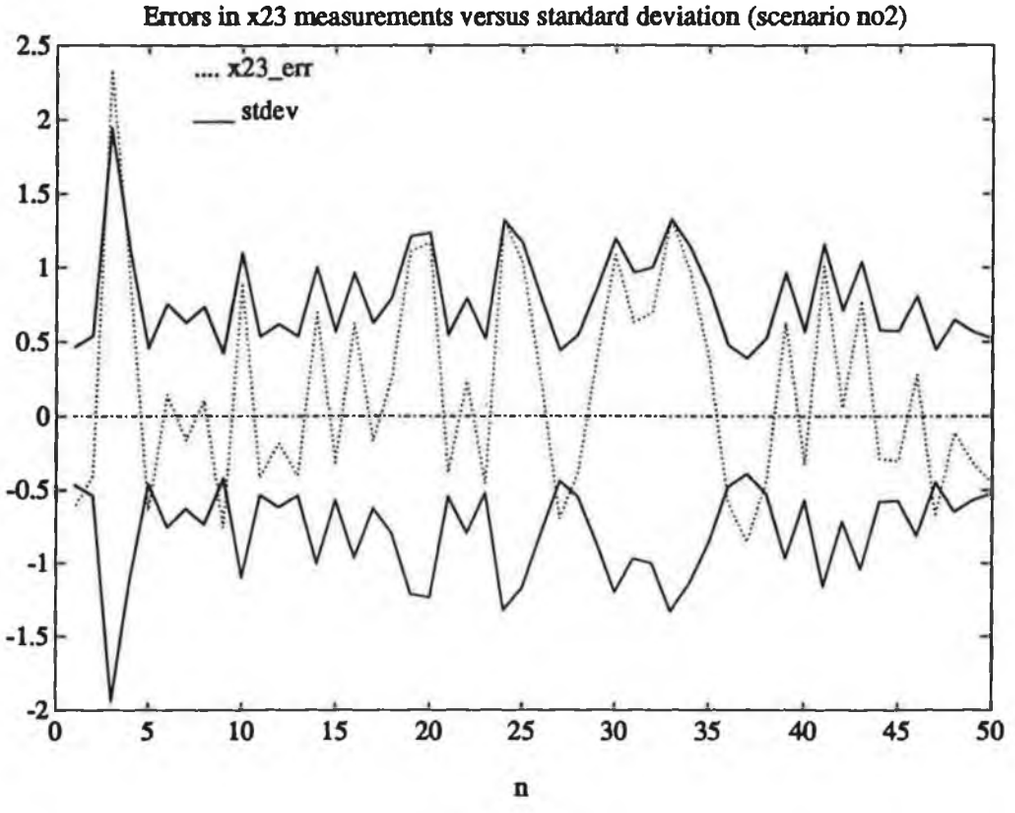

Figure (5.25)

.... x23_err represents the actual errors in the noisy measurements x_{23} in low-noise case in scenario no2.

____ stdev represents the square root of $P_{z12}(2,2)$, the theoretical standard deviation of the errors according to the first-order approximation to the covariance matrix.

Figure (5.26) shows the percentage errors in the fused estimate in low-noise case in scenario no2 in x position.

We observe from the figure that the fused estimate (solid line) clips the peak errors in the measurements. We see the fused estimate clips the large errors in the noisy measurements x_{23}, and remains close to the higher accuracy noisy measurements x_{12} when the errors in the two noisy measurements x_{12}, and x_{23} are the of same algebraic sign. For example at n = 18, both the errors in the noisy measurements x_{12}, and x_{23} are positive; we see the fused estimate is close to x_{12}. We observe the same effect at n = 21, 43, and n = 46. But when the errors in the noisy measurements x_{12}, and x_{23} are of opposite algebraic signs, the fusion algorithm produces a smaller error than the smallest measurement error. For example at n = 3 , the error in the noisy measurements x_{12} is negative and small and in the noisy measurements x_{23} is positive and large, we see that the error in the fused estimate is smaller than the smallest magnitude error which is in x_{12}. We see the same effect at n = 4, 6, 10, 12, 24, 25, and many cases between n = 27, and n = 50.

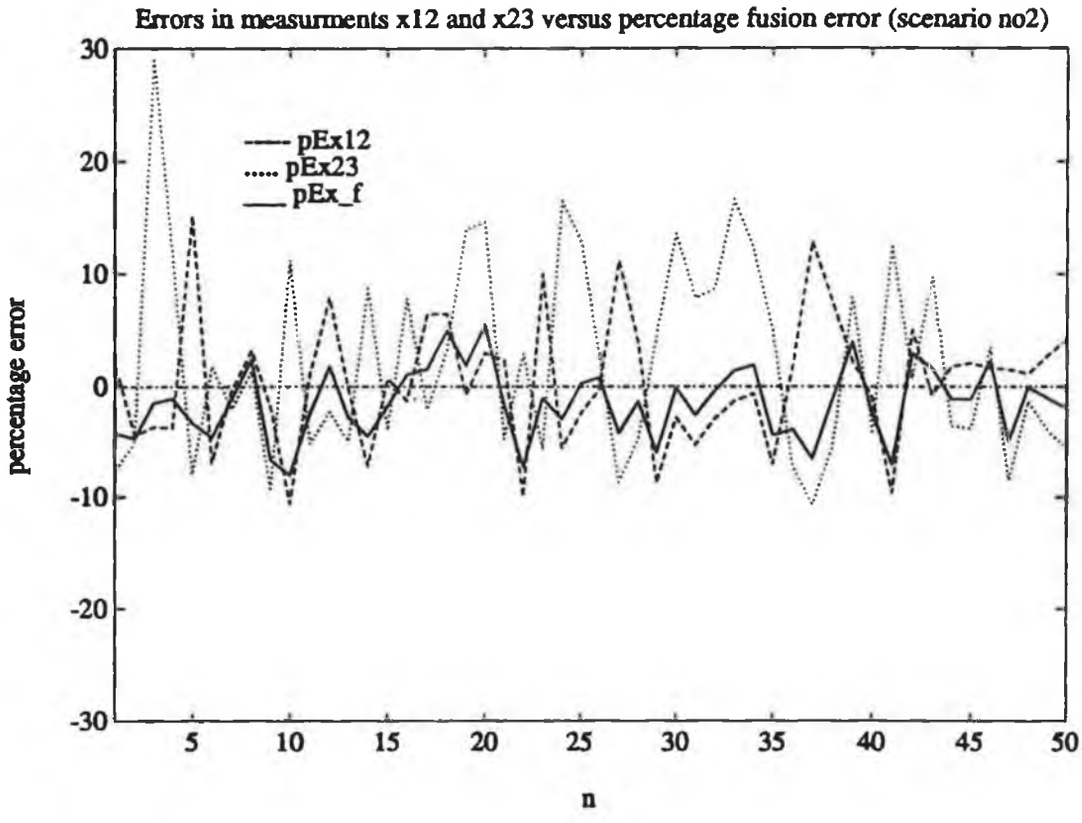

Figure (5.26)

--- pEx12 represents the percentage error in the noisy measurements x_{12} in low-noise case in scenario no2 in x position.

.... pEx23 represents the percentage error in the noisy measurements x_{23} in low-noise case in scenario no2 in x position.

____ pEx_f represent the percentage error in the fused estimate in low-noise case in scenario no2 in x position.

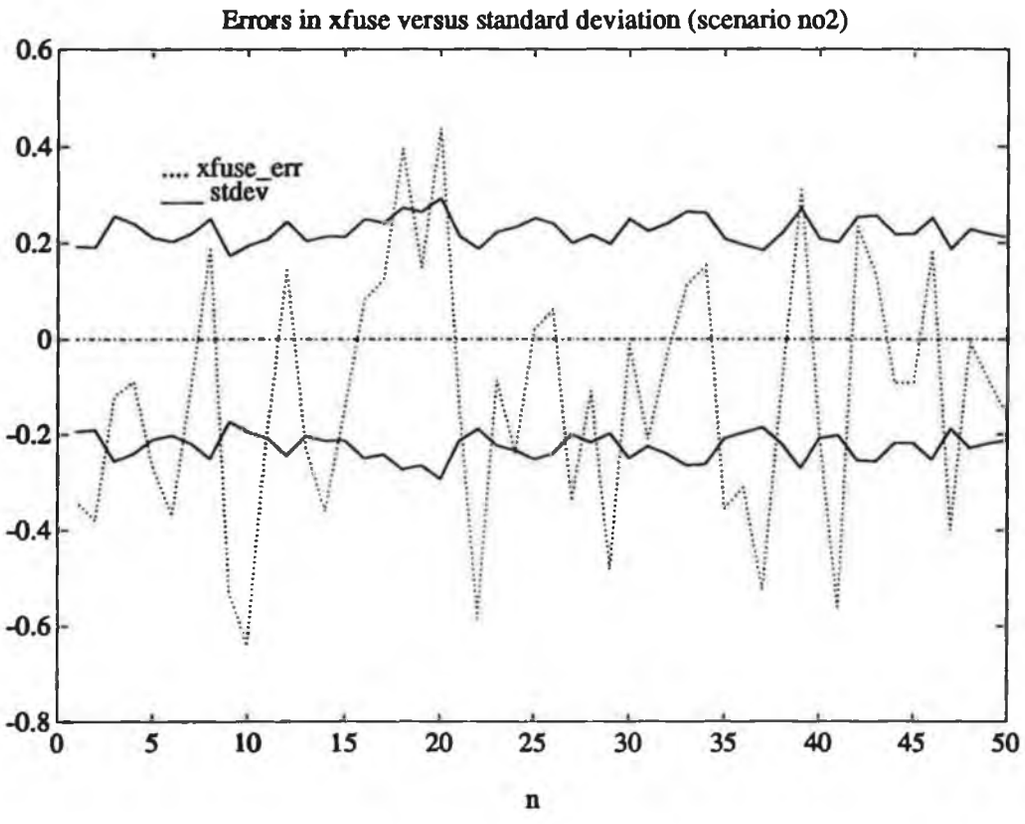

Figure (5.27)

.... xfuse_err_f represents the errors in the fused estimate in low-noise case in scenario no2 in x position.

____ represents the square root of $P_o(1,1)$, the theoretical standard deviation of the errors in the fused estimate in low-noise case in scenario no2 in x position.

Figure (5.28) shows the actual errors in the noisy measurements y_{12} and the theoretical standard deviation of the errors in low-noise case in scenario no2 .

In general, we see from the figure the theoretical standard deviation tracks the magnitude of the errors.

Figure (5.29) shows the actual errors in the noisy measurements y_{23} and the theoretical standard deviation of the errors in low-noise case in scenario no2.

We can see from the figure the noisy measurements y_{23} are less accurate than the noisy measurements y_{12} because the errors in the noisy measurements y_{12} are less than the errors in the noisy measurements y_{23}, also the standard deviation of the errors in y_{12} is less than the standard deviation of the errors in y_{23}. We see the standard deviation in the figure tracks the magnitude of the errors.

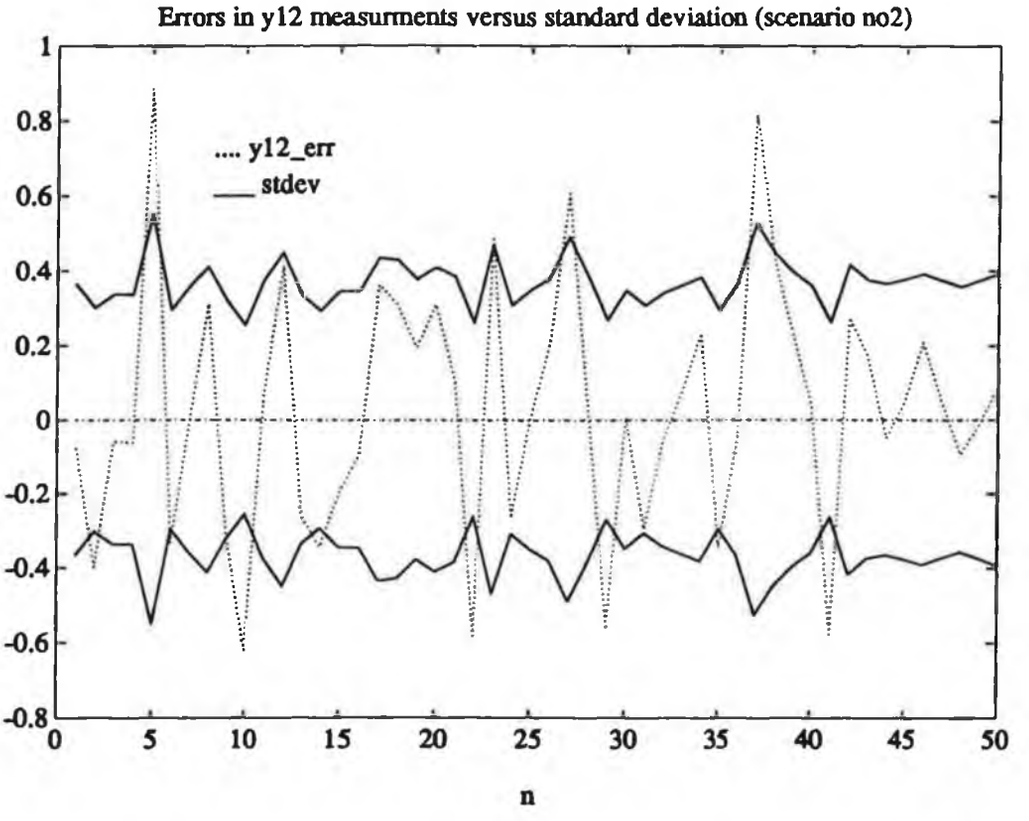

Figure (5.28)

.... y12_err represents the actual errors in the noisy measurements y_{12} in low-noise case in scenario no2 in y position.

_____ stdev represent the square root of $P_{z12}(2,2)$, the theoretical standard deviation of the errors according to the first-order approximation to the covariance matrix.

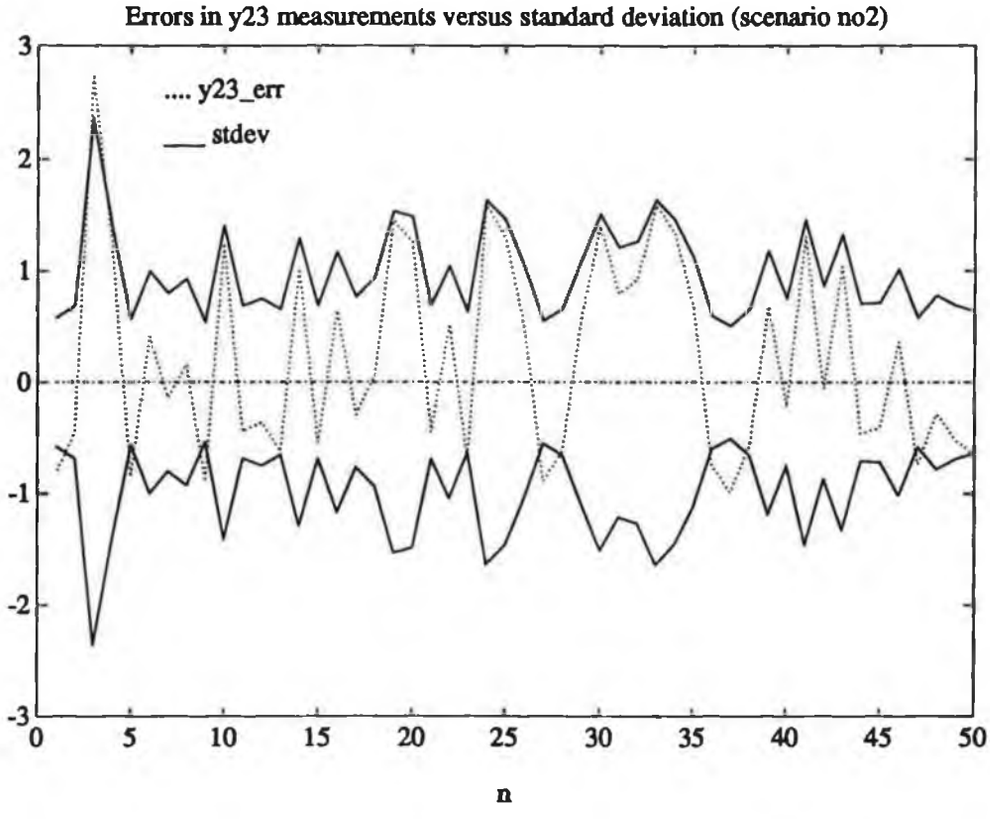

Figure (5.29)

.... y23_err represents the actual errors in the noisy measurements y_{23} in low-noise case in scenario no2.

____ stdev represents the square root of $P_{z23}(2,2)$, the theoretical standard deviation of the errors according to the first-order approximation to the covariance matrix.

Figure (5.30) shows the percentage errors in the fused estimate in y position in low-noise case in scenario no2 in y position.

From the figure we see when the errors in the noisy measurements y_{12}, and y_{23} are of opposite algebraic signs the fused estimate clips the peak error in both noisy measurements y_{12}, and y_{23} and the fused error is smaller than the smallest one. For example at n = 3, the error in the noisy measurements y_{23} is positive and large and in y_{12} is negative and small, we see that the error in the fused estimate is smaller than the smallest magnitude error which is in y_{12}. We see the same effect at n = 4, 5, 10, 12, 14, 17, 24, and in many cases between n = 27 and n = 50. But we see when the errors in the noisy measurements y_{12}, and y_{23} are of the same algebraic sign, the error in the fused estimate is not less than the smallest measurement error. Instead, it clips the peak error and remains close to the smaller one. For example at n = 33, both the errors in the noisy measurements y_{12}, and y_{23} are positive; we see the fused estimate is close to y_{12}. We see the same effect at n = 34 and n = 46.

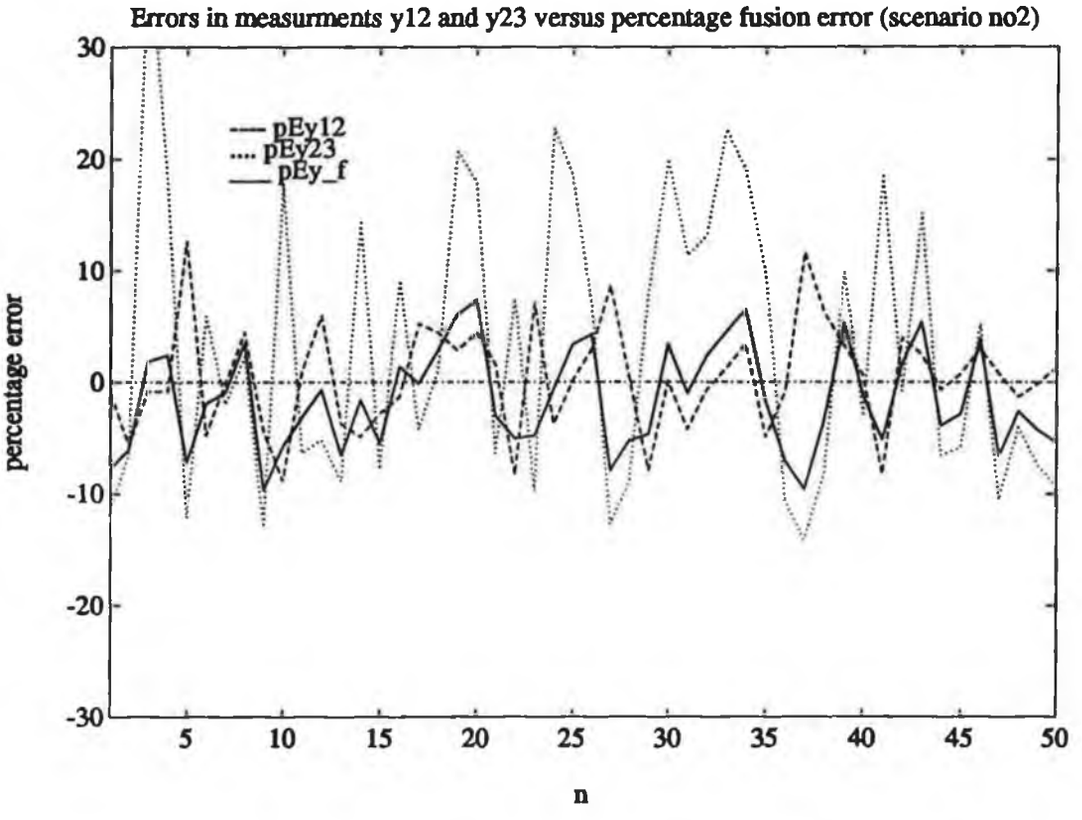

Figure (5.30)

---- pEy12 represents the percentage error in the noisy measurements y_{12} in low-noise case in scenario no2 in y position.

.... pEy23 represents the percentage error in the noisy measurements y_{23} in low-noise case in scenario no2 in y position.

_____ pEy_f represents the percentage error in the fused estimate in low-noise case in scenario no2 in y position.

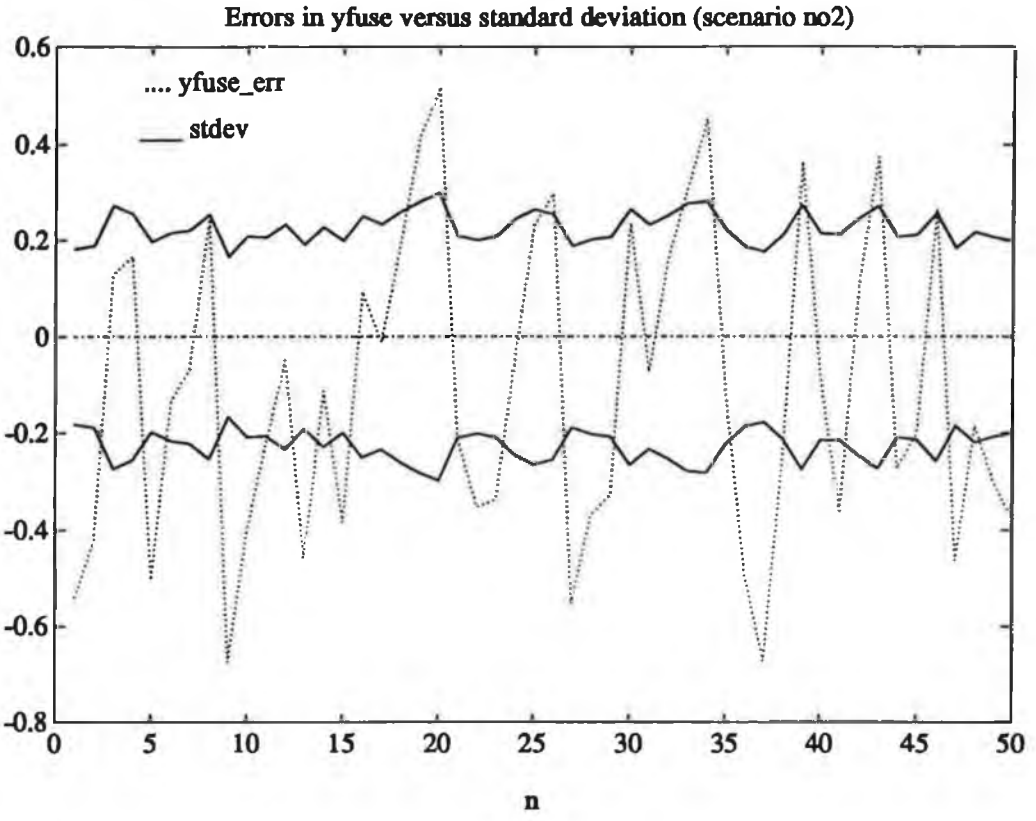

Figure (5.31)

.... xfuse_err represents the errors in the fused estimate in low-noise case in scenario no2 in y position.

____ stdev represents the square root of $P_o(2,2)$, the theoretical standard deviation of the errors in the fused estimate in low-noise case in scenario no2 in y position.

5.5.1.1 Trace of Covariance Matrices

Figure (5.32) shows the trace of the error covariance matrices in low-noise case in scenario no2.

From the figure we see that the trace of the optimum error covariance matrix is less than the trace of the individual error covariance matrices P_{z12}, and P_{z23}.

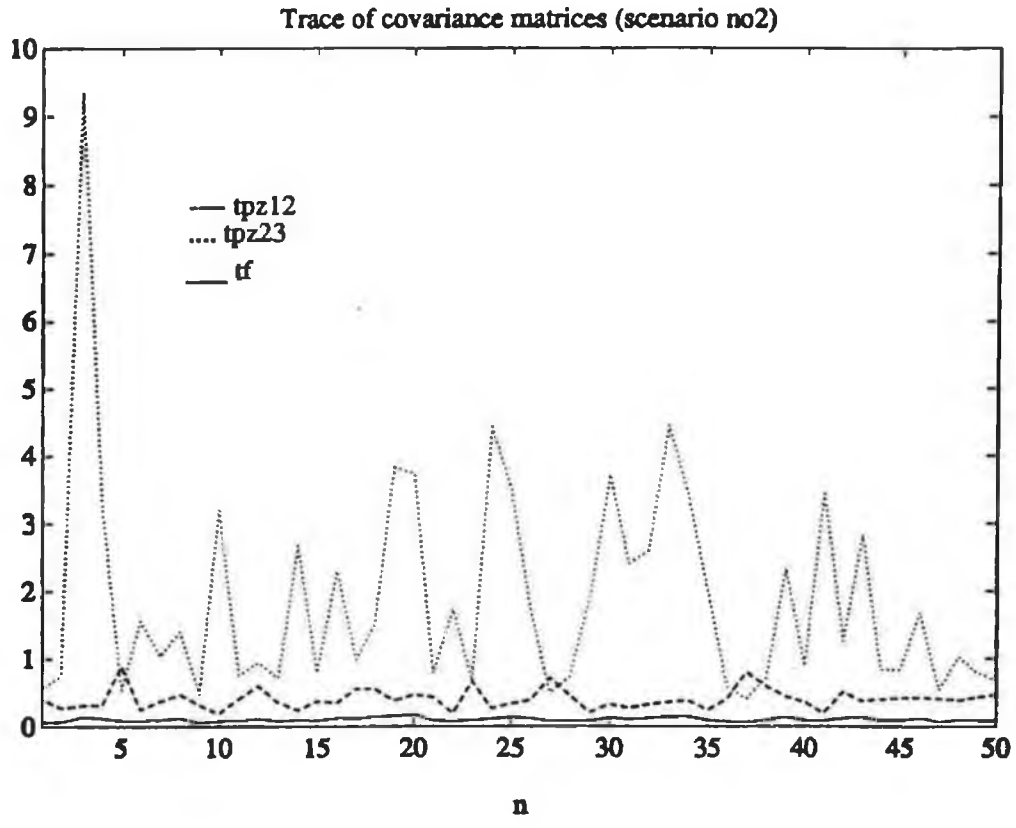

Figure (5.32)

---- tpz12 represents the trace of the error covariance matrix between sensor S1, and sensor S2 in low-noise case in scenario no2.

.... tpz23 represents the trace of the error covariance matrix between sensor S2, and sensor S3 in low-noise case in scenario no2.

____ tf represents the trace of the optimum error covariance matrix in low-noise case in scenario no2.

Figure (5.33) shows the correlation coefficient elements for the cross-covariance matrix p_{z1223} in low-noise in scenario no2.

From the figure we see all the correlation coefficients have magnitude less than one. The figure also shows that there is a strong correlation between the components of the two vectors z_{12}, and z_{23}.

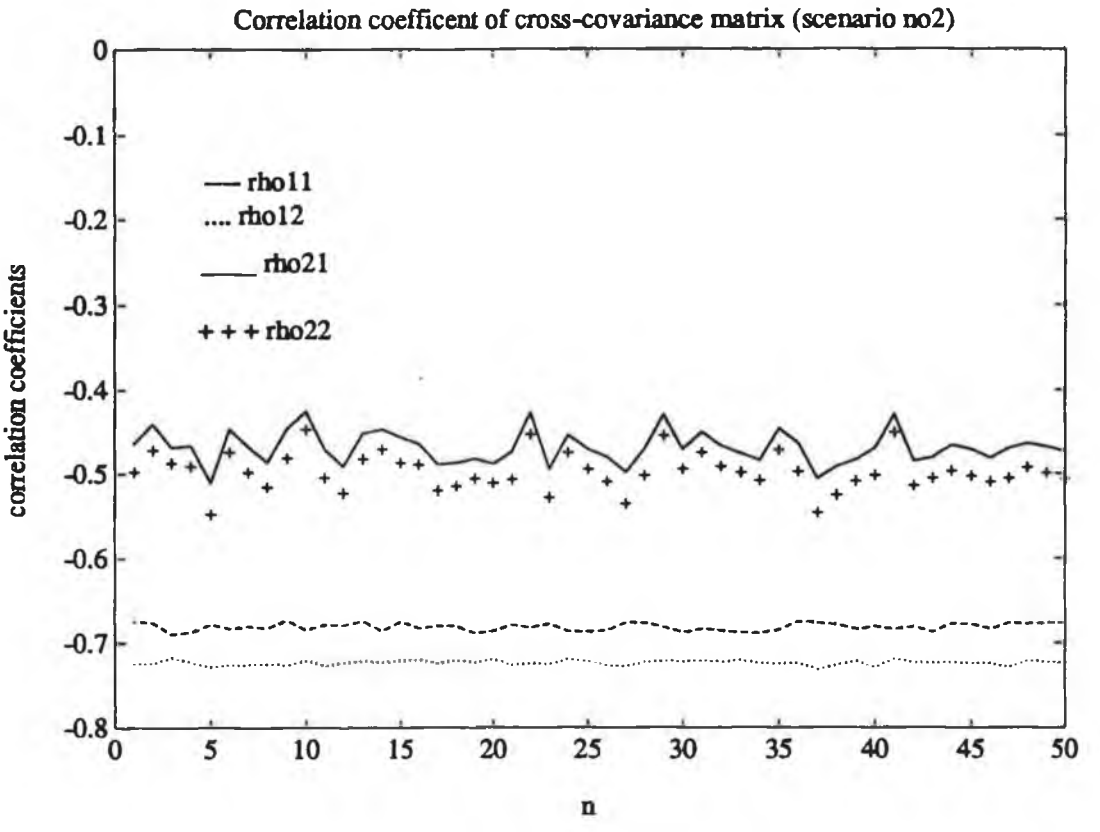

Figure (5.33)

---- rho11 = ρ_{x12x23} represents the correlation between the noisy measurements x_{12}, and the noisy measurements x_{23} in low-noise case in scenario no2.

.... rho12 = ρ_{x12y23} represents the correlation between noisy measurements x_{12}, and the noisy measurements y_{23} in low-noise case in scenario no2.

____ rho21 = ρ_{y12x23} represents the correlation between the noisy measurements y_{12}, and the noisy measurements x_{23} in low-noise case in scenario no2.

++++ rho22 = ρ_{y12y23} represents the correlation between the noisy measurements y_{12}, and the noisy measurements y_{23} in low-noise case in scenario no2.

The next section discusses the simulation results for high-noise case in scenario no2.

5.6 Scenario no2, High-Noise case

In this section we describe some simulation results for high-noise case, scenario no2.

The high-noise case has the same geometrical configuration as the low-noise case. The difference between the high-noise case and the low-noise case is in the measurement noise variances.

Each sensor calculates the true object angle-of-arrival. These are:

$$\theta_{1t} = 26.56° = 0.4636 \text{ radians}$$

$$\theta_{2t} = 44.99° = 0.7854 \text{ radians}$$

$$\theta_{3t} = 53.12° = 0.9273 \text{ radians}$$

Noise pdfs in the three sensors S1,S2, and S3 are as follows:

$$\delta_u = 5 \text{ degrees} = 0.0873 \text{ radians}$$

$$\sigma_u = 2.88 \text{ degrees} = 0.0504 \text{ radians}$$

$$\delta_s = 4 \text{ degrees} = 0.0698 \text{ radians}$$

$$\sigma_s = 2.83 \text{ degrees} = 0.0494 \text{ radians}$$

$$\delta_t = 6 \text{ degrees} = 0.1047 \text{ radians}$$

$$\sigma_t = 2.45 \text{ degrees} = 0.0428 \text{ radians}$$

The same equations as used in the low-noise case are used to compute the standard deviation above. The difference between θ_{2t} and θ_{3t} is 8 degrees. But with δ_s = 4 degrees and δ_t = 6 degrees, this represents a very large noise component. Indeed, the errors could well exceed the magnitude of the difference ($\theta_{3t} - \theta_{2t}$)

resulting in very large errors in the triangulation process between S2 and S3. In addition, the first-order approximation to the covariance matrix P_{z23} for the noisy position vector z_{23} will also have large errors because we see from figure (5.1) and section 5.2.4 that we need the noisy position measurements in equation (3.16) to compute the partial derivative matrix A_{23}. These noisy position measurements are not accurate and have large errors. Therefore the partial derivative matrix A_{23} will not be accurate. For these reasons the covariance matrix of the noisy position vector P_{z23} will not be accurate too.

5.6.1 Discussion of Simulation results, Scenario no2, high-Noise Case

The computer simulation was run 50 times and the results are plotted and discussed in the next several pages.

Figure (5.34) shows the actual errors in the noisy measurements x_{12} from triangulation between sensors S1, and S2. The dotted line represents the actual errors in the noisy measurements x_{12}, and the solid line represents the square root of $P_{z12}(1,1)$ in high-noise case in scenario no2 in x position. The solid line is the theoretical standard deviation of the errors according to the first-order approximation to the covariance matrix. The numeric mean value of the

errors in the noisy measurements x_{12} in figure (5.34) is Mx12_err = -0.1310. The numeric standard deviation is Sx12_err = 0.7364. This value is slightly off with respect to the theoretical standard deviation given by the solid line in the figure. This is due to the high noise situation and slant triangulation lines. Comparing this figure with figure (5.24), we see that the errors and the standard deviation are now much larger.

Figure (5.35) shows the actual errors in the noisy measurements x_{23} from triangulation between sensors S2, and S3. The dotted line represents the actual errors in the noisy measurements x_{23}, and the solid line represents the square root of $P_{z23}(1,1)$. The solid line is the theoretical standard deviation of the errors according to the first-order approximation to the covariance matrix. The numeric mean value of the errors in the noisy measurements x_{23} in the figure is Mx23_err = 0.1565. The numeric standard deviation is Sx23_err = 3.713. Clearly there is a very significant difference between the actual errors and the theoretical standard deviation given by the solid line. This is due to the high noise situation because of the large noise in the triangulation process between sensors S2, and S3. The difference between θ_{2t}, and θ_{3t} is 8 degrees, but δ_s = 4 degrees and δ_t = 6 degrees which represent a very large noise

component.

Figure (5.37) shows the errors in the fused estimate in x position obtained by fusion of the noisy measurements x_{12}, and x_{23}. The dotted line represents the errors in the fused estimate, and the solid line represents the square root of $P_o(1,1)$. The numeric mean value of the errors in the fused estimate in figure (5.37) in x dimension is Mxfuse_err = -0.5153. The numeric standard deviation of the errors in the fused estimate is Sxfuse_err = 0.5385. Compared with low-noise mean value of the error in the fused estimate in low-noise case which is equals 0.12, we see the numeric mean value in high-noise equals five times the numeric mean value of the errors in low-noise case. This is quite large. But it is a small percentage (6.25%) compared with the true value of the object position in x position which is equals to 8. Also we see the theoretical standard deviation is varying around the numeric value of 0.5385. Although the mean value is slightly biased the standard deviation is reasonably accurate.

Figure (5.38) shows the actual errors in the noisy measurements y_{12} from triangulation between sensors S1, and S2. The dotted line represents the actual errors in the noisy measurements y_{12}, and the solid line represents the square root of $P_{z12}(2,2)$. The solid

line is the theoretical standard deviation of the errors according to the first-order approximation to the covariance matrix. The numeric mean value of the errors in the noisy measurements y_{12} in the figure is My12_err = -0.1238. The numeric standard deviation is Sy12_err = 0.5667. From the figure we see no single value for the theoretical standard deviation-it has a large variation. The numeric standard deviation is at the bottom of the theoretical values.

Figure (5.39) shows the actual errors in the noisy measurements y_{23} from triangulation between sensors S2, and S3. The dotted line represents the actual errors in the noisy measurements y_{23}, and the solid line represents the square root of $P_{z23}(2,2)$. The solid line is the theoretical standard deviation of the errors according to the first-order approximation to the covariance matrix. The numeric mean value of the errors in the noisy measurements y_{23} in the figure is My23_err = 0.2896. The numeric standard deviation is Sy23_err = 4.2797. Clearly there is a very significant difference between the actual errors (dotted line) and the theoretical standard deviation (solid line). This is obvious in the figure (5.39) at n = 4 for example. We see the theoretical standard deviation is greater than the actual error by about 3 times. We see the same thing at n = 29, 36, and n = 37. This is due to the high noise situation because

of the large noise in the triangulation process between sensors S2, and S3. The slant angles in the triangulation process make the situation worse. Referring to the y_{23} noisy measurements in low-noise case in scenario no2 figure (5.29) we see that the theoretical standard deviation varies around the numeric standard deviation of 0.8934. Compared with the y_{23} noisy measurements in high-noise case in the same scenario figure (5.39), the numeric standard deviation is 4.279 which is approximately four times bigger than the actual standard deviation of the measurements in low-noise case in the same scenario. This means that the covariance matrix is inaccurate in the high-noise case.

Figure (5.41) shows the errors in the fused estimate in y position obtained by fusing the noisy measurements y_{12}, and y_{23}. The dotted line represents the errors in the fused estimate in y position, and the solid line represents the square root of $P_o(2,2)$. The numeric mean value of the errors in the fused estimate in figure (5.41) is Myfuse_err = -0.4673. The numeric standard deviation of the errors in the fused estimate is Syfuse_err = 0.6220. Compared with the mean value of the error in low-noise which is equal to 0.1093, we see it is about four times bigger in high-noise case. This is a quite large. But it is a small percentage (8.87%) compared with the true

value of the object y position which is equal to 7. Also we see from the figure the theoretical standard deviation varies around the numeric value.

The results of the simulations of scenario no2 for high-noise case are discussed in the next several pages.

Figure (5.34) shows the actual errors in the noisy measurements x_{12} (Mx12_err) and the numeric standard deviation of the errors in high-noise case in scenario no2 in x position.
We can see from figure (5.34) the errors in the noisy measurements x_{12} have a magnitude bigger than the magnitude of the errors in the x_{12} noisy measurements in low-noise case figure (5.24). In general we see the theoretical standard deviation tracks the magnitude of the errors.

Figure (5.35) shows the actual errors in the noisy measurements x_{23} and the theoretical standard deviation of the errors in high-noise case in scenario no2 in x position.
We can see from the figure that the errors in the x_{23} noisy measurements have a magnitude much bigger than the magnitude of the errors in the noisy measurements x_{23} in low-noise case in figure (5.25). Also we see from the figure that x_{23} noisy measurements are less

accurate than x_{12} noisy measurements in figure (5.34) because the errors and the standard deviation of the errors in x_{23} noisy measurements are much bigger than the errors and the standard deviation of the errors in x_{12} noisy measurements. We see from figure (5.35) there is a very significant difference between the actual errors and the theoretical standard deviation. As we mentioned earlier the large errors in the triangulation process between sensors S2, and S3 makes the measured position vector z_{23} very noisy. Therefore the covariance matrix of the noisy position vector z_{23} (P_{z23}) will not be accurate.

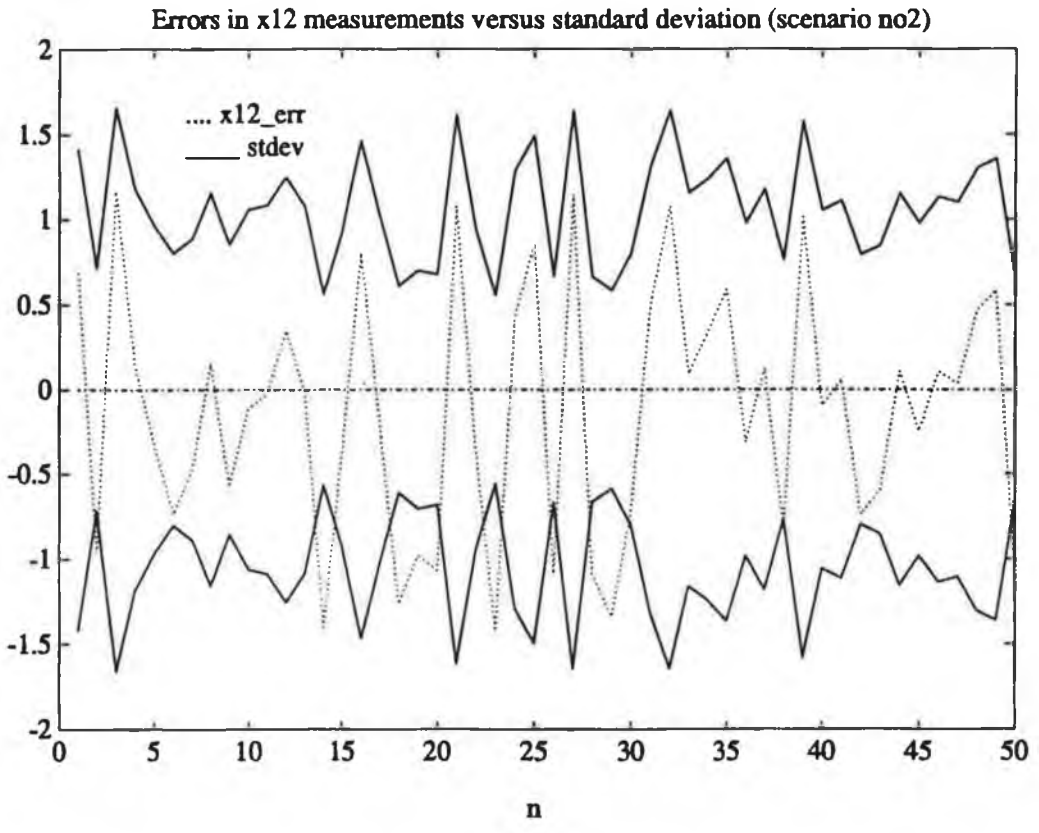

Figure (5.34)

.... x12_err represents the actual errors in the noisy measurements x_{12} in high-noise case in scenario no2 in x position.

____ stdev represents the square root of $P_{z12}(1,1)$, the theoretical standard deviation of the errors according to the first-order approximation to the covariance matrix in high-noise case in scenario no2 in x position.

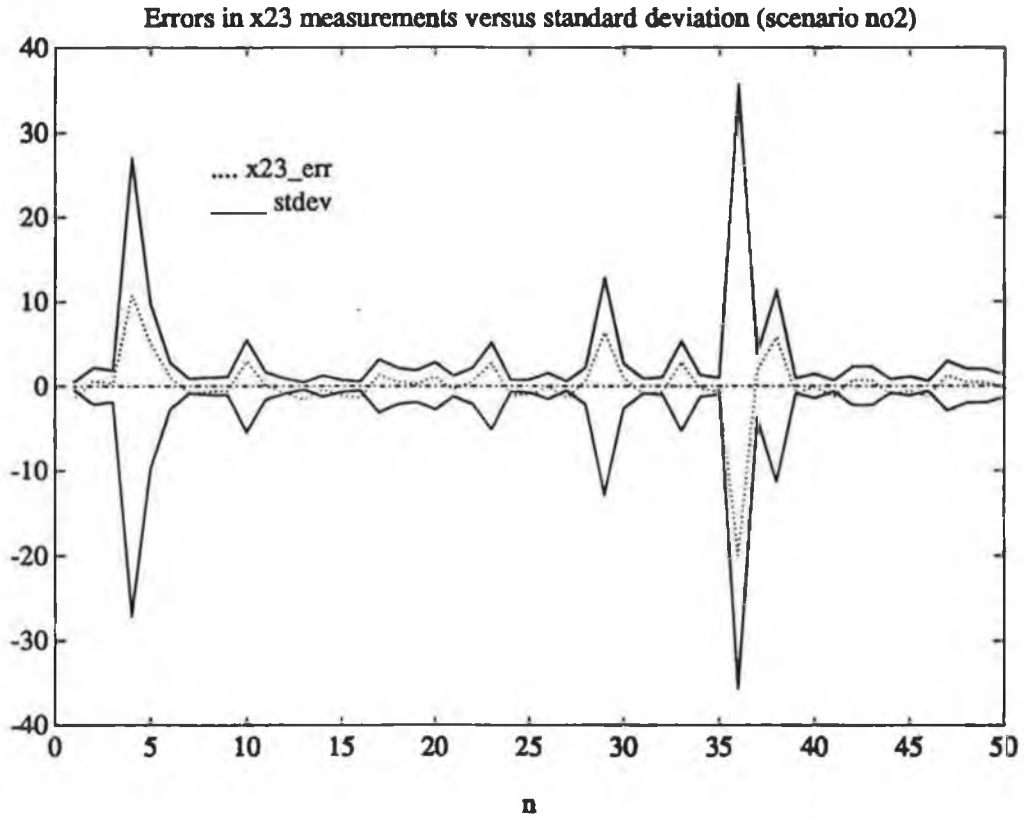

Figure (5.35)

.... x23_err represents the actual errors in the noisy measurements x_{23} in high-noise case in scenario no2 in x position.

____ stdev represents the square root of $P_{z23}(1,1)$, the theoretical standard deviation of the errors according to the first-order approximation to the covariance matrix in high-noise case in scenario no2 in x position.

Figure (5.36) shows the percentage errors in the fused estimate in high-noise case in scenario no2 in x position.

From the figure we see that the fused estimate (the solid line) clips the large errors in the noisy measurements x_{23}, and remains close to the higher accuracy noisy measurements x_{12} when the errors in the two noisy measurements x_{12}, and x_{23} are of the same algebraic sign. For example at n = 3 where the both of the errors in the noisy measurements x_{12}, and x_{23} are positive we see the fused estimate measurements clips the large error in the noisy measurement x_{23}, and remains close to the higher accuracy measurement x_{12}. We see the same effect at n = 37, 47, and n = 48. But when the error in the noisy measurements x_{12}, and x_{23} are of opposite algebraic sign, the fusion algorithm produces a smaller error than the smallest measurement error. For example at n = 11 where the error in the noisy measurement x_{12} is negative and the error in the noisy measurement x_{23} is positive , we see the fused error in the fused estimate is less than the smaller error individually. We also see the same effect at n = 19, 21, 31, 32 39, and n = 43.

In general we see from figure (5.36) that the fused estimate is superior to the individual measurements. This is surprising since the measurements are relatively noisy and the covariance matrix is quite inaccurate.

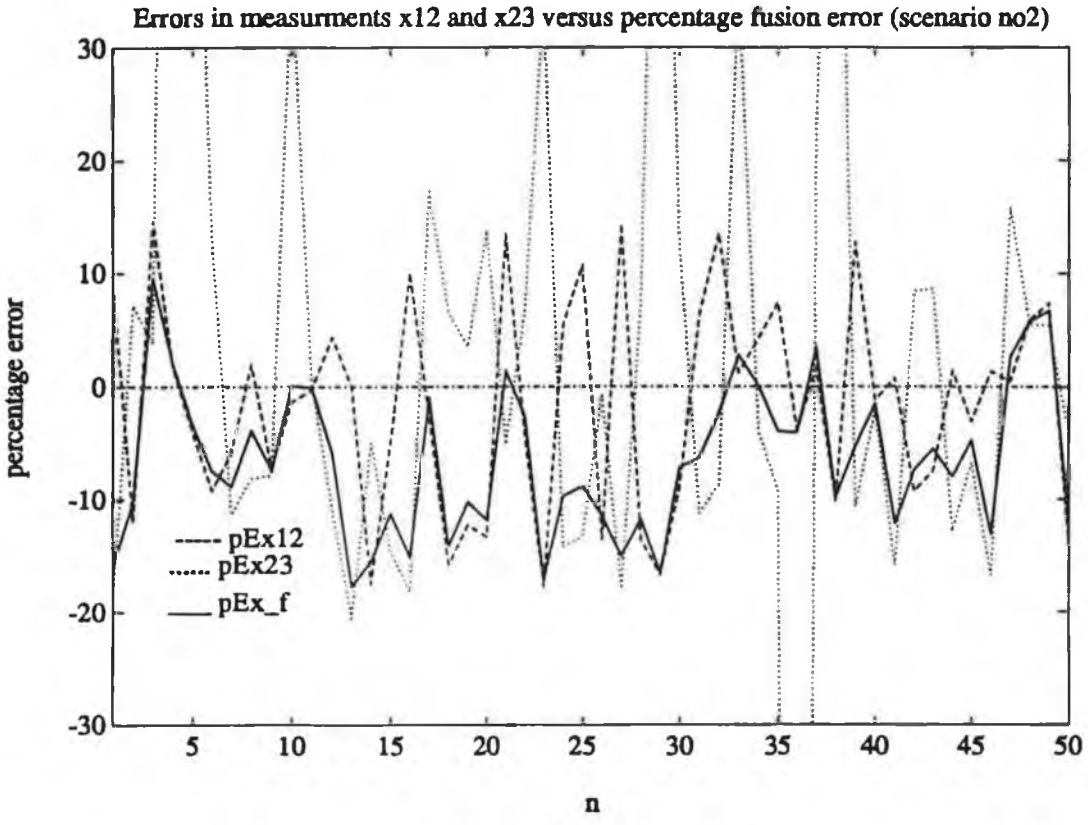

Figure (5.36)

--- pEx12 represents the percentage error in the noisy measurements x_{12} in high-noise case in scenario no2 in x position.

.... pEx23 represents the percentage error in the noisy measurements x_{23} in high-noise case in scenario no2 in x position.

____ pEx_f represents the percentage error in the fused estimate in high-nose case in scenario no2 in x position.

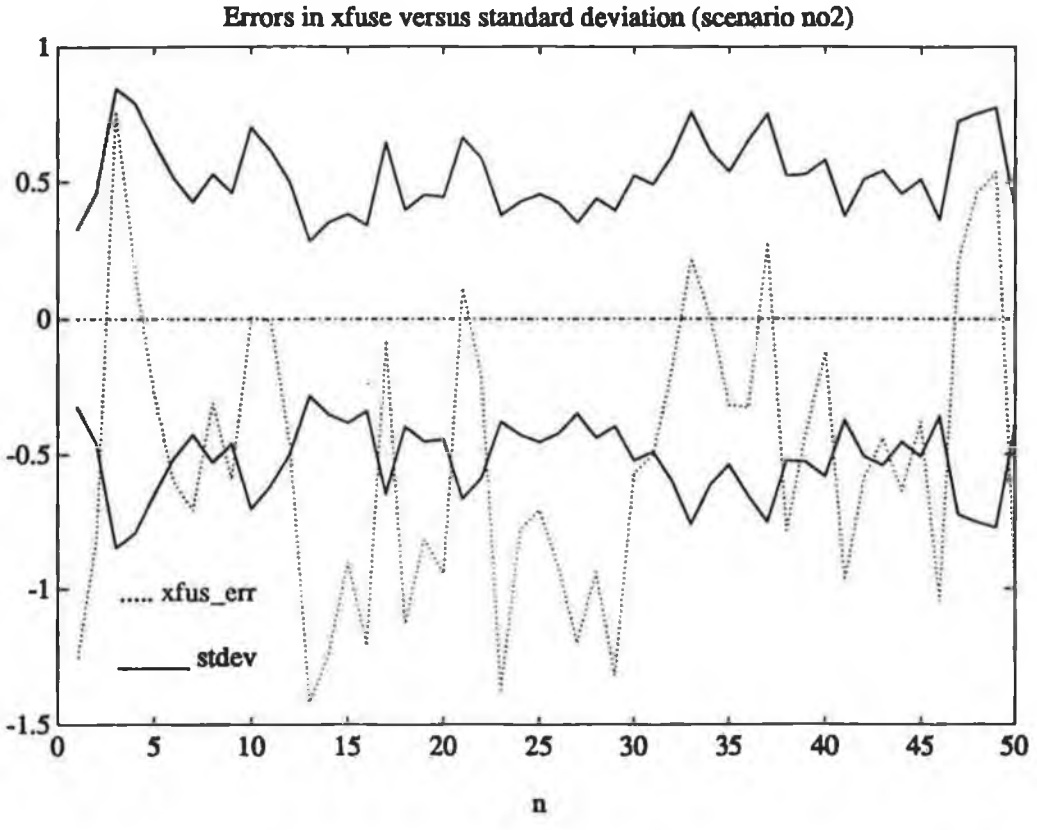

Figure (5.37)

.... xfus_err represents the errors in the fused estimate in high-noise case in scenario no2 in x position.

____ stdev represents the square root of $P_o(1,1)$, the theoretical standard deviation of the errors in the fused estimate in high-noise case in scenario no2 in x position.

Figure (5.38) shows the actual errors in the noisy measurements y_{12}, and the theoretical standard deviation of the errors in high-noise case in scenario no2 in y position.

We see from the figure the actual errors in the noisy measurements y_{12} in high-noise case are bigger than the actual errors in the noisy measurements y_{12} in low-noise case in scenario no2 figure (5.28). Also the theoretical standard deviation is seen to be bigger too.

In general we can see from the figure the theoretical standard deviation tracks the magnitude of the errors.

Figure (5.39) shows the actual errors in the noisy measurements y_{23}, and the theoretical standard deviation of the errors in high-noise case in scenario no2 in y position.

We can see from the figure that the noisy measurements y_{23} are less accurate than the noisy measurements y_{12} in figure (5.38). We see from figure (5.39) there is a very significant difference between the actual errors and the theoretical standard deviation because of the very large errors in the triangulation process between sensors S2, and S3. The noisy position vector z_{23} makes a very large error in the first-order approximation to the covariance matrix P_{z23}.

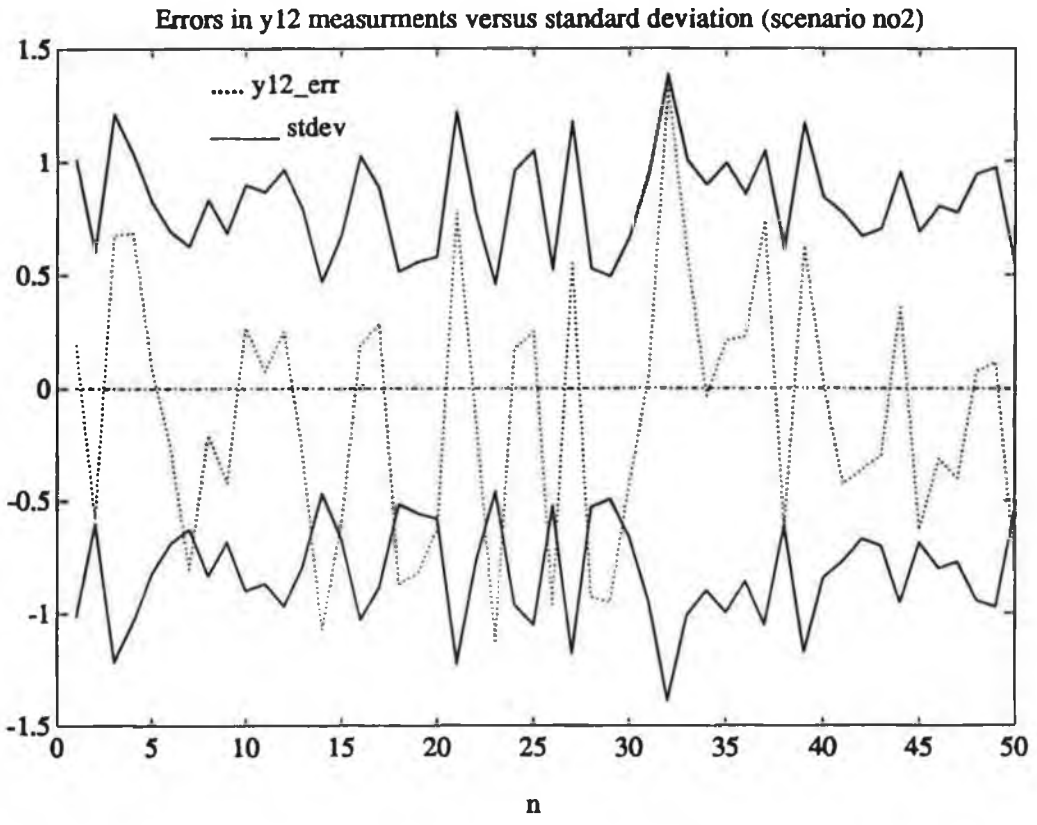

Figure (5.38)

.... y12_err represents the actual errors in the noisy measurements y_{12} in high-noise case in scenario no2 in y position.

____ stdev represents the square root of $P_{z12}(2,2)$, the theoretical standard deviation of the errors according to the first-order approximation to the covariance matrix.

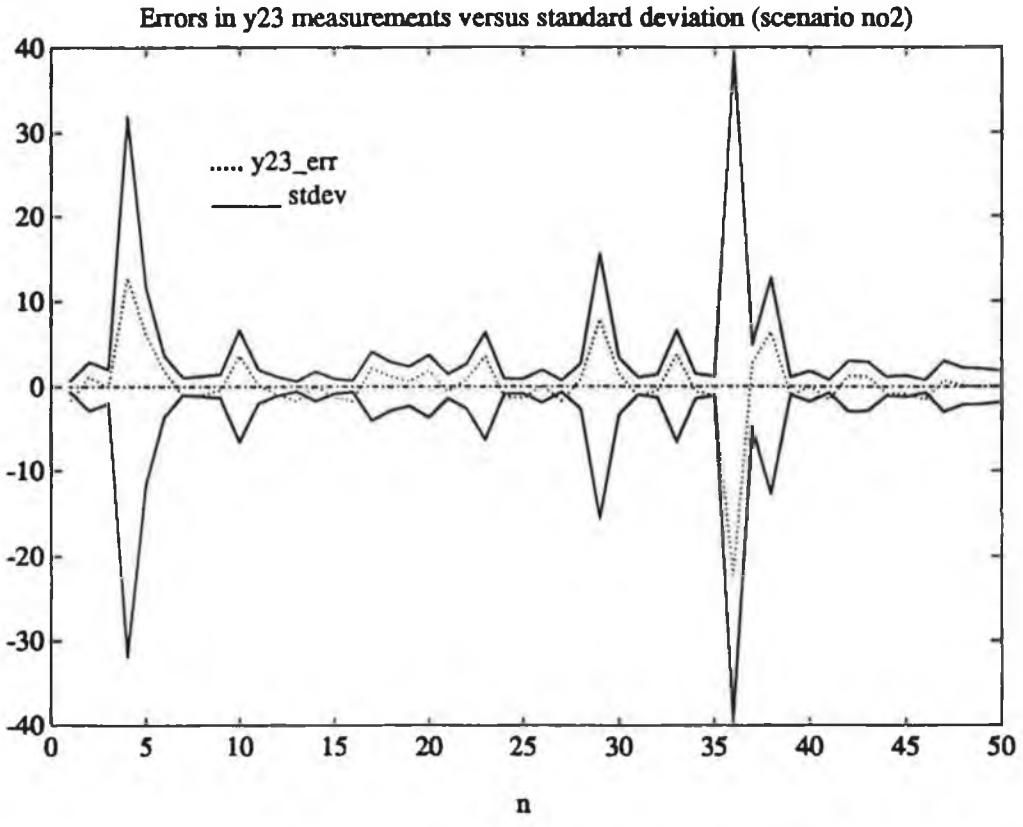

Figure (5.39)

.... y23_err represents the actual errors in the noisy measurements y_{23} in high-noise case in scenario no2 in y position.

_____ stdev represents the square root of $P_{z23}(2,2)$, the theoretical standard deviation of the error according to the first-order approximation to the covariance matrix in high-noise case in scenario no2 in y position.

Figure (5.40) shows the percentage errors in the fused estimate in y position in high-noise case in scenario no2.

From figure (5.40) we can see the fusion algorithm clips the peak error in both noisy measurements y_{12}, and y_{23}. For example at n = 19, the error in the noisy measurement y_{12} is negative and small and in the noisy measurement y_{23} is positive and large, we see that the fused error is smaller than the smallest magnitude error which is in y_{12}. We see the same effect at n = 28, 43, and n = 44. But we see when the errors in the noisy measurements y_{12}, and y_{23} are of the same algebraic sign, the fused error is not less than the smallest measurement error. Instead, it clips the peak error and remains close to the smaller one. For example at n = 5, both the errors in the noisy measurements y_{12}, and y_{23} are positive; we see the fused estimate is close to y_{12}. We see the same effect at n = 10, 17, and n = 40. The fusion algorithm occasionally gives a poorer estimate than the best measurement. For example at n = 25 we see the error in the fused estimate is not smaller than the smallest errors in the noisy measurements y_{12}, and y_{23}. We see the same thing at n = 26, 42, 46, and n = 47. This is not a fault in the algorithm, but a fault in the high noise measurements themselves. On average, however, we see that the fused estimate clips the peak errors in the noisy measurements in most cases

and is often superior to the best measurements. This is surprising since figure (5.39) shows the covariance matrix P_{z23} is a very inaccurate representation of the actual errors. Because of the presence of noise, even under optimal conditions all algorithms will sometimes yield poorer results than the measurements themselves. The important thing is that on average the algorithm gives better results than the raw data.

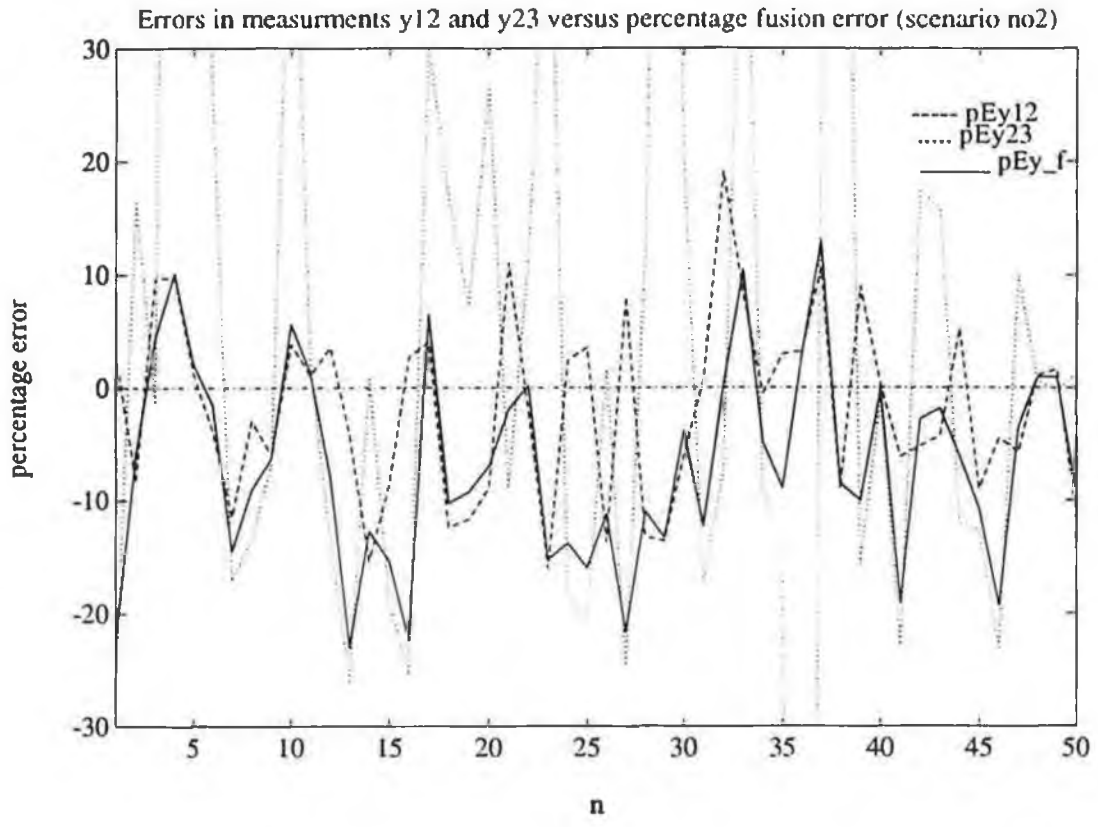

Figure (5.40)

--- pEy12 represents the percentage error in the noisy measurement y_{12} in high-noise case in scenario no2 in y position.

... pEy23 represents the percentage error in the noisy measurements y_{23} in high-noise case in scenario no2 in y position.

___ pEy_f represent the percentage error in the fused estimate in high-noise case in scenario no2 in y position.

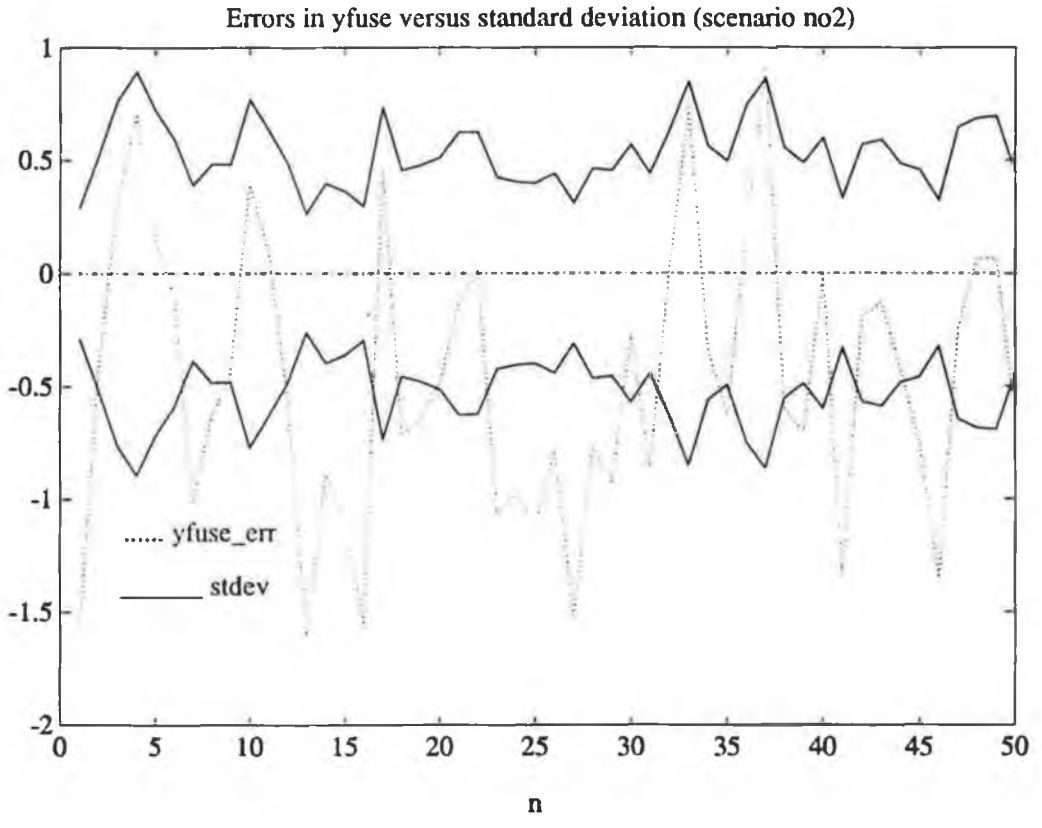

Figure (5.41)

.... yfuse_err represents the errors in the fused estimate in high-noise case in scenario no2 in y position.

_____ stdev represents the square root of $P_o(2,2)$, the theoretical standard deviation of the errors in the fused estimate in high-noise case in scenario no2 in y position.

5.6.1.1 Trace of Covariance Matrices

Figure (5.42) shows the trace of the error covariance matrices in high-noise case in scenario no2.

From the figure we see the trace of the optimum error covariance matrix is always less than the trace of the individual error covariance matrices P_{z12}, and P_{z23}. Clearly the trace of P_{z12} is much smaller than the trace of P_{z23}. Nevertheless, the trace of the optimum covariance matrix is always less than the trace of P_{z12}. From figure (5.42) we see the trace of the optimum covariance matrix (the solid line) is quite close to the trace of the covariance matrix P_{z12} (the dashed line) and some times is nearly the same. For example at n = 28, 29, the optimum covariance matrix has a trace which is almost the same as (but slightly less than) the trace of P_{z12}. The reason for this that since P_{z23} has much a larger trace compared to the high accuracy P_{z12}, the algorithm ignores P_{z23} and simply uses P_{z12} alone. At n = 21, the trace of P_{z12} and P_{z23} are about the same. Therefore the trace of the optimum covariance matrix is now much smaller than either of the covariance matrices. We see when both covariance matrices have a trace which is approximately the same, the trace of the optimum covariance matrix is then much smaller that either. But when the trace of one covariance matrix is much larger than the other the trace of the optimum covariance matrix is close to the smaller trace.

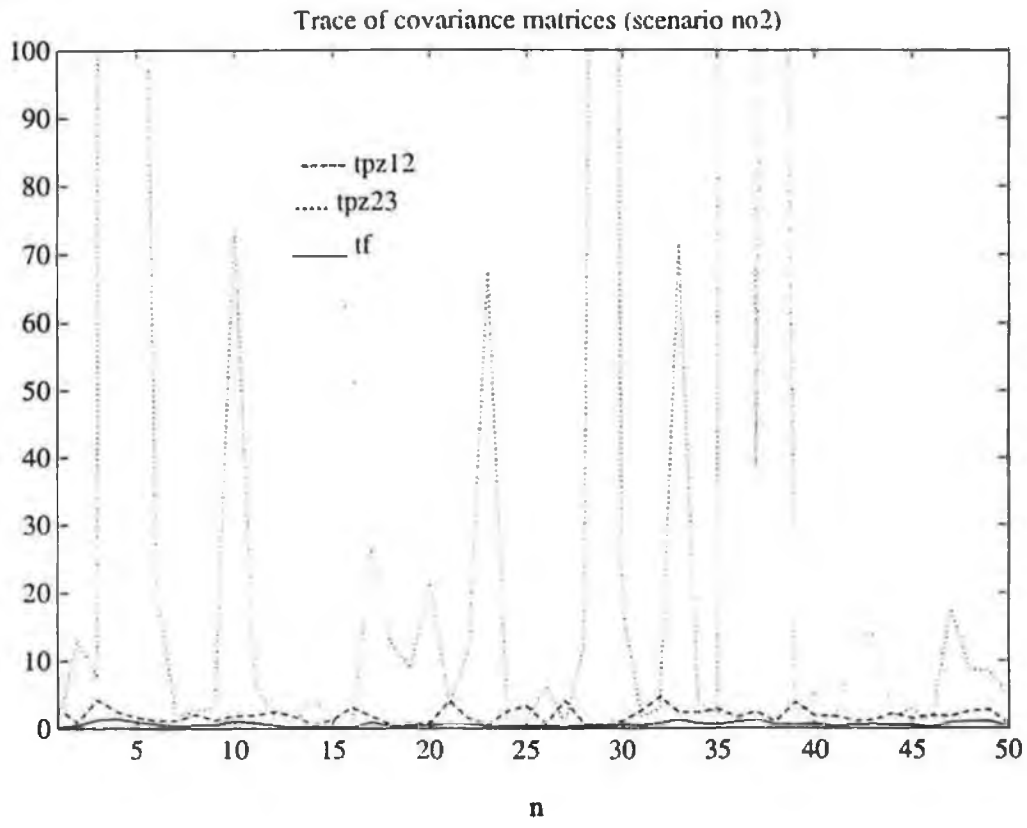

Figure (5.42)

---- tpz12 represents the trace of the error covariance matrix between sensor S1 and sensor S2 in high-noise case in scenario no2 case.

.... tpz23 represents the trace of the error covariance matrix between sensor S2, and sensor S3 in high-noise case in scenario no2.

____ tf represents the trace of the optimum error covariance matrix in high-noise case in scenario no2. case.

Regardless of the size of the trace of P_{z12} and P_{z23}, the trace of the optimum covariance matrix is always less than the trace of either of them. The fusion algorithm is designed to produce an optimum covariance matrix which has a trace less than the trace of the individual error covariance matrices.The algorithm does not know that in the high noise case in scenario no2, the covariance matrices are not accurate. The optimum covariance matrix may not accurately represent the statistics of the fused estimate. This is not the fault of the algorithm. It is the fault of the high-noise case and the first-order approximation. Also the algorithm does not know the pdf which is governing the errors in the data. The only things known by the algorithm are the covariance matrices and the noisy triangulation position measurements.

Figure (5.43) shows the correlation coefficient elements of the cross-covariance matrix p_{z1223}.
From the figure we see all the correlation coefficients have magnitude less than one. The figure also shows that there is a strong correlation between the components of the two vectors z_{12}, and z_{23}.

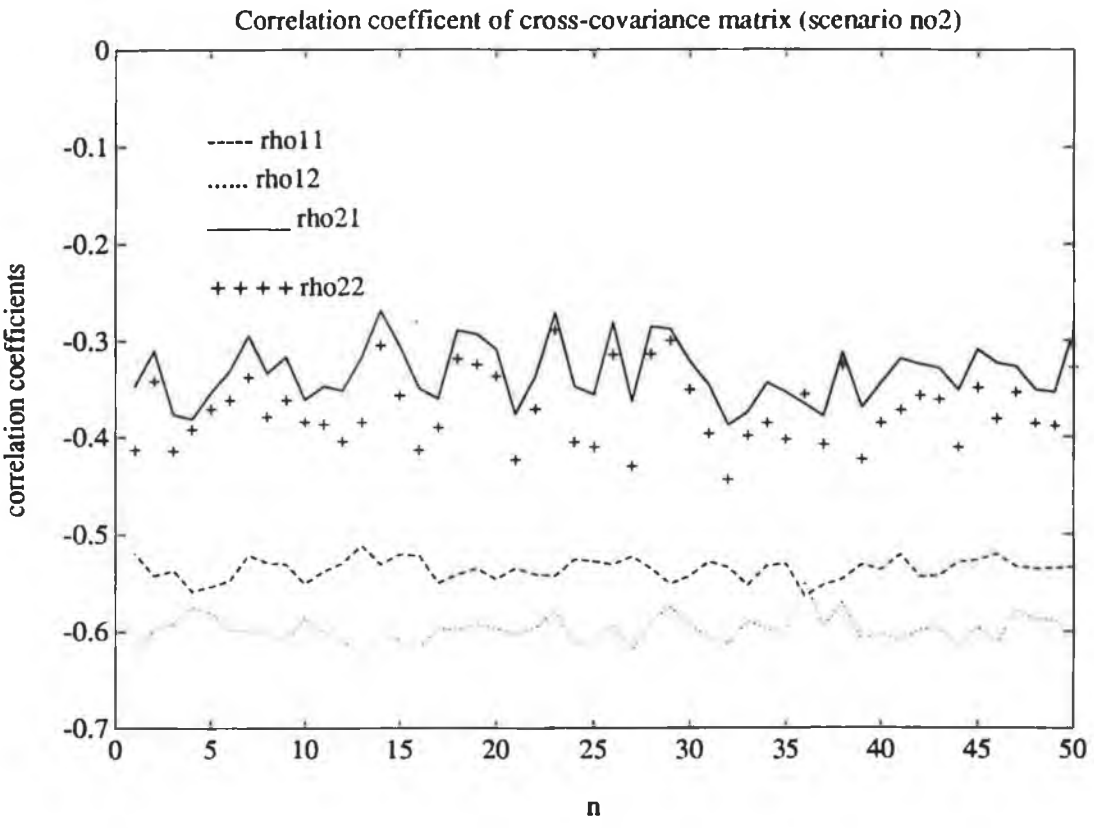

Figure (5.43)

---- rho11 = ρ_{x12x23} represents the correlation between the noisy measurements x_{12}, and x_{23} in high-nois case in scenario no2.

.... rho12 = ρ_{x12y23} represents the correlation between the noisy measurements x_{12}, and y_{23} in high-noise case in scenario no2.

____ rho21 = ρ_{y12x23} represents the correlation between the noisy measurements y_{12}, and x_{23} in high-noise case in scenario no2.

++++ rho22 = ρ_{y12y23} represents the correlation between the noisy measurements y_{12}, and y_{23} in high-noise case in scenario no2.

In the next chapter we investigate the impact of high-order terms in the approximation to the error covariance matrix.

CHAPTER VI

HIGH-ORDER TERMS IN COVARIANCE MATRIX

In this chapter, we invesitgate the impact of using higher-order terms in the approximation to the error covariance matrix.

We see what improvement results by including the second-order terms in the Taylor expansion of the covariance matrix.

6.1 The Second-Order Terms of TAYLOR'S Expansion FORMULA

From the equation (2) chapter VI in reference [12] we see the second-order terms in the expansion of f(x,y) in 2-dimensional space for TAYLOR'S FORMULA are:

$$f(x,y) = f(x_o,y_o) + D_1 f(x,y)\,\Delta x + D_2 f(x,y)\,\Delta y +$$

$$\frac{1}{2}\left[D_1^2 f(x,y)\,\Delta x^2 + D_2^2 f(x,y)\,\Delta y^2 + 2D_1 D_2 f(x,y)\,\Delta x\,\Delta y\right] \qquad (6.1)$$

where:

$\Delta x = (x - x_0)$

$\Delta y = (y - y_o)$

$D_1 f(x,y) = \partial f(x,y)/\partial x$

$D_2 f(x,y) = \partial f(x,y)/\partial y$

$D_1^2 f(x,y) = \partial^2 f(x,y)/\partial x^2$

$D_2^2 f(x,y) = \partial^2 f(x,y)/\partial y^2$ and

$D_1 D_2 f(x,y) = \partial^2 f(x,y)/\partial x \partial y$

In our approach there are two noisy measurements

vectors z_{12}, and z_{23}:

$$z_{12} = \begin{bmatrix} x_{12} \\ y_{12} \end{bmatrix}$$

and

$$z_{23} = \begin{bmatrix} x_{23} \\ y_{23} \end{bmatrix}$$

These are expanded to include the second-order terms as follows:

$$x_{12} = x_{12}(\theta_{1t}, \theta_{2t}) + a_{11}\Delta\theta_1 + a_{12}\Delta\theta_2 + \frac{1}{2}a_{13x}\Delta\theta_1^2 + \frac{1}{2}a_{14x}\Delta\theta_2^2 + a_{15x}\Delta\theta_1\Delta\theta_2 \qquad (6.2)$$

Where:

$a_{11} = D_1 f = \partial x_{12}/\partial\theta_1$ and is given by the equation (3.7)

$a_{12} = D_2 f = \partial x_{12}/\partial\theta_2$ and is given by the equation (3.8)

$$a_{13x} = D_1^2 f = \frac{\partial^2 x_{12}}{\partial\theta_1^2} = \frac{\partial}{\partial\theta_1}\left[\frac{\partial x_{12}}{\partial\theta_1}\right] = \frac{\partial}{\partial\theta_1}[a_{11}]$$

$$a_{14x} = D_2^2 f = \frac{\partial^2 x_{12}}{\partial\theta_2^2} = \frac{\partial}{\partial\theta_2}\left[\frac{\partial x_{12}}{\partial\theta_2}\right] = \frac{\partial}{\partial\theta_2}[a_{12}] \qquad \text{and}$$

$$a_{15x} = D_1 D_2 f = \frac{\partial^2 x_{12}}{\partial\theta_1\partial\theta_2} = \frac{\partial}{\partial\theta_1}\left[\frac{\partial x_{12}}{\partial\theta_2}\right] = \frac{\partial}{\partial\theta_1}[a_{12}]$$

From equation (6.1) we compute the second-order derivatives for the noisy measurement y_{12} as follows:

$$y_{12} \approx y_{12}(\theta_{1t}, \theta_{2t}) + a_{21}\Delta\theta_1 + a_{22}\Delta\theta_2 + \frac{1}{2}a_{13y}\Delta\theta_1^2 + \frac{1}{2}a_{14y}\Delta\theta_2^2 + a_{15y}\Delta\theta_1\Delta\theta_2 \qquad (6.3)$$

Where:

$a_{21} = \partial y_{12}/\partial\theta_1$ and given by the equation (3.9),

$a_{22} = \partial y_{12}/\partial\theta_2$ and given by the equation (3.10),

$$a_{13y} = \frac{\partial^2 y_{12}}{\partial\theta_1^2} = \frac{\partial}{\partial\theta_1}\left[\frac{\partial y_{12}}{\partial\theta_1}\right] = \frac{\partial}{\partial\theta_1}[a_{21}]$$

$$a_{14y} = \frac{\partial^2 y_{12}}{\partial\theta_2^2} = \frac{\partial}{\partial\theta_2}\left[\frac{\partial y_{12}}{\partial\theta_2}\right] = \frac{\partial}{\partial\theta_2}[a_{22}]$$

$$a_{15y} = \frac{\partial^2 y_{12}}{\partial\theta_1\partial\theta_2} = \frac{\partial}{\partial\theta_1}\left[\frac{\partial y_{12}}{\partial\theta_2}\right] = \frac{\partial}{\partial\theta_1}[a_{22}]$$

A similar set of equations hold to compute the second derivatives terms for the noisy measurements x_{23}, and y_{23} as follow:

$$x_{23} = x_{12}(\theta_{2t}, \theta_{3t}) + a_{11}\Delta\theta_2 + a_{12}\Delta\theta_3 + \frac{1}{2}a_{13x}\Delta\theta_2^2 + \frac{1}{2}a_{14x}\Delta\theta_3^2 + a_{15x}\Delta\theta_2\Delta\theta_3 \qquad (6.4)$$

where:

$a_{11} = \dfrac{\partial x_{23}}{\partial\theta_2}$ *and is given by the equation* (3.14)

$$a_{12} = \frac{\partial x_{23}}{\partial \theta_3} \qquad \textit{and is given by the equation (3.15)}$$

$$a_{13x} = \frac{\partial^2 x_{23}}{\partial \theta_2^2} = \frac{\partial}{\partial \theta_2}\left[\frac{\partial x_{23}}{\partial \theta_2}\right] = \frac{\partial}{\partial \theta_2}[a_{11}]$$

$$a_{14x} = \frac{\partial^2 x_{23}}{\partial \theta_3^2} = \frac{\partial}{\partial \theta_3}\left[\frac{\partial x_{23}}{\partial \theta_3}\right] = \frac{\partial}{\partial \theta_3}[a_{12}] \qquad \text{and}$$

$$a_{15x} = \frac{\partial^2 x_{23}}{\partial \theta_2 \partial \theta_3} = \frac{\partial}{\partial \theta_2}\left[\frac{\partial x_{23}}{\partial \theta_3}\right] = \frac{\partial}{\partial \theta_2}[a_{12}]$$

From the equation (6.1) we compute the noisy measurements y_{23} includes the high-order terms as follows:

$$y_{23} = y_{23}(\theta_{2t}, \theta_{3t}) + a_{21}\Delta\theta_2 + a_{22}\Delta\theta_3 + \frac{1}{2}a_{13y}\Delta\theta_2^2 + \frac{1}{2}a_{14y}\Delta\theta_3^2 + a_{15y}\Delta\theta_2\Delta\theta_3 \qquad (6.5)$$

where:

$$a_{21} = \frac{\partial y_{23}}{\partial \theta_2} \qquad \textit{and is given by the equation (3.16)}$$

$$a_{22} = \frac{\partial y_{23}}{\partial \theta_3} \qquad \textit{and is given by the equation (3.17)}$$

$$a_{13y} = \frac{\partial y_{23}^2}{\partial \theta_2^2} = \frac{\partial}{\partial \theta_2}\left[\frac{\partial y_{23}}{\partial \theta_2}\right] = \frac{\partial}{\partial \theta_2}[a_{21}]$$

$$a_{14y} = \frac{\partial^2 y_{23}}{\partial \theta_3^2} = \frac{\partial}{\partial \theta_3}\left[\frac{\partial y_{23}}{\partial \theta_3}\right] = \frac{\partial}{\partial \theta_3}[a_{22}] \quad \text{and}$$

$$a_{15y} = \frac{\partial^2 y_{23}}{\partial \theta_2 \partial \theta_3} = \frac{\partial}{\partial \theta_2}\left[\frac{\partial y_{23}}{\partial \theta_3}\right] = \frac{\partial}{\partial \theta_3}[a_{22}]$$

Of course we use θ_{im} instead of θ_{it} since we only measure θ_{im}.

6.2 The Second-Order Terms for the Noisy Measurements x_{12}, and y_{12}

6.2.1 Calculation of a_{13x} for the Noisy Measurement x_{12}

$$a_{13x} = \frac{\partial^2 x_{12}}{\partial \theta_1^2} = \frac{\partial}{\partial \theta_1}\left[\frac{\partial x_{12}}{\partial \theta_1}\right] = \frac{\partial}{\partial \theta_1}[a_{11}]$$

where

$$a_{11} = \frac{\partial x_{12}}{\partial \theta_1} = \frac{\sec^2\theta_1\left[(x_2 - x_1)\tan\theta_2 + (y_1 - y_2)\right]}{(\tan\theta_1 - \tan\theta_2)^2}$$

Therefore

$$a_{13x} = \frac{\partial}{\partial \theta_1}\left\{\frac{\sec^2\theta_1\left[(x_2 - x_1)\tan\theta_2 + (y_1 - y_2)\right]}{(\tan\theta_1 - \tan\theta_2)^2}\right\}$$

After some algebra, we get

$$a_{13x} = 2\frac{[(x_2-x_1)\tan\theta_2+(y_1-y_2)]\sec^2\theta_1\tan\theta_1(\tan\theta_1-\tan\theta_2)^2}{(\tan\theta_1-\tan\theta_2)^4} -$$

$$2\frac{[x_2-x_1)\tan\theta_2+(y_1-y_2)][(\tan\theta_1-\tan\theta_2)\sec^4\theta_1]}{(\tan\theta_1-\tan\theta_2)^4} \qquad (6.6)$$

6.2.2 Calculation of a_{14x} for the Noisy Measurement x_{12}

$$a_{14x} = \frac{\partial^2 x_{12}}{\partial\theta_2^2} = \frac{\partial}{\partial\theta_2}[\frac{\partial x_{12}}{\partial\theta_2}] = \frac{\partial}{\partial\theta_2}[a_{12}]$$

where

$$a_{12} = \frac{\partial x_{12}}{\partial\theta_2} = \frac{\sec^2\theta_2[(x_1-x_2)\tan\theta_2 + (y_2-y_1)]}{(\tan\theta_1-\tan\theta_2)^2}$$

Therefore

$$a_{14x} = \frac{\partial}{\partial\theta_2}\{\frac{\sec^2\theta_2[(x_1-x_2)\tan\theta_1+(y_2-y_1)]}{(\tan\theta_1-\tan\theta_2)^2}\}$$

$$a_{14x} = 2\frac{[(x_1-x_2)\tan\theta_1+(y_2-y_1)](\tan\theta_1-\tan\theta_2)^2\sec\theta_2^2\tan\theta_2}{(\tan\theta_1-\tan\theta_2)^4} +$$

$$2\frac{[(x_1-x_2)\tan\theta_1+(y_2-y_1)](\tan\theta_1-\tan\theta_2)\sec^4\theta_2}{(\tan\theta_1-\tan\theta_2)^4} \qquad (6.7)$$

6.2.3 Calcualation of a_{15x} for the Noisy Measurement x_{12}

$$a_{15x} = \frac{\partial}{\partial\theta_1}\left[\frac{\partial x_{12}}{\partial\theta_2}\right] = \frac{\partial}{\partial\theta_1}[a_{12}]$$

$$= \frac{\partial}{\partial\theta_1}\left\{\frac{\sec^2\theta_2\left[(x_1-x_2)\tan\theta_1+(y_2-y_1)\right]}{(\tan\theta_1-\tan\theta_2)^2}\right\}$$

$$a_{15x} = \frac{\left[(x_2-x_1)\sec^2\theta_1\sec^2\theta_2\right](\tan\theta_1-\tan\theta_2)^2}{(\tan\theta_1-\tan\theta_2)^4} +$$

$$2\frac{\left[(x_2-x_1)\tan\theta_2+(y_1-y_2)\right]\sec^2\theta_1\sec^2\theta_2(\tan\theta_1-\tan\theta_2)}{(\tan\theta_1-\tan\theta_2)^4} \qquad (6.8)$$

6.2.4 Calculation of a_{13y} for the Noisy Measurement y_{12}

$$a_{13y} = \frac{\partial^2 y_{12}}{\partial\theta_1^2} = \frac{\partial}{\partial\theta_1}\left[\frac{\partial y_{12}}{\partial\theta_1}\right] = \frac{\partial}{\partial\theta_1}[a_{21}]$$

where a_{21} is given by:

$$a_{21} = a_{11}\tan\theta_1 + \sec^2\theta_1(x_{12} - x_1)$$

Therefore

$$a_{13y} = \frac{\partial}{\partial\theta_1}\left[a_{11}\tan\theta_1+\sec^2\theta_1(x_{12}-x_1)\right]$$

$$a_{13y} = a_{13x}\tan\theta_1 + 2a_{11}\sec^2\theta_1 + 2(x_{12}-x_1)\sec^2\theta_1\tan\theta_1 \qquad (6.9)$$

where x_{12}, a_{11}, and a_{13x} are given by equations (2.9),

(3.7), and (6.6) respectively.

6.2.5 Calculation of a_{14y} for the Noisy Measurement y_{12}

$$a_{14y} = \frac{\partial^2 y_{12}}{\partial \theta_2^2} = \frac{\partial}{\partial \theta_2}\left[\frac{\partial y_{12}}{\partial \theta_2}\right] = \frac{\partial}{\partial \theta_2}[a_{22}]$$

Where equation (3.10)

$$a_{22} = a_{12}\tan\theta_1$$

Therefore

$$a_{14y} = \frac{\partial}{\partial \theta_2}[a_{12}\tan\theta_1] = \frac{\partial}{\partial \theta_2}[a_{12}]\tan\theta_1 = \frac{\partial}{\partial \theta_2}\{[\frac{\partial x_{12}}{\partial \theta_2}]\}\tan\theta_1$$

$$= a_{14x}\tan\theta_1 \qquad (6.10)$$

where a_{14x} is given by equation (6.7)

6.2.6 Calculation of a_{15y} for the Noisy Measurement y_{12}

$$a_{15y} = \frac{\partial}{\partial \theta_1}\left[\frac{\partial y_{12}}{\partial \theta_2}\right] = \frac{\partial}{\partial \theta_1}[a_{22}]$$

where:

$$a_{22} = a_{12}\tan\theta_1 \quad \text{and}$$

$$a_{12} = \frac{\partial x_{12}}{\partial \theta_2}$$

Therefore

$$a_{15y} = \frac{\partial}{\partial\theta_1}\{[\frac{\partial x_{12}}{\partial\theta_2}\tan\theta_1]\}$$

$$= \frac{\partial x_{12}}{\partial\theta_1\partial\theta_2}\tan\theta_1 + \frac{\partial x_{12}}{\partial\theta_2}\sec^2\theta_1$$

Therefore

$$a_{15y} = a_{15x}\tan\theta_1 + a_{12}\sec^2\theta_1 \qquad (6.11)$$

where a_{12}, and a_{15x} are given by equations (3.8) and (6.8) respectively.

6.3 The Second-Order Terms for the Noisy Measurements x_{23}, and y_{23}

It is not necessary to rederive the expressions for a_{13x}, a_{14x}, a_{15x}, a_{13y}, a_{14y}, and a_{15y} for the noisy measurements x_{23}, y_{23}. The equations derived for the noisy measurements x_{12}, and y_{12} may be used for the noisy measurements x_{23}, and y_{23}. This is accomplished by replacing θ_1, x_1, θ_2, x_2, y_1, y_2, and x_{12} with θ_2, x_2, θ_3, x_3, y_2, y_3, and x_{23} respectively. The resulting equations are as follow:

$$a_{13x} = \frac{\partial^2 x_{23}}{\partial\theta_2^2} = 2\frac{[(x_3-x_2)\tan\theta_3+(y_2-y_3)]\sec^2\theta_2\tan\theta_2(\tan\theta_2-\tan\theta_3)^2}{(\tan\theta_2-\tan\theta_3)^4}$$

$$- 2\frac{[x_3-x_2)\tan\theta_3+(y_2-y_3)](\tan\theta_2-\tan\theta_3)\sec^4\theta_2}{(\tan\theta_2-\tan\theta_3)^4} \qquad (6.12)$$

$$a_{14x} = \frac{\partial^2 x_{23}}{\partial \theta^2_3} = 2\frac{[(x_2-x_3)\tan\theta_2+(y_3-y_2)](\tan\theta_2-\tan\theta_3)^2\sec\theta_3^2\tan\theta_3}{(\tan\theta_2-\tan\theta_3)^4}$$

$$+ 2\frac{[(x_2-x_3)\tan\theta_2+(y_3-y_2)](\tan\theta_2-\tan\theta_3)\sec^4\theta_3}{(\tan\theta_2-\tan\theta_3)^4} \qquad (6.13)$$

$$a_{15x} = \frac{\partial}{\partial\theta_2}\left[\frac{\partial x_{23}}{\partial\theta_3}\right] = \frac{[(x_3-x_2)\sec^2\theta_2\sec^2\theta_3(\tan\theta_2-\tan\theta_3)^2}{(\tan\theta_2-\tan\theta_3)^4} +$$

$$2\frac{[(x_3-x_2)\tan\theta_3+(y_2-y_3)\sec^2\theta_2\sec^2\theta_3(\tan\theta_2-\tan\theta_3)}{(\tan\theta_2-\tan\theta_3)^4} \qquad (6.14)$$

$$a_{13y} = \frac{\partial}{\partial\theta_2}\left[\frac{\partial y_{23}}{\partial\theta_2}\right] = a_{13x}\tan\theta_2+2a_{11}\sec^2\theta_2+2(x_{23}-x_2)\sec^2\theta_2\tan\theta_2 \qquad (6.15)$$

$$a_{14y} = a_{14x}\tan\theta_2 \qquad (6.16) \text{ and}$$

$$a_{15y} = a_{15x}\tan\theta_2 + a_{12}\sec^2\theta_2 \qquad (6.17)$$

where a_{11}, a_{12}, a_{13x}, a_{14x}, and a_{15x} are given by equations (3.14), (3.15), (6.12), (6.13), and (6.14) respectively.

We now have expressions for all the high-order terms in the covariance matrices. We now formulate the

expected values of these high-order terms.

6.4 The Error Covariance Matrices P_{z12}, and P_{z23}

In our scenario as we said previously there are two noisy position vectors z_{12}, and z_{23} which are given as follow:

$$z_{12} = [x_{12}, y_{12}]^T \text{ and}$$

$$z_{23} = [x_{23}, y_{23}]^T$$

The error in the noisy x_{12} measurements (ε_{x12}) is given by

$$\varepsilon_{x12} = x_{12} - \bar{x}_{12}$$

From equation (6.2) we compute the expected value for the noisy measurements x_{12}, ($\bar{x}_{12}$)

$$\bar{x}_{12} = E(x_{12})$$

$$\overline{x_{12}} = E(x_{12}) \approx x_{12}(\theta_{1t}, \theta_{2t}) + a_{11}E(\Delta\theta_1) + a_{12}E(\Delta\theta_2) + \frac{1}{2}a_{13x}E(\Delta\theta_1^2) +$$

$$\frac{1}{2}\, a_{14x}\, E(\Delta\theta_2^2) + a_{15x}\, E(\Delta\theta_1\Delta\theta_2)$$

Since $E(\Delta\theta_i) = 0$ (the sensor makes an unbiased measurement, sensor errors are zero mean)

$$E(\Delta\theta_1^2) = \sigma^2_{\theta 1}$$

$$E(\Delta\theta_2^2) = \sigma^2_{\theta 2}$$

Also $\Delta\theta_1$, and $\Delta\theta_1$ are assumed to be statistically independent,

$$E[\Delta\theta_1\Delta\theta_2] = E(\Delta\theta_1)E(\Delta\theta_2) = 0$$

Therefore

$$\overline{x_{12}} = x_{12}(\theta_{1t}, \theta_{2t}) + \frac{1}{2}a_{13x}\sigma^2_{\theta 1} + \frac{1}{2}a_{14x}\sigma^2_{\theta 2} \qquad (6.18)$$

From equations (6.2) and (6.18) we get

$$(x_{12} - \overline{x_{12}}) = x_{12}(\theta_{1t}, \theta_{2t}) + a_{11}\Delta\theta_1 + a_{12}\Delta\theta_2 + \frac{1}{2}a_{13x}\Delta\theta_1^2 + \frac{1}{2}a_{14x}\Delta\theta_2^2 +$$

$$a_{15x}\Delta\theta_1\Delta\theta_2 - x_{12}(\theta_{1t}, \theta_{2t}) - \frac{1}{2}a_{13x}\sigma^2_{\theta 1} - \frac{1}{2}a_{14x}\sigma^2_{\theta 2}$$

$$\epsilon_{x12} = (x_{12} - \overline{x_{12}}) = a_{11}\Delta\theta_1 + a_{12}\Delta\theta_2 + \frac{1}{2}a_{13x}(\Delta\theta_1^2 - \sigma^2_{\theta 1}) +$$

$$\frac{1}{2}a_{14x}(\Delta\theta_2^2 - \sigma^2_{\theta_2}) + a_{15x}\Delta\theta_1\Delta\theta_2 \qquad (6.19)$$

The error in the y_{12} noisy measurements (ϵ_{y12}) is given by:

$$\epsilon_{y12} = y_{12} - \bar{y}_{12}$$

From the equation (6.3) we compute the expected value $\bar{y}_{12}$

$$\overline{y_{12}} = E\{ y_{12}(\theta_{1t}, \theta_{2t}) + a_{21}\Delta\theta_1 + a_{22}\Delta\theta_2 + \frac{1}{2}a_{13y}\Delta\theta_1^2 + \frac{1}{2}\Delta\theta_2^2 + a_{15y}\Delta\theta_\Delta\theta_2 \}$$

$$= E[y_{12}(\theta_{1t}, \theta_{2t})] + a_{21}E(\Delta\theta_1) + a_{22}E(\Delta\theta_2) + \frac{1}{2}a_{13y}E(\Delta\theta_1^2) + \frac{1}{2}a_{14y}E(\Delta\theta_2^2)$$

$$+ E(a_{15y}\Delta\theta_1\Delta\theta_2)$$

where:

$$E[y_{12}(\theta_{1t},\theta_{2t})] = y_{12}(\theta_{1t},\theta_{2t}),$$

$$E(\Delta\theta_i) = 0,$$

$$E(\Delta\theta_1\Delta\theta_2) = 0 \text{ (statistically independent)}$$

$$E(\Delta\theta_1^2) = \sigma_{\theta 1}^2, \text{ and}$$

$$E(\Delta\theta_2^2) = \sigma_{\theta 2}^2$$

Therefore

$$\overline{y_{12}} = y_{12}(\theta_{1t},\theta_{2t}) + \frac{1}{2}a_{13y}\sigma_{\theta 1}^2 + \frac{1}{2}a_{14y}\sigma_{\theta 2}^2 \qquad (6.20)$$

From (6.3), and (6.20) we get ε_{y12}

$$\epsilon_{y12} = y_{12} - \overline{y_{12}} = a_{21}\Delta\theta_1 + a_{22}\Delta\theta_2 + \frac{1}{2}a_{13y}[\Delta\theta_1^2 - \sigma_{\theta 1}^2] +$$

$$\frac{1}{2}a_{14y}(\Delta\theta^2{}_2 - \sigma^2{}_{\theta 2}) + A_{15y}\Delta\theta_1\Delta\theta_2 \qquad (6.21)$$

The error in the estimate of a state vector z_{12} is ε_{z12} and is given by:

$$\epsilon_{z12} = \begin{bmatrix} \epsilon_{x12} \\ \epsilon_{y12} \end{bmatrix}$$

6.4.1 The Error Covariance matrix P_{z12}

The error covariance matrix of the error ε_{z12}, is P_{z12}, and is then given by

$$P_{z12} = E[\varepsilon_{z12}\varepsilon_{z12}^T]$$

$$= E\left\{ \begin{vmatrix} \epsilon_{x12} \\ \epsilon_{y12} \end{vmatrix} [\ \epsilon_{x12}\ \epsilon_{y12}\ ]\ \right\}$$

$$= E \begin{vmatrix} \epsilon_{x12}^2 & \epsilon_{x12}\epsilon_{y12} \\ \epsilon_{y12}\epsilon_{x12} & \epsilon_{y12}^2 \end{vmatrix}$$

$$= E \begin{vmatrix} (x_{12}-\overline{x_{12}})^2 & (x_{12}-\overline{x_{12}})\,(y_{12}-\overline{y_{12}}) \\ (y_{12}-\overline{y_{12}})\,(x_{12}-\overline{x_{12}}) & (y_{12}-\overline{y_{12}})^2 \end{vmatrix}$$

$$= \begin{vmatrix} E(x_{12}-\overline{x_{12}})^2 & E[(x_{12}-\overline{x_{12}})\,(y_{12}-\overline{y_{12}})] \\ E[(y_{12}-\overline{y_{12}})\,(x_{12}-\overline{x_{12}})] & E(y_{12}-\overline{y_{12}})^2 \end{vmatrix} \quad (6.22)$$

6.4.1.1 Calculation of $P_{z12}(1,1)$

From the equation (6.20) we compute the first element of the error covariance matrix P_{12}, $[P_{z12}(1,1)]$, as follows:

$$P_{z12}(1,1) = E\,[(x_{12}-\overline{x_{12}})^2] = E\{[a_{11}\Delta\theta_1+a_{12}\Delta\theta_2+\frac{1}{2}a_{13x}(\Delta\theta_1^2-\sigma_{\theta1}^2) +$$

$$\frac{1}{2}a_{14x}(\Delta\theta_2^2-\sigma_{\theta2}^2)+a_{15x}\Delta\theta_1\Delta\theta_2]^2\}$$

$$= E\,[a_{11}^2\Delta\theta_1^2+a_{12}^2\Delta\theta_2^2+\frac{1}{4}a_{13x}^2(\Delta\theta_1^2-\sigma_{\theta1}^2)^2+\frac{1}{4}a_{14x}^2(\Delta\theta_2^2-\sigma_{\theta2}^2)^2 +$$

$$a_{15x}^2\Delta\theta_1^2\Delta\theta_2^2+a_{11}\Delta\theta_1 a_{12}\Delta\theta_2+a_{11}\Delta\theta_1(\frac{1}{2})a_{13x}(\Delta\theta_1^2-\sigma_{\theta 2}^2)\ +$$

$$a_{11}\Delta\theta_1(\frac{1}{2})a_{14x}(\Delta\theta_2^2-\sigma_{\theta 2}^2)+a_{11}\Delta\theta_1 a_{15x}\Delta\theta_1\Delta\theta_2\ +$$

$$a_{12}\Delta\theta_2(\frac{1}{2})a_{13x}(\Delta\theta_1^2-\sigma_{\theta 1}^2)+a_{12}\Delta\theta_2(\frac{1}{2})a_{14x}(\Delta\theta_2^2-\sigma_{\theta 2}^2)\ +$$

$$a_{12}\Delta\theta_2 a_{15x}\Delta\theta_1\Delta\theta_2+\frac{1}{2}a_{13x}(\Delta\theta_1^2-\sigma_{\theta 1}^2)\frac{1}{2}a_{14x}(\Delta\theta_2^2-\sigma_{\theta 2}^2)\ +$$

$$\frac{1}{2}a_{13x}(\Delta\theta_1^2-\sigma_{\theta 1}^2)a_{15x}\Delta\theta_1\Delta\theta_2+\frac{1}{2}a_{14x}(\Delta\theta_2^2-\sigma_{\theta 2}^2)a_{15x}\Delta\theta_1\Delta\theta_2$$

$$=a_{11}^2E(\Delta\theta_1^2)+a_{12}^2E(\Delta\theta_2^2)+\frac{1}{4}a_{13x}^2E[(\Delta\theta_1^2-\sigma_{\theta 1}^2)^2]+\frac{1}{4}a_{14x}^2E[(\Delta\theta_2^2-\sigma_{\theta 2}^2)]\ +$$

$$a_{15x}^2E(\Delta\theta_1^2\Delta\theta_2^2)+a_{11}a_{12}E(\Delta\theta_1\Delta\theta_2)+\frac{1}{2}a_{11}a_{13x}E[\Delta\theta_1(\Delta\theta_1^2-\sigma_{\theta 1}^2)]\ +$$

$$\frac{1}{2}a_{11}a_{14x}E[\Delta\theta_1(\Delta\theta_2^2-\sigma_{\theta 2}^2)]+a_{11}a_{15x}E(\Delta\theta_1^2\Delta\theta_2)\ +$$

$$\frac{1}{2}a_{12}a_{13x}E[\Delta\theta_2(\Delta\theta_1^2-\sigma_{\theta 1}^2)]+\frac{1}{2}a_{12}a_{14x}E[\Delta\theta_2(\Delta\theta_2^2-\sigma_{\theta 2}^2)]\ +$$

$$a_{12}a_{15x}E(\Delta\theta_1\Delta\theta_2^2)+\frac{1}{4}a_{13x}a_{14x}E[(\Delta\theta_1^2-\sigma_{\theta1}^2(\Delta\theta_2^2-\sigma_{\theta2}^2)] +$$

$$\frac{1}{2}a_{13x}a_{15x}E[(\Delta\theta_1^2-\sigma_{\theta1}^2)\Delta\theta_1\Delta\theta_2]+\frac{1}{2}a_{14x}a_{15x}E[(\Delta\theta_2^2-\sigma_{\theta2}^2)\Delta\theta_1\Delta\theta_2]$$

From appendix D, equation (D-1) is follows that

$$E(\Delta\theta_i)^3 = 0$$

also we know $E(\Delta\theta_i) = 0$

Therefore

$$P_{z12}(1,1) = a_{11}^2\sigma_{\theta1}^2+a_{12}^2\sigma_{\theta2}^2+\frac{1}{4}a_{13x}^2E(\Delta\theta_1^4-2\Delta\theta_1^2\sigma_{\theta1}^2+\sigma_{\theta1}^4) +$$

$$\frac{1}{4}a_{14x}^2E(\Delta\theta_2^4-2\Delta\theta_2^2\sigma_{\theta2}^2+\sigma_{\theta2}^4)+a_{15x}^2\sigma_{\theta1}^2\sigma_{\theta2}^2 +$$

$$\frac{1}{4}a_{13x}a_{14x}E(\Delta\theta_1^2\Delta\theta_2^2-\Delta\theta_1^2\sigma_{\theta2}^2-\sigma_{\theta1}^2\Delta\theta_2^2+\sigma_{\theta1}^2\sigma_{\theta2}^2)$$

$$= a_{11}^2\sigma_{\theta1}^2+a_{12}^2\sigma_{\theta2}^2+\frac{1}{4}a_{13x}^2E(\Delta\theta_1)^4 - \frac{1}{2}a_{13x}^2\sigma_{\theta1}^2\sigma_{\theta1}^2+\frac{1}{4}a_{13x}^2(\sigma_{\theta1}^2)^2 +$$

$$\frac{1}{4}a_{14x}^2E(\Delta\theta_2)^4-\frac{1}{2}a_{14x}^2\sigma_{\theta_2}^2\sigma_{\theta2}^2+\frac{1}{4}a_{14x}^2(\sigma_{\theta2}^2)^2+a_{15x}^2\sigma_{\theta1}^2\sigma_{\theta2}^2 +$$

$$\frac{1}{4}a_{13x}a_{14x}\sigma_{\theta1}^2\sigma_{\theta2}^2-\frac{1}{4}a_{13x}a_{14x}\sigma_{\theta1}^2\sigma_{\theta2}^2-\frac{1}{4}a_{13x}a_{14x}\sigma_{\theta1}^2\sigma_{\theta2}^2+\frac{1}{4}a_{13x}a_{14x}\sigma_{\theta1}^2\sigma_{\theta2}^2$$

From equations (A-7), and (B-10)

$$E(\Delta\theta_1^4) = \frac{\delta_u^4}{5}$$

$$E(\Delta\theta_2^4) = \frac{\delta_s^4}{3}$$

Therefore

$$P_{z12}(1,1) = a_{11}^2\sigma_{\theta1}^2 + a_{12}^2\sigma_{\theta2}^2 + \frac{a_{13x}^2\delta_u^4}{20} - \frac{1}{4}a_{13x}^2(\sigma_{\theta1}^2)^2 + \frac{a_{14x}^2\delta_s^4}{12} -$$

$$\frac{1}{4}a_{14x}^2(\sigma_{\theta2}^2)^2 + a_{15x}^2\sigma_{\theta1}^2\sigma_{\theta2}^2 \qquad (6.23)$$

6.4.1.2 Calculation of $P_{z12}(1,2)$

From the equations (6.19), and (6.20) we compute the second element of the covariance matrix P_{z12}, $[P_{z12}(1,2)]$, as follows:

$$P_{z12}(1,2) = \varepsilon_{x12}\varepsilon_{y12} = E[(x_{12} - \bar{x}_{12})(y_{12} - \bar{y}_{12})]$$

$$= \{ [a_{11}\Delta\theta_1 + a_{12}\Delta\theta_2 + \frac{1}{2}a_{13x}(\Delta\theta_1^2 - \sigma_{\theta1}^2) + \frac{1}{2}a_{14x}(\Delta\theta_2^2 - \sigma_{\theta2}^2) + a_{15x}\Delta\theta_1\Delta\theta_2] *$$

$$[a_{21}\Delta\theta_1 + a_{22}\Delta\theta_2 + \frac{1}{2}a_{13y}(\Delta\theta_1^2 - \sigma_{\theta1}^2) + \frac{1}{2}a_{14y}(\Delta\theta_2^2 - \sigma_{\theta2}^2) + a_{15y}\Delta\theta_1\Delta\theta_2] \}$$

$$= E\left[a_{11}a_{21}\Delta\theta_1^2+a_{11}a_{22}\Delta\theta_1\Delta\theta_2+\frac{1}{2}a_{11}a_{13y}\Delta\theta_1(\Delta\theta_1^2-\sigma_{\theta 1}^2)\right.+$$

$$a_{11}\Delta\theta_1\frac{1}{2}a_{14y}(\Delta\theta_2^2-\sigma_{\theta 2}^2)+a_{11}a_{15y}\Delta\theta_1^2\Delta\theta_2^2+a_{12}a_{21}\Delta\theta_2\Delta\theta_1+a_{12}a_{22}\Delta\theta_2^2+$$

$$\frac{1}{2}a_{12}a_{13y}\Delta\theta_2(\Delta\theta_1^2-\sigma_{\theta 1}^2)+a_{12}\Delta\theta_2\frac{1}{2}a_{14y}(\Delta\theta_2^2-\sigma_{\theta 2}^2)+a_{12}a_{15y}\Delta\theta_1\Delta\theta_2^2+$$

$$\frac{1}{2}a_{13x}(\Delta\theta_1^2-\sigma_{\theta 1}^2)\,(a_{21}\Delta\theta_1)+\frac{1}{2}a_{13x}a_{22}(\Delta\theta_1^2-\sigma_{\theta 1}^2)\Delta\theta_2+$$

$$\frac{1}{4}a_{13x}a_{13y}(\Delta\theta_1^2-\sigma_{\theta 1}^2)\,(\Delta\theta_1^2-\sigma_{\theta 1}^2)+\frac{1}{4}a_{13x}a_{14y}(\Delta\theta_1^2-\sigma_{\theta 1}^2)\,(\Delta\theta_2^2-\sigma_{\theta 2}^2)+$$

$$\frac{1}{2}a_{13x}a_{15y}(\Delta\theta_1^2-\sigma_{\theta 1}^2)\Delta\theta_1\Delta\theta_2+\frac{1}{2}a_{14x}a_{21}(\Delta\theta_2^2-\sigma_{\theta 2}^2)\Delta\theta_1+$$

$$\frac{1}{2}a_{14x}a_{22}(\Delta\theta_2^2-\sigma_{\theta 2}^2)\Delta\theta_2+\frac{1}{4}a_{14x}a_{13y}(\Delta\theta_2^2-\sigma_{\theta 2}^2(\Delta\theta_1^2-\sigma_{\theta 1}^2)+$$

$$\frac{1}{4}a_{14x}a_{14y}(\Delta\theta_2^2-\sigma_{\theta 2}^2)\,(\Delta\theta_2^2-\sigma_{\theta 2}^2)+\frac{1}{2}a_{14x}a_{15y}(\Delta\theta_2^2-\sigma_{\theta 2}^2)\Delta\theta_1\Delta\theta_2+$$

$$a_{15x}a_{21}\Delta\theta_1^2\Delta\theta_2+a_{15x}a_{22}\Delta\theta_1\Delta\theta_2^2+\frac{1}{2}a_{15x}a_{13y}\Delta\theta_1\Delta\theta_2(\Delta\theta_1^2-\sigma_{\theta 1}^2)+$$

$$\frac{1}{2}a_{15x}a_{14y}\Delta\theta_1\Delta\theta_2(\Delta\theta_2^2-\sigma_{\theta 2}^2)+a_{15x}a_{15y}\Delta\theta_1^2\Delta\theta_2^2]$$

Where

$$E(\Delta\theta_i) = 0,$$

$$E(\Delta\theta_i^3) = 0,$$

$$E(\Delta\theta_1^2) = \sigma_{\theta 1}^2, \text{ and}$$

$$E(\Delta\theta_2^2) = \sigma_{\theta 2}^2$$

Therefore

$$P_{x12}(1,2) = a_{11}a_{21}\sigma_{\theta 1}^2+a_{12}a_{22}\sigma_{\theta 2}^2+\frac{1}{4}a_{13x}a_{13y}E[\Delta\theta_1^4-\Delta\theta_1^2\sigma_{\theta 1}^2-\sigma_{\theta 1}^2\Delta\theta_1^2+\sigma_{\theta 1}^4]+$$

$$\frac{1}{4}a_{13x}a_{14y}E[\Delta\theta_1^2\Delta\theta_2^2-\Delta\theta_1^2\sigma_{\theta 2}^2-\sigma_{\theta 1}^2\Delta\theta_2^2+\sigma_{\theta 1}^2\sigma_{\theta 2}^2] +$$

$$\frac{1}{4}a_{14x}a_{13y}E[\Delta\theta_2^2\Delta\theta_1^2-\Delta\theta_2^2\sigma_{\theta 1}^2-\sigma_{\theta 2}^2\Delta\theta_1^2+\sigma_{\theta 1}^2\sigma_{\theta 2}^2] +$$

$$\frac{1}{4}a_{14x}a_{14y}E[\Delta\theta_2^4-\Delta\theta_2^2\sigma_{\theta 2}^2-\sigma_{\theta 2}^2\Delta\theta_2^2+\sigma_{\theta 2}^4]+a_{15x}a_{15y}E(\Delta\theta_1^2\Delta\theta_2^2)$$

$$= a_{11}a_{12}\sigma_{\theta 1}^2+a_{12}a_{22}\sigma_{\theta 2}^2+\frac{1}{4}a_{13x}a_{13y}E(\Delta\theta_1^4)-\frac{1}{2}a_{13x}a_{13y}(\sigma_{\theta 1}^2)^2 +$$

$$\frac{1}{4}a_{13x}a_{13y}(\sigma_{\theta 1}^2)^2+\frac{1}{4}a_{13x}a_{14y}\sigma_{\theta 1}^2\sigma_{\theta 2}^2-\frac{1}{4}a_{13x}a_{14y}\sigma_{\theta 1}^2\sigma_{\theta 2}^2 -$$

$$\frac{1}{4}a_{13x}a_{14y}\sigma_{\theta 1}^2\sigma_{\theta 2}^2+\frac{1}{4}a_{13x}a_{14y}\sigma_{\theta 1}^2\sigma_{\theta 2}^2+\frac{1}{4}a_{14x}a_{13y}\sigma_{\theta 2}^2\sigma_{\theta 1}^2 -$$

$$\frac{1}{2}a_{14x}a_{13y}\sigma_{\theta 1}^2\sigma_{\theta 2}^2+\frac{1}{4}a_{14x}a_{13y}\sigma_{\theta 1}^2\sigma_{\theta 2}^2+\frac{1}{4}a_{14x}a_{14y}E(\Delta\theta_2^4) -$$

$$\frac{1}{2}a_{14x}a_{14y}(\sigma_{\theta 2}^2)^2+\frac{1}{4}a_{14x}a_{14y}(\sigma_{\theta 2}^2)^2+a_{15x}a_{15y}\sigma_{\theta 1}^2\sigma_{\theta 2}^2$$

From equations (A-7), and (B-10) we see

$$E(\Delta\theta_1^4)=\frac{\delta_u}{5}$$

$$E(\Delta\theta_2^4)=\frac{\delta_s^4}{3}$$

Therefore

$$P_{x12}(1,2) = E\left[(x_{12}-\overline{x_{12}})(y_{12}-\overline{y_{12}})\right]$$

$$= a_{11}a_{21}\sigma_{\theta 1}^2+a_{12}a_{22}\sigma_{\theta 2}^2 + \frac{1}{20}a_{13x}a_{13y}\delta_u^4-\frac{1}{4}a_{13x}a_{13y}(\sigma_{\theta 1}^2)^2 +$$

$$\frac{1}{12}a_{14x}a_{14y}\delta_s^4-\frac{1}{4}a_{14x}a_{14y}(\sigma_{\theta 2}^2)^2+a_{15x}a_{15y}\sigma_{\theta 1}^2\sigma_{\theta 2}^2 \qquad (6.24)$$

6.4.1.3 Calculation of $P_{x12}(2,1)$

From the equation (6.22) we see:

$$P_{z12}(2,1) = E[(y_{12}-\bar{y}_{12})(x_{12}-\bar{x}_{12})]$$

$$= P_{z12}(1,2)$$

Therefore

$$P_{z12}(2,1) = E\{[(y_{12}-\overline{y_{12}})(x_{12}-\overline{x_{12}})]\}$$

$$= a_{11}a_{21}\sigma_{\theta 1}^2+a_{12}a_{22}\sigma_{\theta 2}^2+\frac{1}{20}a_{13x}a_{13y}\delta_u^4-\frac{1}{4}a_{13x}a_{13y}(\sigma_{\theta 1}^2)^2 +$$

$$\frac{1}{12}a_{14x}a_{14y}\delta_s^4-\frac{1}{4}a_{14x}a_{14y}(\sigma_{\theta 2}^2)^2+a_{15x}a_{15y}\sigma_{\theta 1}^2\sigma_{\theta 2}^2 \qquad (6.25)$$

6.4.1.4 Calculation $P_{z12}(2,2)$

From the equation (6.21) we compute the fourth element for the error covariance matrix P_{z12}, $[P_{z12}(2,2)]$, as follows:

$$P_{z12}(2,2) = E\{[(y_{12}-\bar{y}_{12})^2]\}$$

$$= E\{[a_{21}\Delta\theta_1+a_{22}\Delta\theta_2+\frac{1}{2}a_{13y}(\Delta\theta_1^2-\sigma_{\theta 1}^2)+\frac{1}{2}a_{14y}(\Delta\theta_2^2-\sigma_{\theta 2}^2) +$$

$$a_{15y}\Delta\theta_1\Delta\theta_2]^2\}$$

$$= E\{[a_{21}^2\Delta\theta_1^2+a_{22}^2\Delta\theta_2^2+\frac{1}{4}a_{13y}^2(\Delta\theta_1^2-\sigma_{\theta 1}^2)^2+\frac{1}{4}a_{14y}^2(\Delta\theta_2^2-\sigma_{\theta 2}^2)^2 +$$

$$a_{15y}^2\Delta\theta_1^2\Delta\theta_2^2+a_{21}a_{22}\Delta\theta_1\Delta\theta_2+a_{21}\frac{1}{2}a_{13y}\Delta\theta_1(\Delta\theta_1^2-\sigma_{\theta 1}^2) +$$

$$a_{21}\frac{1}{2}a_{14y}\Delta\theta_1(\Delta\theta_2^2-\sigma_{\theta 2}^2)+a_{21}a_{15y}\Delta\theta_1^2\Delta\theta_2+a_{22}\frac{1}{2}a_{13y}\Delta\theta_2(\Delta\theta_1^2-\sigma_{\theta 1}^2)\ +$$

$$a_{22}\frac{1}{2}a_{14y}\Delta\theta_2(\Delta\theta_2^2-\sigma_{\theta 2}^2)+a_{22}a_{15y}\Delta\theta_1\Delta\theta_2+\frac{1}{4}a_{13y}a_{14y}(\Delta\theta_1^2-\sigma_{\theta 1}^2)(\Delta\theta_2^2-\sigma_{\theta 2}^2)\ +$$

$$\frac{1}{2}a_{13y}a_{15y}(\Delta\theta_1^2-\sigma_{\theta 1}^2)\Delta\theta_1\Delta\theta_2+\frac{1}{2}a_{14y}(\Delta\theta_1^2-\sigma_{\theta 2}^2)a_{15y}\Delta\theta_1\Delta\theta_2]\ \}$$

Where:

$E(\Delta\theta_i) = 0,$

$E(\Delta\theta_i^2) = \sigma_{\theta i}^2$

$E(\Delta\theta_1\Delta\theta_2) = E(\Delta\theta_1)E(\Delta\theta_2) = 0$ and

$E(\Delta\theta_i)^3 = 0$

Therefore

$$P_{x12}(2,2) = a_{21}^2\sigma_{\theta 1}^2+a_{22}^2\sigma_{\theta 2}^2+\frac{1}{4}a_{13y}^2E(\Delta\theta_1^2-\sigma_{\theta 1}^2)^2+\frac{1}{4}a_{14y}^2E(\Delta\theta_2^2-\sigma_{\theta 2}^2)^2\ +$$

$$a_{15y}^2\sigma_{\theta 1}^2\sigma_{\theta 2}^2+\frac{1}{4}a_{13y}a_{14y}E\{[(\Delta\theta_1^2-\sigma_{\theta 1}^2)(\Delta\theta_2^2-\sigma_{\theta 2}^2)]\ \}$$

$$= a_{21}^2\sigma_{\theta 1}^2+a_{22}^2\sigma_{\theta 2}^2+\frac{1}{4}a_{13y}^2E\{[\Delta\theta_1^4-2\Delta\theta_1^2\sigma_{\theta 1}^2+(\sigma_{\theta 1}^2)^2]\ \}\ +$$

$$\frac{1}{4}a_{14y}^2E\{[\Delta\theta_2^4-2\Delta\theta_2^2\sigma_{\theta 2}^2+(\sigma_{\theta 2}^2)^2]\ \}+a_{15y}^2\sigma_{\theta 1}^2\sigma_{\theta 2}^2\ +$$

$$\frac{1}{4}a_{13y}a_{14y}E\{[\Delta\theta_1^2\Delta\theta_2^2-\Delta\theta_1^2\sigma_{\theta 2}^2-\sigma_{\theta 1}^2\Delta\theta_2^2+\sigma_{\theta 1}^2\sigma_{\theta 2}^2]\}$$

$$= a_{21}^2\sigma_{\theta 1}^2+a_{22}^2\sigma_{\theta 2}^2+\frac{1}{4}a_{13y}^2E(\Delta\theta_1^4)-\frac{1}{2}a_{13y}^2(\sigma_{\theta 1}^2)^2+\frac{1}{4}a_{13y}^2(\sigma_{\theta 1}^2)^2 +$$

$$\frac{1}{4}a_{14y}^2E(\Delta\theta_2^4)-\frac{1}{2}a_{14y}^2(\sigma_{\theta 2}^2)^2+\frac{1}{4}a_{14y}^2(\sigma_{\theta 2}^2)^2+a_{15y}^2\sigma_{\theta 1}^2\sigma_{\theta 2}^2 +$$

$$\frac{1}{4}a_{13y}a_{14y}\sigma_{\theta 1}^2\sigma_{\theta 2}^2-\frac{1}{4}a_{13y}a_{14y}\sigma_{\theta 1}^2\sigma_{\theta 2}^2-\frac{1}{4}a_{14y}a_{13y}\sigma_{\theta 1}^2\sigma_{\theta 2}^2+\frac{1}{4}a_{13y}a_{14y}\sigma_{\theta 1}^2\sigma_{\theta 2}^2$$

$$= a_{21}^2\sigma_{\theta 1}^2+a_{22}^2\sigma_{\theta 2}^2+\frac{1}{4}a_{13y}^2E(\Delta\theta_1^4)-\frac{1}{4}a_{13y}^2(\sigma_{\theta 1}^2)^2 +$$

$$\frac{1}{4}a_{14y}^2E(\Delta\theta_2^4)-\frac{1}{4}a_{14y}^2(\sigma_{\theta 2}^2)^2+a_{15y}^2\sigma_{\theta 1}^2\sigma_{\theta 2}^2$$

From equations (A-7), and (B-10)

$$E(\Delta\theta_1^4) = \frac{\delta_u^4}{5}$$

$$E(\Delta\theta_2^4) = \frac{\delta_s^4}{3}$$

Therefore

$$P_{z12}(2,2) = a_{21}^2\sigma_{\theta 1}^2 + a_{22}^2\sigma_{\theta 2}^2 + \frac{1}{20}a_{13y}^2\delta_u^4 - \frac{1}{4}a_{13y}^2(\sigma_{\theta 1}^2)^2 +$$

$$\frac{1}{12}a_{14y}^2\delta_s^4 - \frac{1}{4}a_{14y}^2(\sigma_{\theta 2}^2)^2 + a_{15y}^2\sigma_{\theta 1}^2\sigma_{\theta 2}^2 \qquad (6.26)$$

6.4.2 The Error Covariance Matrix P_{z23}

It is not necessary to recompute the expressions for the elements of P_{z23}. The equations computed the elements of P_{z12} may be used to compute the elements of P_{z23}. This is accomplished by replacing θ_1, θ_2, $\sigma_{\theta 1}$, $\sigma_{\theta 2}$, x_{12}, y_{12}, ε_{x12}, and ε_{y12} with θ_2, θ_3, $\sigma_{\theta 2}$, $\sigma_{\theta 3}$, x_{23}, y_{23}, ε_{x23}, and ε_{y23} respectively, and using equation (C-10) to computes $E(\Delta\theta_3)^4$.

From equation (C-10) we see

$$E(\Delta\theta_3)^4 = \frac{(\delta_t)^4}{15}$$

The resulting equations are as follow:

$$P_{z23}(1,1) = E\{(x_{23} - \bar{x}_{23})^2\}$$

$$= a_{11}^2\sigma_{\theta 2}^2 + a_{12}^2\sigma_{\theta 3}^2 + \frac{a_{13x}^2\delta_s^4}{12} - \frac{1}{4}a_{13x}^2(\sigma_{\theta 2}^2)^2 +$$

$$\frac{a_{14x}^2\delta_t^4}{60} - \frac{1}{4}a_{14x}^2(\sigma_{\theta 3}^2)^2 + a_{15x}^2\sigma_{\theta 2}^2\sigma_{\theta 3}^2 \qquad (6.27)$$

$$P_{z23}(1,2) = E\{(x_{23}-\bar{x}_{23})(y_{23}-\bar{y}_{23})\}$$

$$= a_{11}a_{21}\sigma_{\theta 2}^2 + a_{12}a_{22}\sigma_{\theta 3}^2 + \frac{a_{13x}a_{13y}\delta_s^4}{12} - \frac{1}{4}a_{13x}a_{13y}(\sigma_{\theta 2}^2)^2 +$$

$$\frac{a_{14x}a_{14y}\delta_s^4}{60} - \frac{1}{4}a_{14x}a_{14y}(\sigma_{\theta 3}^2)^2 + a_{15x}a_{15y}\sigma_{\theta 2}^2\sigma_{\theta 3}^2 \qquad (6.28)$$

$$P_{z23}(2,1) = E\{(y_{23}-\bar{y}_{23})(x_{23}-\bar{x}_{23})\} = P_{z23}(1,2)$$

$$= a_{11}a_{21}\sigma_{\theta 2}^2 + a_{12}a_{22}\sigma_{\theta 3}^2 + \frac{a_{13x}a_{13y}\delta_s^4}{12} - \frac{1}{4}a_{13x}a_{13y}(\sigma_{\theta 2}^2)^2 +$$

$$\frac{a_{14x}a_{14y}\delta_s^4}{60} - \frac{1}{4}a_{14x}a_{14y}(\sigma_{\theta 3}^2)^2 + a_{15x}a_{15y}\sigma_{\theta 2}^2\sigma_{\theta 3}^2 \qquad (6.29)$$

$$P_{z23}(2,2) = E\{(y_{23}-\bar{y}_{23})^2\}$$

$$= a_{21}^2\sigma_{\theta 2}^2 + a_{22}^2\sigma_{\theta 3}^2 + \frac{a_{13y}^2\delta_s^4}{12} - \frac{1}{4}a_{13y}^2(\sigma_{\theta 2}^2)^2 + \frac{a_{14y}^2\delta_t^4}{60} -$$

$$\frac{1}{4}a_{14y}^2(\sigma_{\theta 3}^2)^2 + a_{15y}^2\sigma_{\theta 2}^2\sigma_{\theta 3}^2 \qquad (6.30)$$

The next section discusses simulation results for the covariance matrices P_{z12}, and P_{z23} using second-order terms.

6.5 Discussion of Simulation Results, Scenario no1, Low-Noise Case, and High-Noise Case Using Second-Order Terms

The computer simulation was run 50 times and the results are plotted and discussed in the next several pages.

Figure (6.1) shows the actual errors in the noisy measurements x_{12} from triangulation between sensors S1, and S2, where (scenario no1 ho1) means scenario no1 high-order terms, low-noise case, and (scenario no1 hoh) means scenario no1 high-order terms, high-noise case. The dotted line represents the actual errors in the noisy measurements x_{12}, and the solid line represents the square root of $P_{z12}(1,1)$ in low-noise case in scenario no1 using second-order terms in the covariance matrix. The solid line is the theoretical standard deviation of the errors according to the second-order approximation to the covariance matrix.

We are interested in comparing the change in the standard deviation using the second-order terms with the standard deviation using the first-order approximation. Comparing the theoretical standard deviation using the second-order terms in figure

(6.1) with the theoretical standard deviation using first-order approximation in low-noise case in scenario no1 in figure (5.3) we see the theoretical standard deviation in the two cases are almost equal. The second-order terms do not give any large change. This is because in the low-noise case in scenario no1 using the first-order approximation the theoretical standard deviation was found to be close to the actual numeric standard deviation of the errors. So we would not expect any changes by including the second-order terms.

Figure (6.2) shows the actual errors in the noisy measurements x_{23} from triangulation between sensors S2, and S3. The dotted line represents the actual errors in the noisy measurements x_{23}, and the solid line represents the square root of $P_{z23}(1,1)$ in low-noise case in scenario no1 using second-order terms in the covariance matrix. The solid line is the theoretical standard deviation of the errors according to the second-order approximation to the covariance matrix.

Comparing the theoretical standard deviation using the second-order terms in figure (6.2) with the theoretical standard deviation using first-order approximation in low-noise case in scenario no1 in figure (5.4) we see the theoretical standard deviation in the two cases are almost equal. We see

that the second-order terms do not make any large difference. This is because in the low-noise case first-order approximation in scenario no1 the theoretical standard deviation was found to be close to the actual numeric standard deviation of the errors. So we would not expect any changes by including the second-order terms.

Figure (6.3) shows the actual errors in the noisy measurements y_{12} from triangulation between sensors S1, and S2, and figure (6.4) shows the actual errors in the noisy measurements y_{23} from triangulation between sensors S2, and S3.

Likewise in figures (6.3), and (6.4) there was no difference in the theoretical standard deviation of the errors using second-order terms, when compared with those in figures (5.7), and (5.8).

In scenario no1, high-noise case, the second-order terms did not produce any noticeable difference either. Figures (6.5), (6.6), (6.7), and (6.8) are almost identical to the corresponding figures (5.13), (5.14), (5.17), and (5.18) which used only the first-order approximation.

Again, the first-order approximation to the covariance matrix was found to be close to the numerical variances.

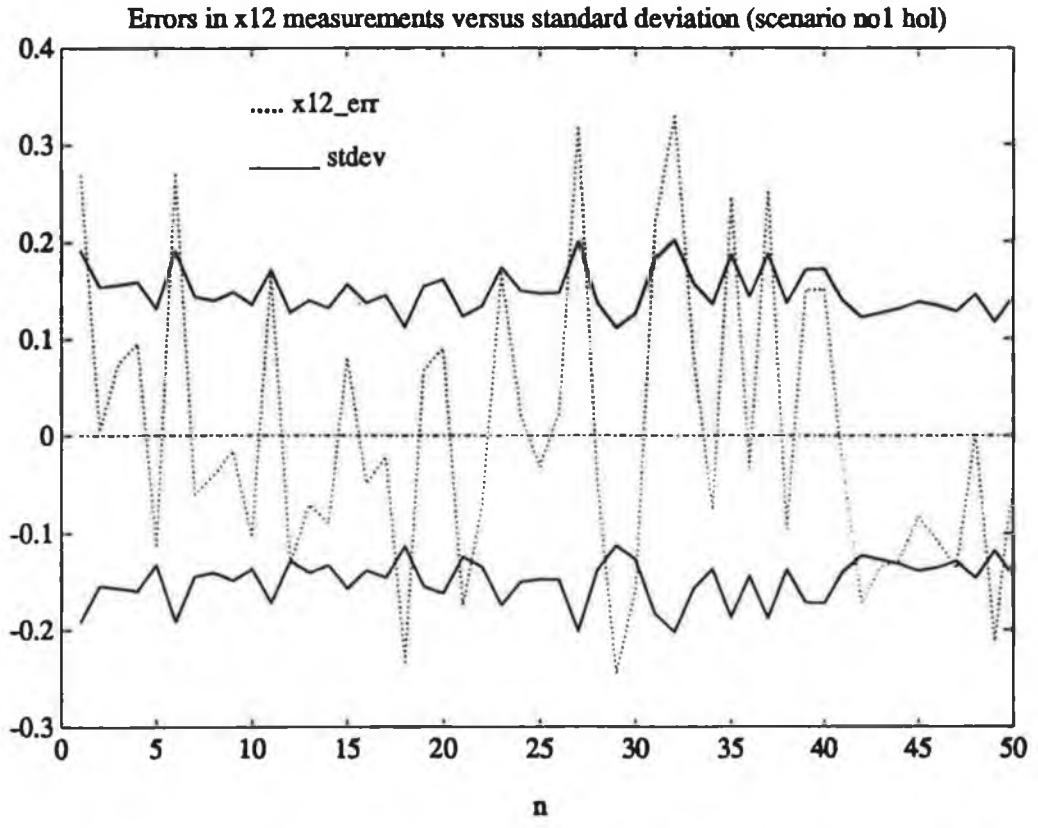

Figure (6.1)

.... x12_err represents the actual errors in the noisy measurements x_{12} in low-noise case in scenario no1 in x position.

___ stdev represents the square root of $P_{z12}(1,1)$, the theoretical standard deviation of the errors according to the second-order approximation to the covariance matrix in low-noise case in scenario no1 in x position.

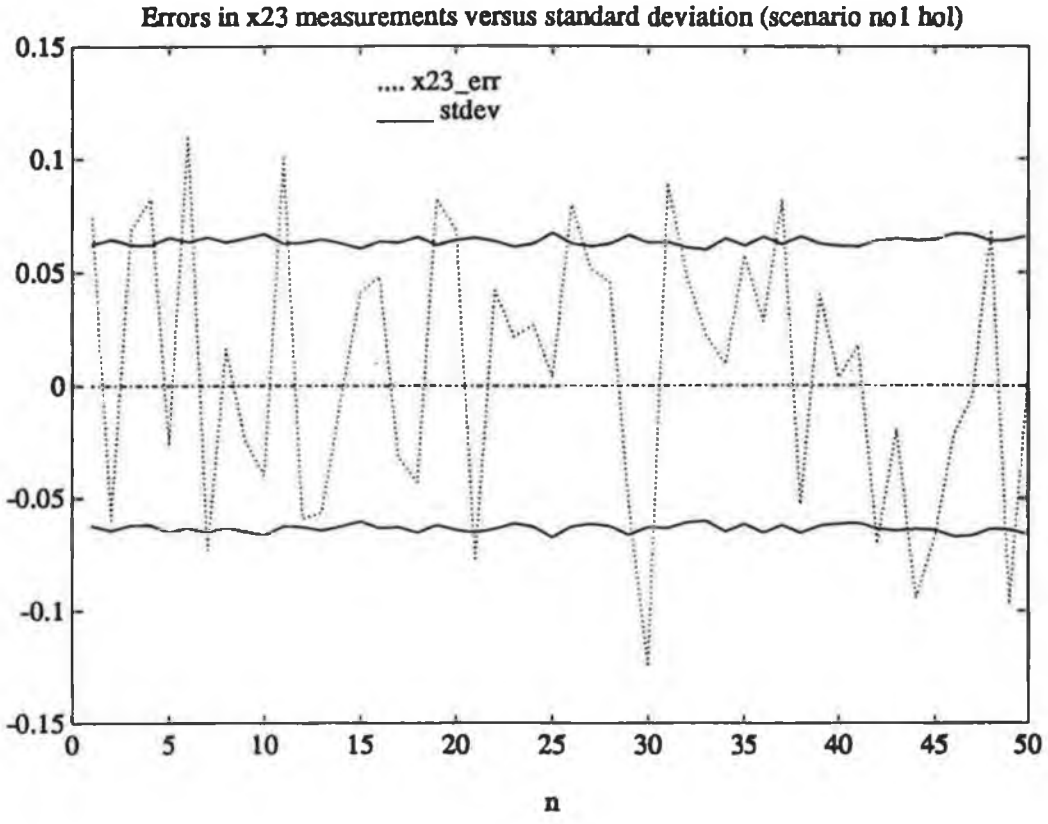

Figure (6.2)

.... x23_err represents the actual errors in the noisy measurements x_{23} in low-noise case in scenario no1 in x position.

___ stdev represents the square root of $P_{z23}(1,1)$, the theoretical standard deviation of the errors according to the second-order approximation to the covariance matrix in low-noise case in scenario no1.

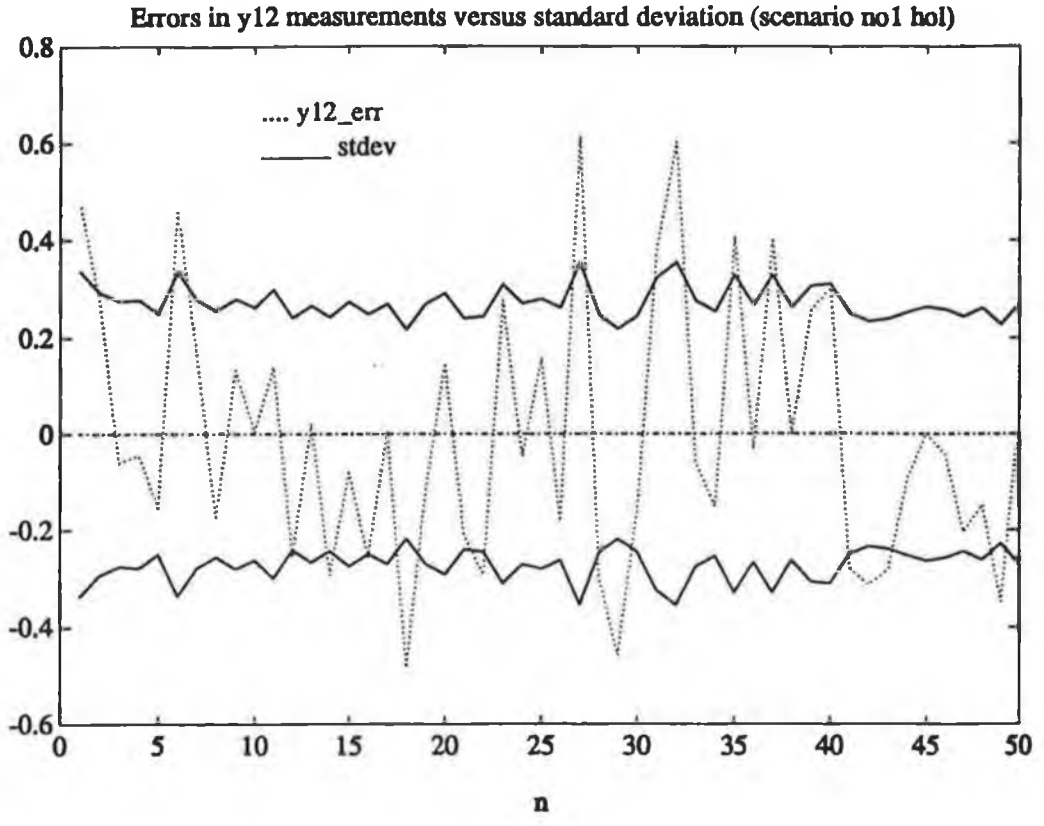

Figure (6.3)

.... y12_err represents the actual errors in the noisy measurements y_{12} in low-noise case in scenario no1 in y position.

_____ stdev represents the square root of $P_{z12}(2,2)$, the theoretical standard deviation of the errors according to the second-order approximation to the covariance matrix in low-noise case in scenario no1.

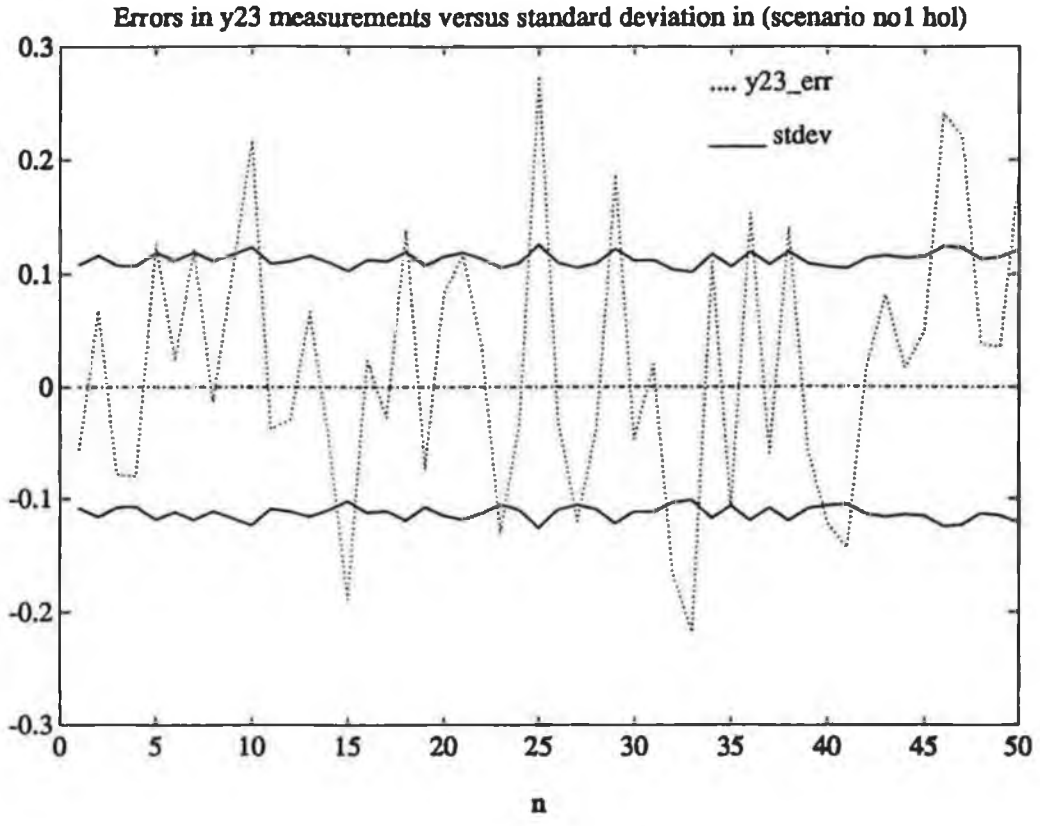

Figure (6.4)

.... represents the actual errors in the noisy measurements y_{23} in low-noise case in scenario no1 in y position.

____ stdev represents the square root of $P_{z23}(2,2)$, the theoretical standard deviation of the errors according to the covariance matrix in low-noise case in scenario no1 in y position using second-order terms.

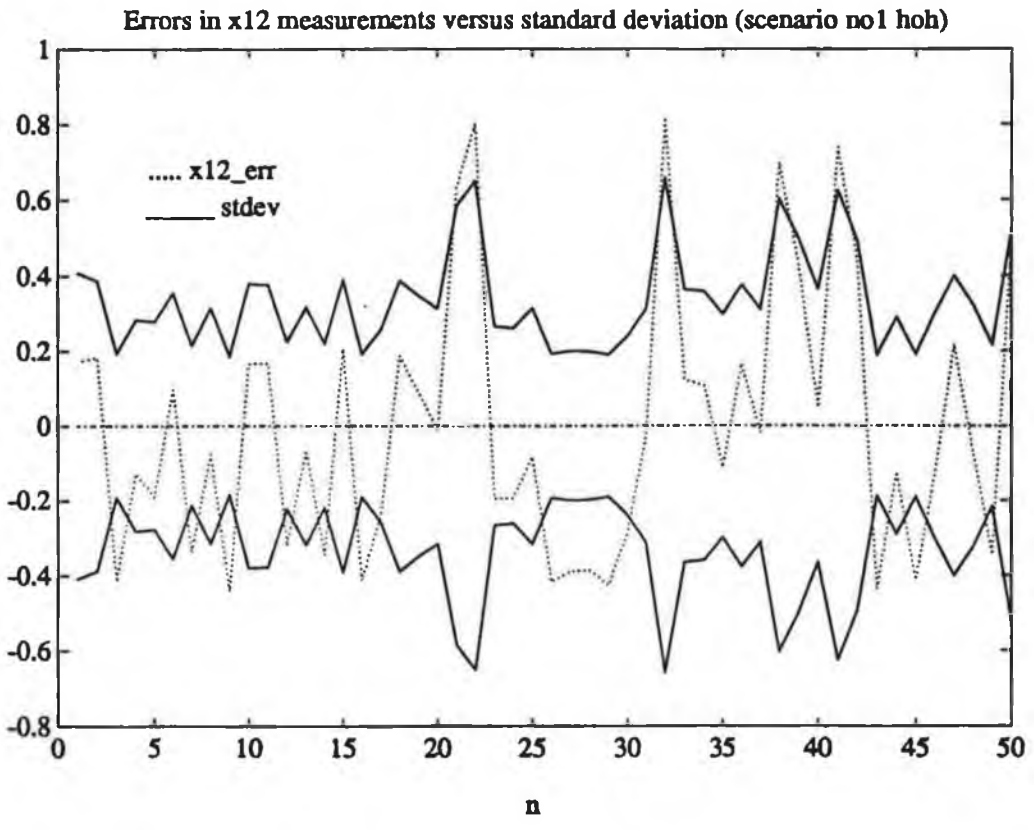

Figure (6.5)

.... x12_err represents the actual errors in the noisy measurements x_{12} in high-noise case in scenario no1 in x position.

___ stdev represents the square root of $P_{z12}(1,1)$, the theoretical standard deviation of the errors according to the second-order approximation to the covariance matrix in high-noise case in scenario no1 in x position.

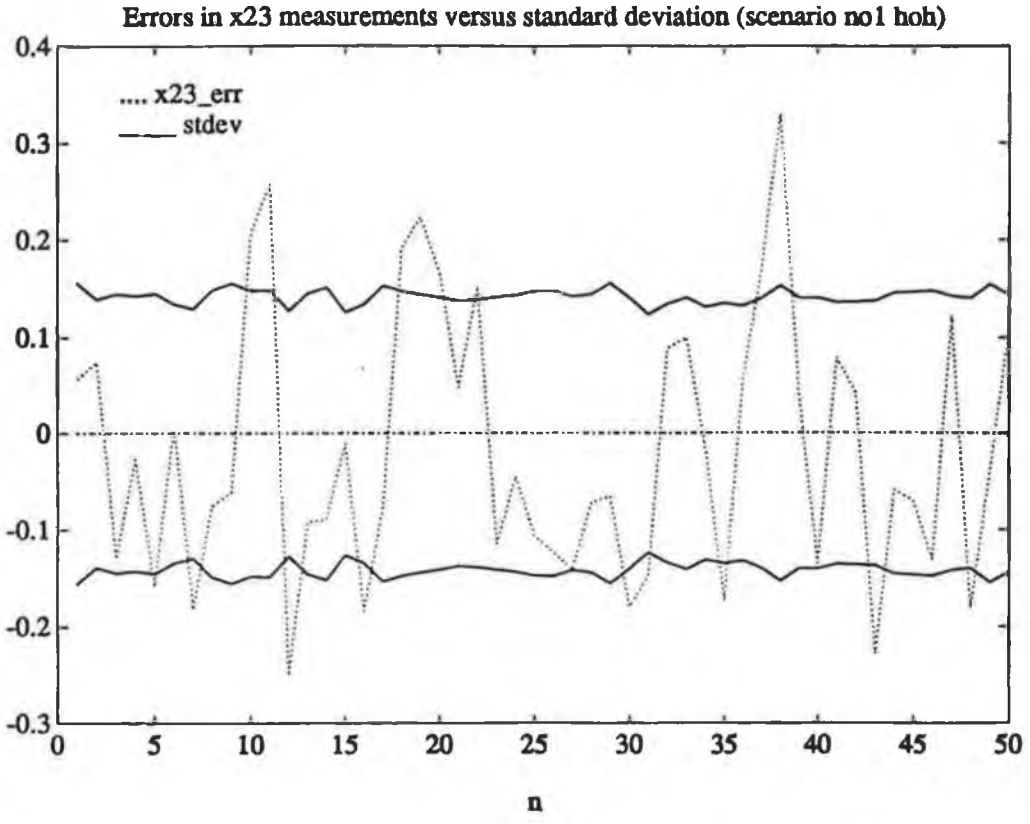

Figure (6.6)

.... x23_err represents the actual errors in the noisy measurements x_{23} in high-noise case in scenario no1 in x position.

___ stdev represents the square root of $P_{z23}(1,1)$, the theoretical standard deviation of the errors according to the second-order approximation to the covariance matrix in high-noise case in scenario no1 in x position.

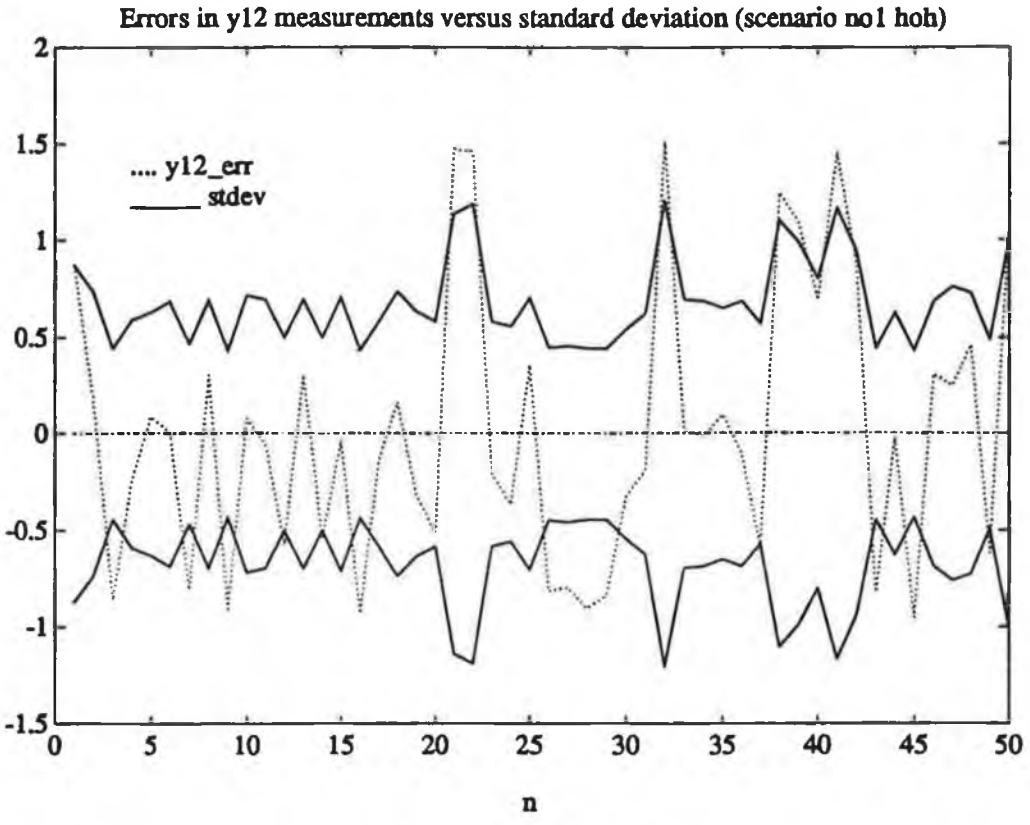

Figure (6.7)

.... y12_err represents the actual errors in the noisy measurements y_{12} in high-noise case in scenario no1 in y position.

_____ stdev represents the square root of $P_{z12}(2,2)$, the theoretical standard deviation of the errors according to the second-order approximation to the covariance matrix in high-noise case in scenario no1 in y position.

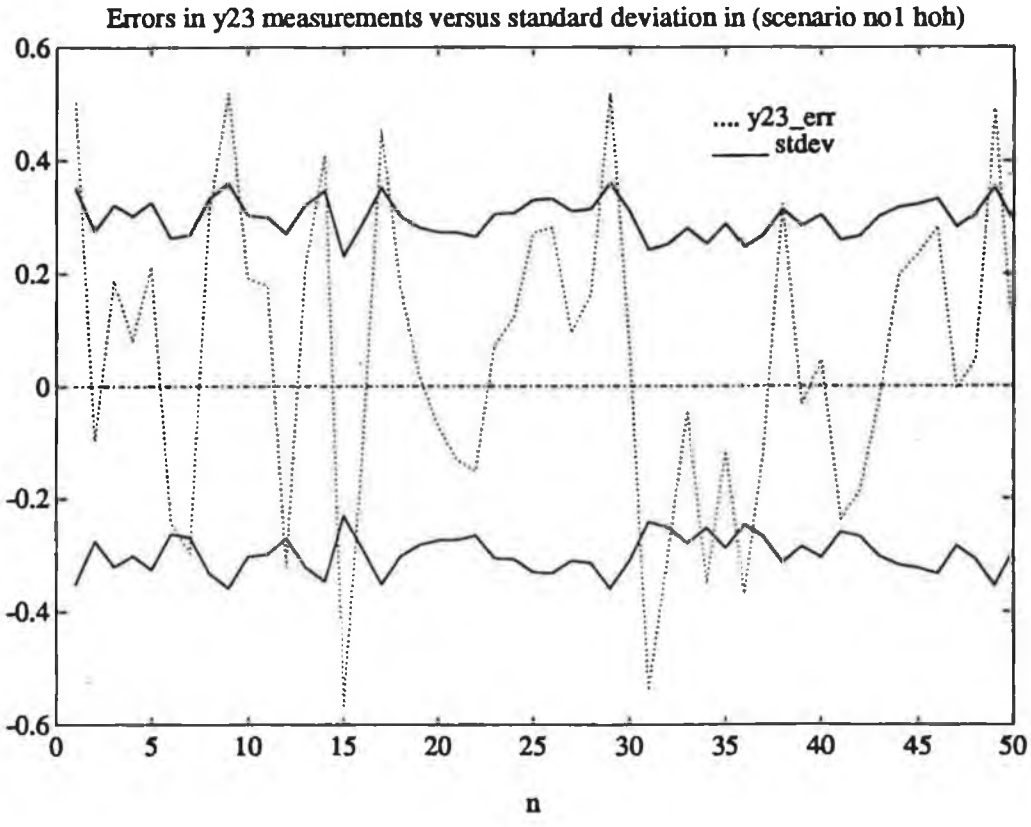

Figure (6.8)

.... y23_err represents the actual errors in the noisy measurements y_{23} in high-noise case in scenario no1 in y position.

____ stdev represents the square of P_{z23} (2,2), the theoretical standard deviation of the errors according to the second-order approximation to the covariance matrix in high-noise case in scenario no1 in y position.

The next section discusses the simulation results for the covariance matrices P_{z12}, and P_{z23} for low-noise case in scenario no2 using the high-order terms.

6.6 Discussion of Simulation Results, Scenario no2, Low-Noise Case Using Second-Order Terms

In this section we describe some simulation results for low-noise case, scenario no2 using second-order terms.

The computer simulation was run 50 times and the results are plotted and discussed in the next several pages.

Figure (6.9) shows the actual errors in the noisy measurements x_{12} from triangulation between sensors S1, and S2, where (scenario no2hol) means scenario number two high-order terms low-noise case. The dotted line represents the actual errors in the noisy measurements x_{12}, and the solid line represents the square root of $P_{z12}(1,1)$ in low-noise case in scenario no2 using the second-order terms in the covariance matrix. The solid line is theoretical standard deviation of the errors according to the second-order approximation to the covariance matrix.

We are interested in comparing the changes in the standard deviation using the second-order terms with the standard deviation using the first-order approximation.

Comparing the theoretical standard deviation in low-

noise case in scenario no2 using the second-order terms in figure (6.9) with the theoretical standard deviation in low-noise case in scenario no2 using the first-order approximation in figure (5.24), the theoretical standard deviation including the second-order terms is slightly greater than the theoretical standard deviation including the first-order approximation. This is not obvious from the graph because of the resolution. For example at n = 5, the theoretical standard deviation in figure (6.9) is equal to 0.77598, but in figure (5.24) it is equal to 0.76883. It is the same thing at n = 27 where the theoretical standard deviation in figure (6.9) is 0.69536, but in figure (5.24) it is equal to 0.68959. The theoretical standard deviation in figure (6.9) is greater than the theoretical standard deviation in figure (5.24) at the most cases.

Figure (6.10) shows the actual errors in the noisy measurements x_{23} from triangulation between sensors S2, and S3. The dotted line represents the actual errors in the noisy measurements x_{23}, and the solid line represents the square root of $P_{z23}(1,1)$ in low-noise case in scenario no2 using the second-order terms in the covariance matrix. The solid line is the theoretical standard deviation of the errors according to the second-order approximation to the covariance matrix.

Comparing the theoretical standard deviation in low-noise case in scenario no2 using the second-order terms in figure (6.10) with the theoretical standard deviation in low-noise case in scenario no2 using the first-order approximation in figure (5.25), the theoretical standard deviation including the second-order terms most of the times is slightly greater than the theoretical standard deviation including the first-order approximation. This it is not obvious from the graph because of the resolution. For example at n = 3, the theoretical standard deviation in figure (6.10) is equal to 2.0553, but in figure (5.25) it is equal to 1.9442. It is the same thing at n = 29 where the theoretical standard deviation in figure (6.9) is 0.8743, but in figure (5.25) is equal to 0.8521. The theoretical standard deviation in figure (6.10) is greater than the theoretical standard deviation in figure (5.25) in most cases. The increase in variances is to be expected as scenario no2 is a noisier triangulation process than scenario no1 between sensors S2, and S3.

Figure (6.11) shows the actual errors in the noisy measurements y_{12} from triangulation between sensors S1, and S2. The dotted line represents the actual errors in the noisy measurements y_{12}, and the solid line represents the square root of $P_{z12}(2,2)$ in low-noise case in scenario no2 using the second-order

terms in the covariance matrix. The solid line is theoretical standard deviation of the errors according to the second-order approximation to the covariance matrix.

Again we see an increase in variances in figure (6.11) and figure (6.12) comparing with Figure (5.28) and figure (5.29) for y_{12}, and y_{23}, respectively which used first-order approximation. For example at n = 5, the theoretical standard deviation in figure (6.11) is equal to 0.5546, but in figure (5.28) is equal to 0.5497. We see the theoretical standard deviation in figure (6.11) is greater than the theoretical standard deviation in figure (5.28) in most cases.

Also at n = 3 the theoretical standard deviation in figure (6.12) is equal to 2.4873, but in figure (5.29) is equal to 2.3623. It is same thing at n = 30 where the theoretical standard deviation in the figure (6.12) is 1.5568, but in figure (5.29) is equal to 1.5076. We see the theoretical standard deviation in figure (6.12) is greater than the theoretical standard deviation in figure (5.29) in most cases.

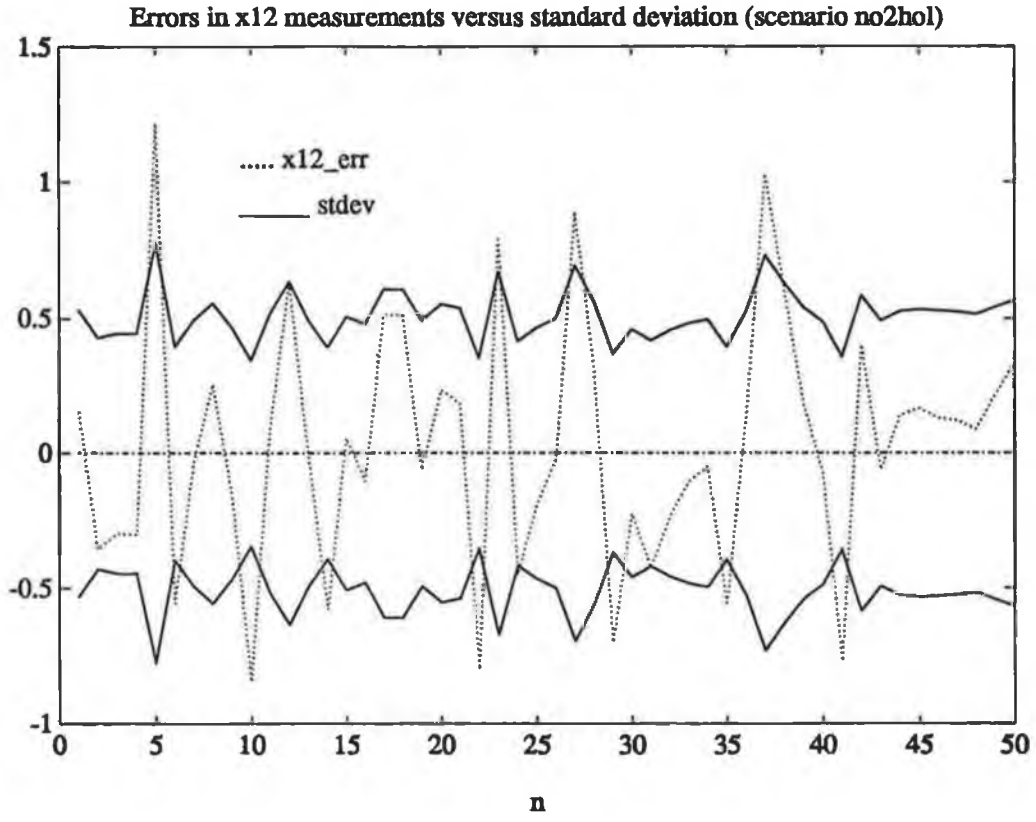

Figure (6.9)

.... x12_err represents the actual errors in the noisy measurements x_{12} in low-noise case in scenario no2 in x position.

_____ stdev represents the square root of $P_{z12}(1,1)$, the theoretical standard deviation of the errors according to the second-order approximation to the covariance matrix in low-noise case in scenario no2.

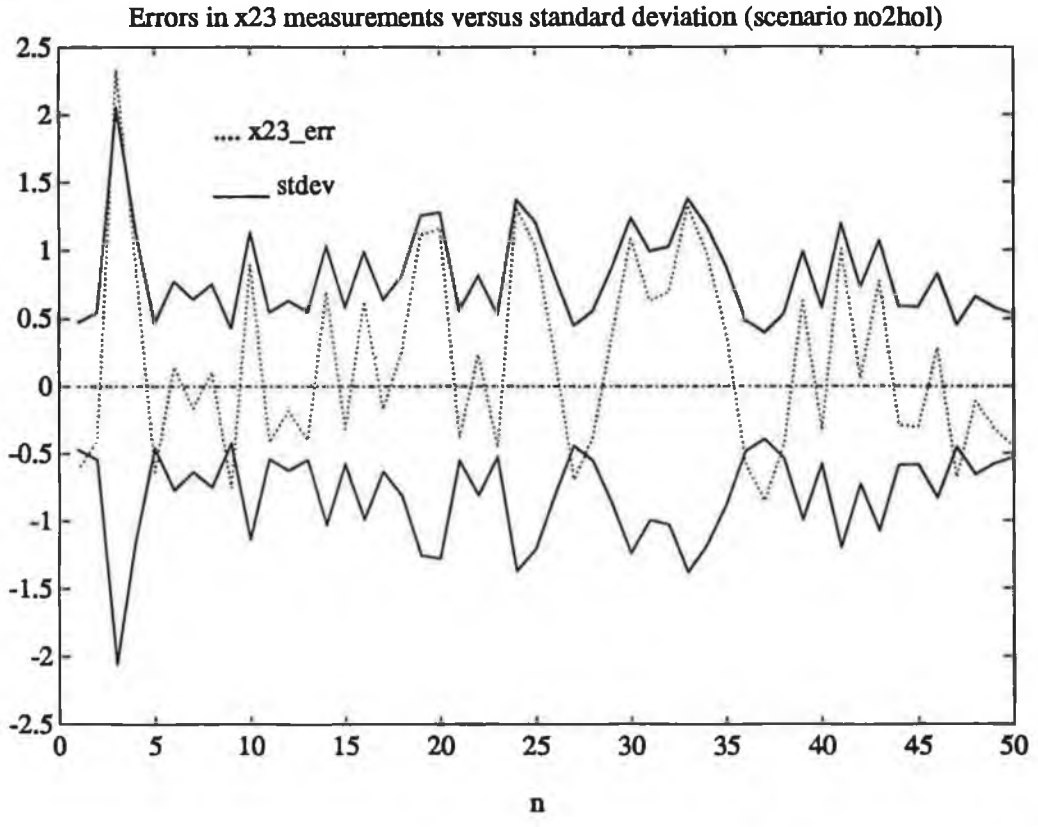

Figure (6.10)

.... x23_err represents the actual errors in the noisy measurements x_{23} in low-noise case in scenario no2 in x position.

____ stdev represents the square root of $P_{z23}(1,1)$, the theoretical standard deviation of the errors according to the second-order approximation to the covariance matrix in low-noise case in scenario no2.

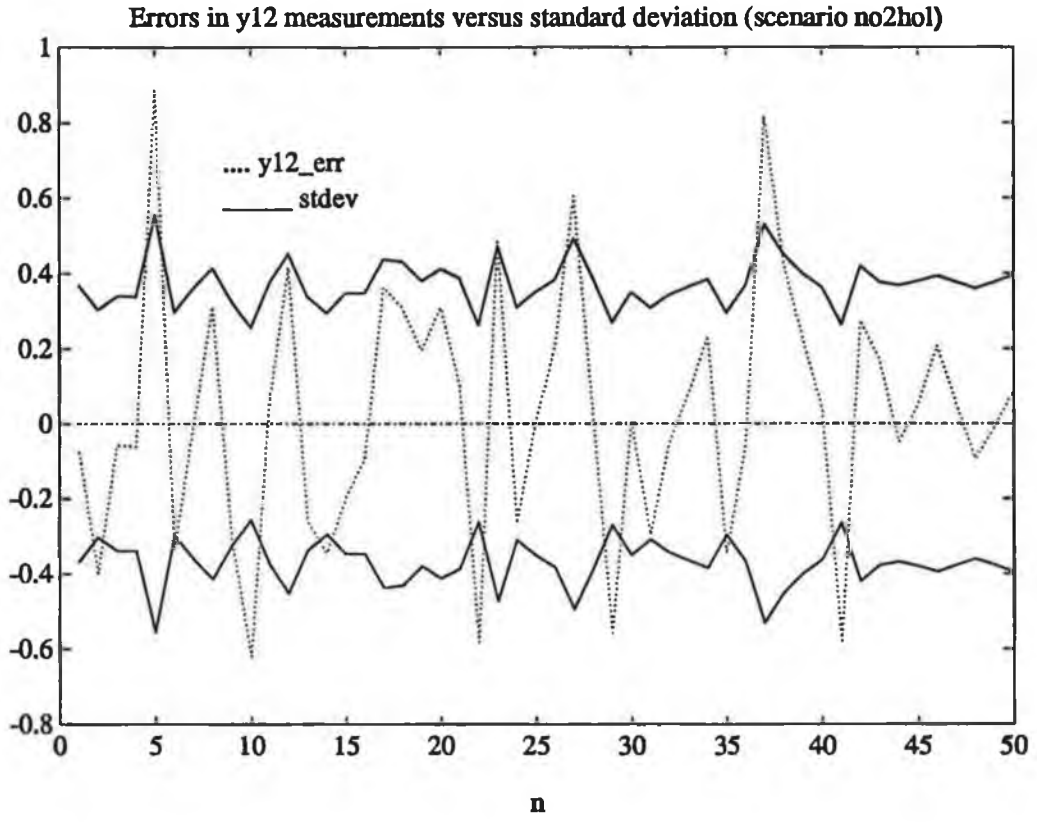

Figure (6.11)

.... y12_err represents the actual errors in the noisy measurements y_{12} in low-noise case in scenario no2 in y position.

_____ stdev represents the square root of $P_{z12}(2,2)$, the theoretical standard deviation of the errors according to the second-order approximation to the covariance matrix in low-noise case in scenario no2.

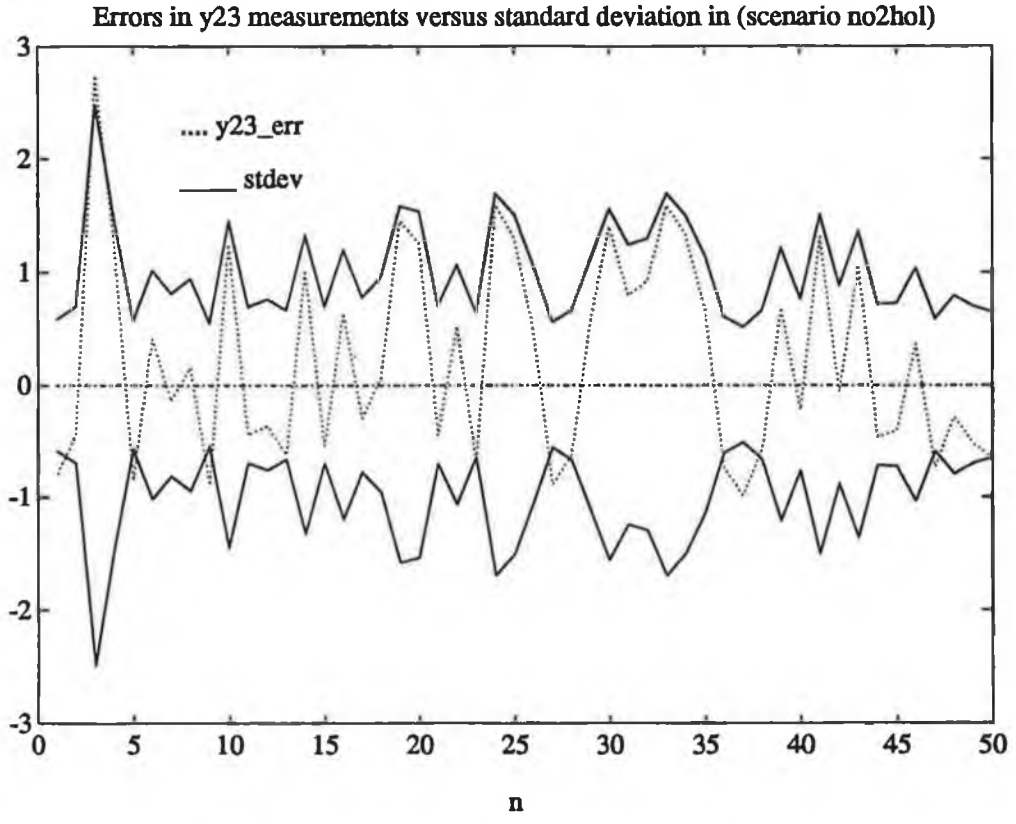

Figure (6.12)

.... y23_err represents the actual errors in the noisy measurements y_{23} in low-noise case in scenario no2 in y position.

____ stdev represents the square root of $P_{z23}(2,2)$, the theoretical standard deviation of the errors according to the second-order approximation to the covariance matrix in low-noise case in scenario no2.

The next section discusses the simulation results for high-noise case in scenario no2 using second-order terms.

6.7 Discussion of Simulation Results, Scenario no2, High-Noise Case Using Second-Order Terms

In this section we describe some simulation results for high-noise case, scenario no2 using second-order terms, and comparing the changes in the standard deviation using the second-order terms with the standard deviation using first-order approximation. The computer simulation was run 50 times and the results are plotted and discussed in the next several pages. The only difference between high-noise case and low-noise case in scenario no2 is in the measurement noise variances.

Figure (6.13) shows the actual errors in the noisy measurements x_{12} from triangulation between sensors S1, and S2, where (scenario no2hoh) means scenario number two using high-order terms in high-noise case. The dotted line represents the actual errors in the noisy measurements x_{12} in high-noise case, and the solid line represents the square root of $P_{z12}(1,1)$ in high-noise case in scenario no2 using second-order terms in x position. Comparing the theoretical standard deviation in high-noise case in scenario no2 using the second-order terms in x position in figure (6.13) with the theoretical standard deviation in high-noise case in scenario no2 using the first-order

approximation in x position in figure (5.34), we see the theoretical standard deviation using the second-order terms is slightly larger than the theoretical standard deviation using first-order approximation. Again the difference is to be expected.
Clearly, the triangulation process between sensors S1, and S2 is still relatively accurate in this case.

Figure (6.14) shows the actual errors in the noisy measurements x_{23} from triangulation between sensors S2, and S3. The dotted line represents the actual errors in the noisy measurements x_{23} in high-noise case, and the solid line represents the square root of $P_{z23}(1,1)$ in high-noise case in scenario no2 using second-order terms in x position. The solid line is the theoretical standard deviation of the errors according to the second-order approximation to the covariance matrix. Comparing the theoretical standard deviation in high-noise case in scenario no2 using the second-order terms in x position in figure (6.14) with the theoretical standard deviation in high-noise case in scenario no2 using the first-order approximation in x position in figure (5.35), we see the theoretical standard deviation using the second-order terms is much larger than the theoretical standard deviation with using first-order approximation. For example at n = 5, we see the theoretical standard deviation including the second-

order terms is twice as large as the theoretical standard deviation including the first-order approximation. We see the same thing at n = 36, and at several other places. In both figures, the standard deviation itself does not accurately model the statistics of the errors. This is due to the high noise distortion in the triangulation process between sensors S2, and S3. The angle-of-arrival errors exceed the magnitude of the difference (θ_{3t} - θ_{2t}) resulting in very large errors in the triangulation process between sensors S2, and S3. Since the covariance matrix is expanded about the noisy triangulated position, this causes the distortion of the covariance matrix which we see in the figures.

Figure (6.15) shows the actual errors in the noisy measurements y_{12} from triangulation between sensors S1, and S2. The dotted line represents the actual errors in the noisy measurements y_{12} in high-noise case, and the solid line represents the square root of $P_{z12}(2,2)$ in high-noise case in scenario no2 using second-order terms in y position. The solid line is the theoretical standard deviation of the errors according to the second-order approximation to the covariance matrix. Comparing the theoretical standard deviation in high-noise case in scenario no2 using the second-order terms in y position in figure (6.15)with the theoretical standard deviation in

high-noise case in scenario no2 using the first-order approximation in y position in figure (5.38), we see the theoretical standard deviation using the second-order terms almost equals the theoretical standard deviation using first-order approximation. We see the second-order terms in this case do not make any change, because of the low noise component in the triangulation process between sensors S1, and S2.

Figure (6.16) shows the actual errors in the noisy measurements y_{23} from triangulation between sensors S2, and S3. The dotted line represents the actual errors in the noisy measurements y_{23} in high-noise case, and the solid line represents the square root of $P_{z23}(2,2)$ in high-noise case in scenario no2 using second-order terms in y position. The solid line is the theoretical standard deviation of the errors according to the second-order approximation to the covariance matrix. Comparing the theoretical standard deviation in high-noise case in scenario no2 using the second-order terms in x position in figure (6.16) with the theoretical standard deviation in high-noise case in scenario no2 using the first-order approximation in y position in figure (5.39), we see the theoretical standard deviation using the second-order terms is much larger than the theoretical standard deviation using first-order approximation. For example at n = 5 we see the theoretical standard

deviation including the second-order terms is bigger than the theoretical standard deviation including the first-order approximation two times. We see the same thing at n = 36, and at the most cases. This is due to the high noise situation because of the large noise in the triangulation process between sensors S2, and S3, where the errors at theses sensors exceed the magnitude of the difference (θ_{3t} - θ_{2t}) resulting in very large errors in the triangulation process between sensors S2, and S3. As mentioned earlier, there is a large distortion of the covariance matrix in this case.

We see in the high-noise case in scenario no2, the second-order terms still are not accurate because of the large errors at the sensors. It is not clear how many high-order terms are needed to get an accurate covariance matrix in high-noise case in scenario no2. Looking at chapter VI we see that a considerable amount of difficult mathematics was necessary to get the second-order terms. To determine the third and fourth-order terms in the approximation would be impossible. The only solution is to use another sensor to get a better slant angle for the triangulation process.

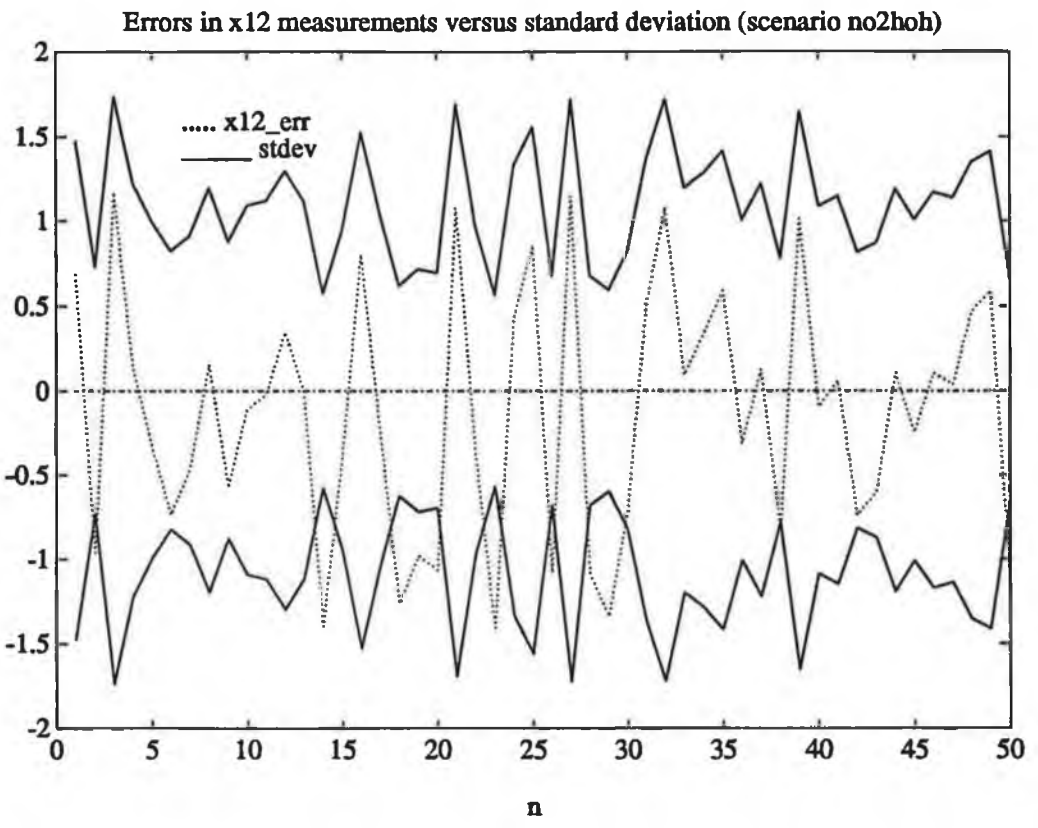

Figure (6.13)

.... x12_err represents the actual errors in the noisy measurements x_{12} in high-noise case in scenario no2 in x position.

_____ stdev represents the square root of $P_{z12}(1,1)$, the theoretical standard deviation of the errors according to the second-order approximation to the covariance matrix in high-noise case in scenario no2.

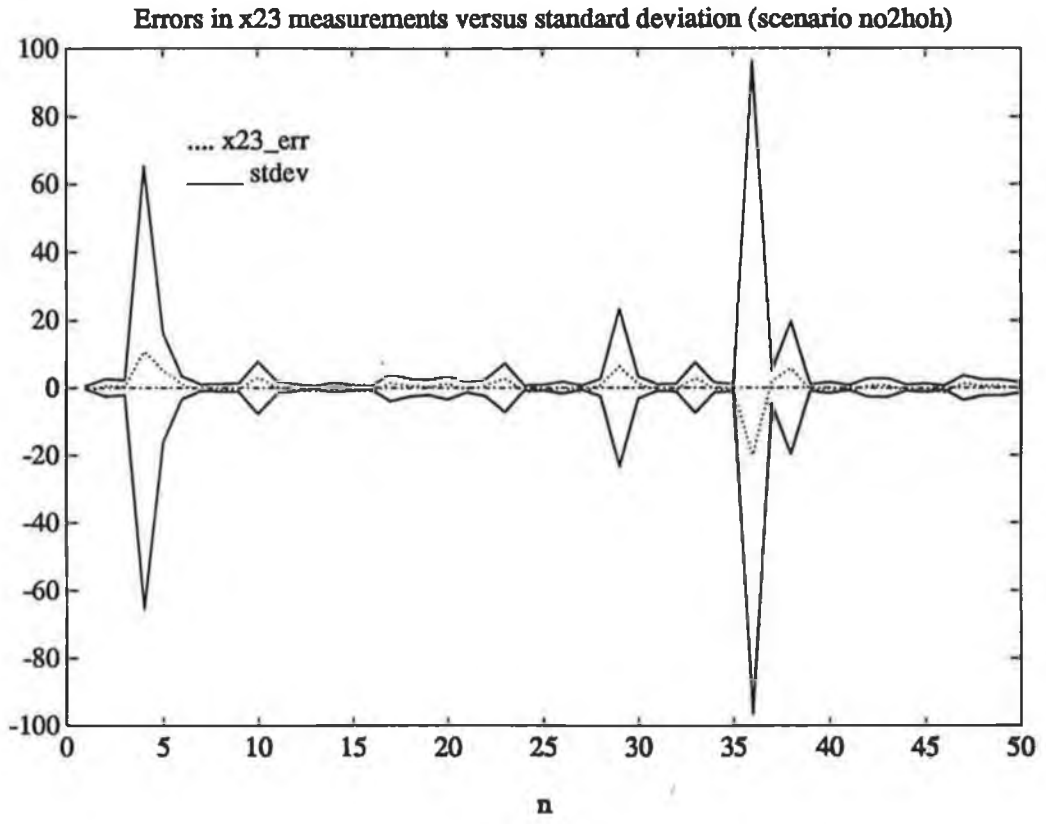

Figure (6.14)

.... x23_err represents the actual errors in the noisy measurements x_{23} in high-noise case in scenario no2 in x position.

____ stdev represents the square root of $P_{z23}(1,1)$, the theoretical standard deviation of the errors according to the second-order approximation to the covariance matrix in high-noise case in scenario no2.

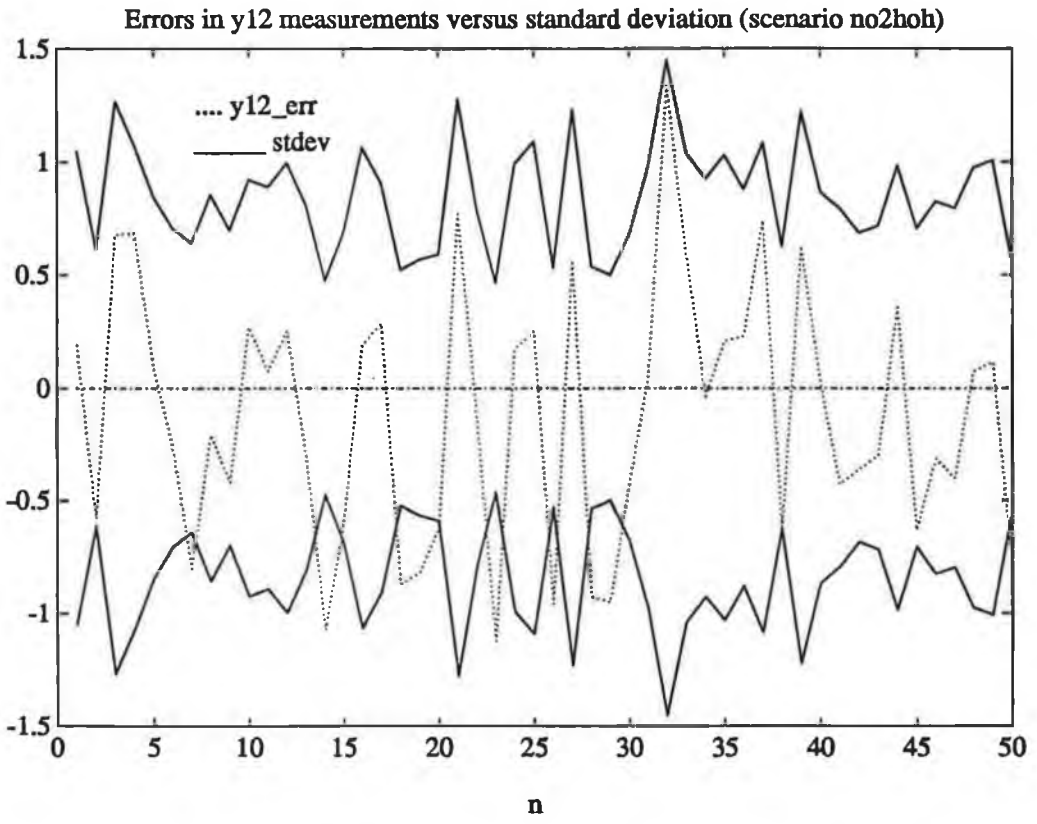

Figure (6.15)

.... y12_err represents the actual errors in the noisy measurements y_{12} in high-noise case in scenario no2 in y position.

____ stdev represents the square root of $P_{z12}(2,2)$, the theoretical standard deviation of the errors according to the second-order approximation to the covariance matrix in high-noise case in scenario no2.

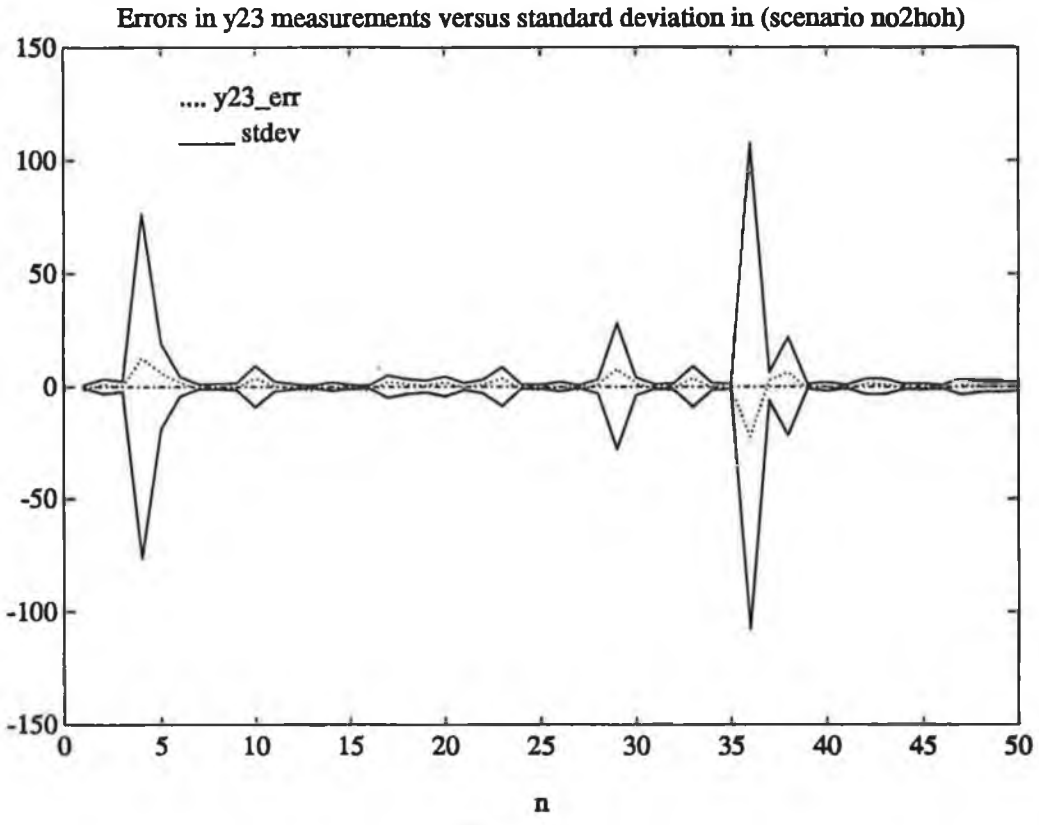

Figure (6.16)

.... y23_err represents the actual errors in the noisy measurements y_{23} in high-noise case in scenario no2 in y position.

____ stdev represents the square root of $P_{z23}(2,2)$, the theoretical standard deviation of the errors according to the second-order approximation to the covariance matrix in high-noise case in scenario no2.

CHAPTER VII

CONCLUSIONS

In this thesis we analyzed data fusion in the presence of non-linear measurements data. Several different areas related to the problem have been examined in this work and we now look at several conclusions from the results presented.

We have shown that the linear fusion algorithm successfully fused nonlinear data using only a first-order approximation to the covariance matrices. The fused estimate is generally better than the individual measurements themselves when the errors in the noisy measurements are of opposite sign. When the measurement errors are of like sign the fused estimate is usually close to the higher accuracy measurement.

We have shown that the fusion algorithm works when we do not know the p.d.f,s governing the errors in the noisy position measurement vectors. In fact by selecting different p.d.f,s for the angle-of-arrival measurements, we have shown that the fusion algorithm is insensitive to p.d.f,s themselves and only needs to know the covariance matrices governing the errors in the noisy position measurement vectors.

A first-order approximation was found to be accurate enough for data fusion except in the high-noise case in scenario no2. In scenario no2, high-noise case we

found that the covariance matrices were very inaccurate for triangulation between sensors S2 and S3. There are several reasons for this. The angle-of-arrival errors are very large compared to the difference in the slant angles (θ_{3m} - θ_{2m}) used for triangulation. This causes large errors in the triangulation process. The covariance matrices are expanded about these errors resulting in the effect we have seen in figures (5.35) and (5.39). In spite of the inaccuracy of the covariance matrices, the fusion algorithm still was effective in fusing the data in many cases. However, there were a few cases where the fused estimate was poorer than the best measurement. In a high-noise situation this is to be expected.

In an attempt to improve the accuracy of the covariance matrices, the impact of the second-order terms in the expansion was analyzed. We found in scenario no1 in both the low-noise and high-noise cases that the first-order approximation to the covariance matrices was close to the statistics of the actual errors themselves. Therefore we found that the second-order terms did not make any difference. In scenario no2 low-noise case we found the theoretical standard deviation of the errors using second-order terms is slightly bigger than the theoretical standard deviation of the errors using first-order approximation for both triangulation

between sensors S1 and S2 and also between sensors S2 and S3. This is because scenario no2 is a noisier triangulation process than scenario no1 and therefore the second-order terms did make a small change. In scenario no2 high-noise case for triangulation between sensors S1 and S2, we found that the second-order terms caused a small increase in the theoretical standard deviation of the errors. The triangulation process between sensors S1 and S2 is still relatively accurate in this case and only a small change is caused by the second-order terms. But the theoretical standard deviation of the errors according to the noisier triangulation process due to the slant angle between sensors S2 and S3 was found to be much larger than the theoretical standard deviation of the errors using the first-order approximation. The covariance matrix is very inaccurate in modelling the errors in this case (between sensors S2, and S3) because of the poor triangulation accuracy. As stated before, this is caused by the noisy angle measurement errors being greater than the difference between the slant angles θ_2 and θ_3. Clearly the second-order terms do not improve the situation. The covariance matrix is still inaccurate when compared to the actual errors in figures (6.14) and (6.16). Many additional terms in the expansion are needed. From chapter VI we see that the mathematics for the second-order terms is quite

difficult. The mathematics for third and higher terms is simply impossible. Another better placed sensor is needed for triangulation.

In spite of the inaccurate covariance matrices, the fusion algorithm does a good job at fusing the data, and produces an optimum covariance matrix which has a trace less than the trace of the individual error covariance matrices in all cases.

REFERENCES

[1] K.Sam Shanmugan (1988).: "RANDOM SIGNALS: Detection, Estimation and Data analysis", John Wiley & Sons.

[2] Peyton Z. Peebles, Jr. (1987).: "PROBABILITY RANDOM VARIABLES, AND RANDOM SIGNAL PRINCIPLES", McGraw-Hill Book Company.

[3] A-Gelb (ed), (1974).:"Applied Optimal Estimation", MIT Press.

[4] Carl Grant Looney, (1989).: "Random Signal Analysis with Random Processes and Introductory Kalman Filtering", IEEE ILP, Published by the institute of Electrical and Electronics. Engineering,Inc. 455 Hoes Lane, PO Box 1331, Piscataway, NJ 08855-1331.

[5] WILLIAM L. BROGAN, (1991).: "Modern Control Theory", Prentice-Hall Inc.

[6] ROBERT M. GRAY (1986), LEE D. DAVISSON.: "RANDOM PROCESSES: A MATHEMATICAL APPROACH FOR ENGINEERS", Prentice-Hall,Inc.

[7] ERWIN KREYSIZIG, (1988).: "ADVANCED ENGINEERING MATHEMATICS", John Wiley & Sons.

[8] Hugh Mc Cabe (1991). "Minimum Trace Fusion of N Sensors with Arbitrarily Correlated Sensor-to-Sensor Errors", IFAC Conference on Distributed Intelligent Systems, August 13-15,1991, Virgenia, USA.

[9] MATI WAX.(1983). "Position Location from Sensors with Position Uncertainty". IEEE Transactions on Aerospace and Electrical Systems VOL. AES-19, NO.5 (september

1983), 658-661.

[10] Vetter, W.J. (1971). "On Linear Estimates, Minimum Variance, and Least-Squares Weighting Matrices". IEEE Transactions on Automatic control (crresp.), 265-266.

[11] Stelios C.A. Thomopoulos, Ramanarayanan Viswanathan, Dimtrios C. Bougoulias. (1987). "Optimal Decision Fusion in Multiple Sensor Systems". IEEE Transactions on Aerospace and Electrical Systems VOL. AES-23, NO.5 September (1987).

[12] Serge Lang. (1987).: "Calculus of Several variables" , Springer-Verlag.

[13] S. Grime, H.F. Durrant-whyte and P. Ho (september 11, 1991), "Communication in Decentralized Data-Fusion Systems", Department of Engineering Science, University of Oxford, Oxford OX1 3PJ.

[14] Mischa Schwartz, Leonard Shaw (1975).: "Signal Processing Discrete Spectral Analysis Detection, and Estimation", Mc-Graw-Hill.

[15] Pervozvnskii, Anatolii Arkadevich (1965).: "Random Process in Nonlinear Control Systems", NEW YORK, ACADEMIC PRESS.

[16] Avez, A. (Ander) (1986).: " Tifferential Culculus", Newyork: J. Wiley.

[17] S.C.A. Thomopoulos*, R. Viswanathan, D.K. Bougoulas (1989).: "Optimal Distributed Decision Fusion", IEEE Transactions on Aerosoace and Electronic Systems vol.25, No. 5.

[18] G.H. Golub and C.F. Van Loan, (1983).: "Matrix

Computations", Johns Hopkins University Press, Baltimore, Maryland.

[19] Julius S. Bendat and Allan G. Piersol (1980).: "Engineering Application of Correlation and Spectral Analysis", John Wiley & Sons.

[20] Walter Poor (1991).: "Statistical Estimation of Navigation Errors", IEEE Transactions on Aerospace and Electronic Systems VOL. 28, NO.2 April 1992.

APPENDIX A

UNIFORM PROBABILITY DENSITY FUNCTION

A-1 The Mean Value of X

Figure (A.1) shows the probability density function (pdf) and cumulative distribution function (cdf) of a uniformly distributed random variable x.

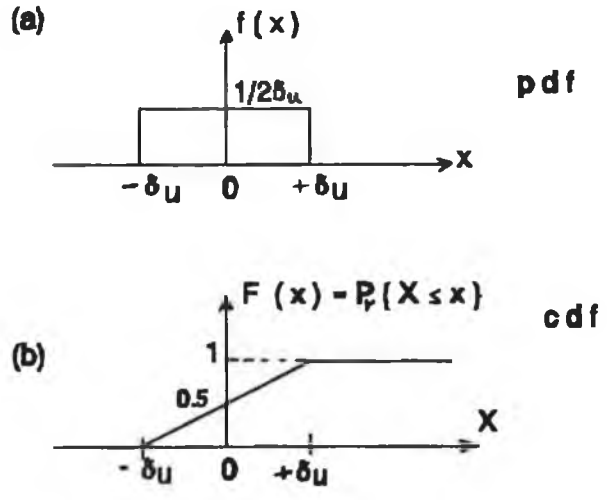

Figure (A.1): (a) probability density function (pdf) (b) cumulative distribution function (cdf).

From figure (A.1) the pdf is given by:

$f_x(x) = 1/2\delta_u$ when $-\delta_u \leq x \leq +\delta_u$ and (A-1)

$f_x(x) = 0$ elsewhere. (A-2)

The mean value of X is given by

$$\mu = E[x] = \overline{x} = \int_{-\delta_u}^{+\delta_u} x f_x(x)\, dx$$

$$= \frac{1}{2\delta_u} \int_{-\delta_u}^{+\delta_u} x dx$$

$$= \frac{1}{2\delta_u} \left[\frac{\delta_u^2}{2} - \frac{\delta_u^2}{2} \right] = 0$$

Therefore the expected value of x, $(\overline{x}) = \mu_x = 0$

A-2 The Variance of X

The variance of x is given by:

$$\sigma_x^2 = \int_{-\delta_u}^{\delta_u} x^2 f_x(x)\, dx$$

$$\sigma_x^2 = \int_{-\delta_u}^{+\delta_u} x^2 \frac{1}{2\delta_u} dx$$

$$= \frac{1}{2\delta_u} \left[\frac{x^3}{3} \right]_{-\delta_u}^{\delta_u}$$

$$\sigma_x^2 = \frac{\delta_u^2}{3} \qquad \text{(A-3)}$$

The square root of the variance of x, or σ_x, is the standard deviation of the random variable x.

A-3 Cumulative Distribution Function (cdf)

For $x \leq -\delta_u$ The cdf is given by:

$$F_X(x) = 0 \qquad \text{(A-4)}$$

For $-\delta_u \leq x \leq \delta_u$ the cdf is given by:

$$F_X(x) = P_r\{X \leq x\} = \int_{-\delta_u}^{x} f_x(x)\,dx = \int_{-\delta_u}^{x} \frac{1}{2\delta_u} d\tau = \frac{1}{2\delta_u}[\tau]_{-\delta_u}^{x}$$

$$F_X(x) = \frac{X+\delta_u}{2\delta_u} \quad when \quad -\delta_u \leq x \leq \delta u \quad \text{(A-5)}$$

$$= 0 \qquad \text{when } x \leq -\delta_u$$

$$= 1 \qquad \text{when } x \geq \delta_u$$

A-4 Use of Probability Integral Transform to Generate Random Draw from $U(-\delta_u, \delta_u)$

Suppose a random variable x has a pdf $f_x(x)$ and a corresponding cdf $F_x(x)$. From the probability integral transform it is shown in reference [2] that if $y = F_x(x)$ then y has a pdf U(0,1). It is also shown that $x = F_x^{-1}(y)$ has pdf $f_x(x)$.

From equation (A-5), we have

$$y = F_X(x) = \frac{X+\delta_u}{2\delta_u} \qquad \text{If } -\delta_u \leq x \leq \delta_u$$

$= 1$ If $x \geq \delta_u$

$= 0$ If $x \leq -\delta_u$

Solving for X, we get

$$X = \delta_u(2y-1) \quad \text{if } -\delta_u \leq x \leq \delta_u \qquad \text{(A-6)}$$

Therefore by generating a random draw from y which is uniform U(0,1), then $X = \delta_u(2y-1)$ has a uniform pdf $U(-\delta_u, \delta_u)$.

This technique is used to generate random angle-of-arrival errors in S1 measurement data.

A-5 The Expected Value of X^4

We need the $E\{x^4\}$, when we discuss high-order terms in the covariance matrices in chapter (VI)

$$E(X^4) = \int_{-\delta_u}^{\delta_u} (x-\bar{x})^4 f_x(X)\, dx = \int_{-\delta_u}^{\delta_u} x^4 f_x(X)\, dx$$

$$E\{X^4\} = \int_{-\delta_u}^{\delta_u} x^4 \frac{1}{2\delta_u} dx$$

$$= \frac{1}{2\delta_u}\left[\frac{x^5}{5}\right]_{-\delta_u}^{\delta_u} = = \frac{1}{10\delta_u}[\delta_u^5+\delta_u^5]$$

Therefore

$$E(X^4) = \frac{1}{5}\delta_u^4 \qquad \text{(A-7)}$$

APPENDIX B

SAWTOOTH PROBABILITY DENSITY FUNCTION

B-1. The Mean Value of X

Figure (B.1) shows the probability density function (pdf) and cumulative distribution function (cdf) of a sawtooth distributed random variable x.

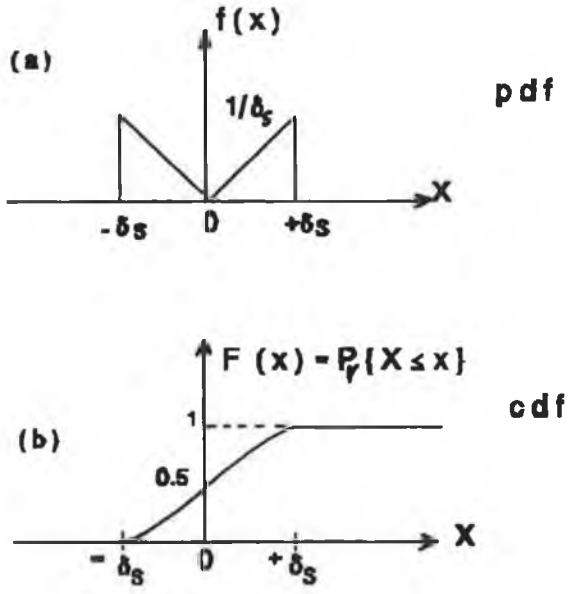

Figure (B.1): (a) Probability density function. (b) Cumulative distribution function.

From the figure (B.1) the pdf is given by:

$$f_x(x) = \frac{x}{\delta_s^2} \quad \text{when } 0 \le x \le \delta_s \quad \text{(B-1)}$$

and

$$f_x(x) = \frac{-x}{\delta_s^2} \quad when \quad -\delta_s \leq x \leq 0 \quad (B\text{-}2)$$

The mean value of x ($\bar{x}$) is given by:

$$E(x) = \bar{x} = \int_{-\delta_s}^{0} x\frac{(-x)}{\delta_s^2}dx + \int_{0}^{\delta_s} x\frac{x}{\delta_s^2}dx$$

$$= \frac{-\delta_s^3}{3\delta_s^2} + \frac{\delta_s^2}{3\delta_s^2} = 0$$

Therefore $\bar{x} = 0$

B-2 The Variance of X

The variance of x is given by:

$$\sigma_x^2 = \int_{-\delta_s}^{\delta_s} x^2 f_x(x)\,dx$$

$$\sigma_x^2 = \int_{-\delta_s^2}^{0} x^2\left(-\frac{x}{\delta_s^2}\right)dx + \int_{0}^{\delta_s} x^2\left(\frac{x}{\delta_s^2}\right)dx$$

$$= \frac{\delta_s^4}{4\delta_s^2} + \frac{\delta_s^4}{4\delta_s^2} = \frac{\delta_s^2}{2}$$

Therefore

$$\sigma_x^2 = \frac{\delta_s^2}{2} \qquad \text{(B-3)}$$

B-3 Cumulative Distribution Function (cdf)

For $-\delta_s \leq x \leq 0$ the pdf is given by:

$$f_x(x) = -x/\delta_s^2$$

Then the cdf is given By:

$$F_X(x) = P_r\{ X \leq x \} = \int_{-\delta_s}^{x} \frac{-\tau}{\delta_s^2} d\tau$$

$$F_X(x) = \frac{-1}{\delta_s^2}\left[\frac{\tau^2}{2}\right]_{-\delta_u}^{x}$$

$$F_X(x) = \frac{\delta_s^2 - X^2}{2\delta_s^2} \quad \text{if } -\delta_u \leq x \leq 0 \qquad \text{(B-4)}$$

$$= 0 \qquad x \leq -\delta_s$$

$$= 0.5 \qquad x = 0$$

For $0 \leq x \leq \delta_s$ the pdf is given by:

$$f_x(x) = \frac{x}{\delta_s^2}$$

Then the cdf is given by:

$$y = F_X(x) = P_r\{ X \leq x \} = \int_{0}^{x} \frac{\tau}{\delta_s^2} d\tau + 0.5$$

$$y = \frac{X^2 + \delta_s^2}{2\delta_s^2} \qquad 0 \le x \le \delta_u \qquad \text{(B-5)}$$

In summary,

$$F_X(x) = \frac{\delta_s^2 - X^2}{2\delta_s^2} \quad if \quad -\delta_s \le x \le 0 \qquad \text{(B-6)}$$

$$= 0 \qquad\qquad x \le -\delta_s$$

$$= 0.5 \qquad\qquad x = 0$$

and

$$F_X(x) = \frac{X^2 + \delta_s^2}{2\delta_s^2} \qquad 0 \le x \le \delta_s \qquad \text{(B-7)}$$

$$= 0.5 \qquad\qquad x = 0$$

$$= 1 \qquad\qquad x \ge \delta_s$$

Equations (B-6) and (B-7) summarize the cdf function for the sawtooth.

B-4 Use of Probability Integral Transform to Generate Random Draw of a sawtooth pdf.

As discussed in section (A-4) of appendix A if y a random number y is U(0,1), then a random draw for X is obtained from $X = F_X^{-1}(y)$ where $F_X(x)$ = cdf of X.

If $0 \le y \le 0.5$ then from equation (B-6) we get

$$X^2 = \delta_s^2(1-2y)$$

Solving for X we get two roots for X, X_1, and X_2

$$X_1 = -\delta_s\sqrt{(1-2y)}$$

and

$$X_2 = \delta_s\sqrt{(1-2y)}$$

The second root X_2 is refused because when y = 0, X_2 must be $-\delta_s$, and therefore the first root is the correct one. Therefore

$$X = -\delta_s\sqrt{(1-2y)} \quad for \quad 0 \leq y \leq 0.5 \quad \text{(B-8)}$$

From equation (B-7), the random draw must be inverse mapped through the cdf function onto the X axis. This is accomplished as follows: If $0.5 \leq y \leq 1$ and from the equation (B-7) we get

$$X^2 = \delta_s^2(2y - 1)$$

Solving for X we get two roots for X, X_1, and X_2

$$X_1 = \delta_s\sqrt{(2y-1)}$$

and

$$X_2 = -\delta_s\sqrt{(2y-1)}$$

X_2 is refused because when y = 1, X must be δ_s. Therefore

$$X = \delta_s\sqrt{(2y-1)} \quad \text{if } 0.5 \leq y \leq 1 \quad \text{(B-9)}$$

Therefore there are two equations (B-8), and (B-9) needed to generate random angle-of-arrival errors in S2 measurement data. For a give draw of y from

U(0,1),

$$X = -\delta_s\sqrt{(1-2y)} \qquad \text{if} \qquad 0 \le y \le 0.5$$

and

$$X = \delta_s\sqrt{(2y-1)} \qquad \text{if} \qquad 0.5 \le y \le 1$$

This technique is used to generate random angle-of-arrival errors in S2 measurement data.

B-5 The Expected value x^4

We need the $E\{x^4\}$, when we discuss high-order approximation terms in the covariance matrices in chapter (VI)

$$E(x^4) = \int_{-\delta_s}^{\delta_s} (x-\overline{x})\, f_x(x)\, dx$$

$$E(x^4) = \int_{-\delta_s}^{0} x^4 \left(\frac{-x}{\delta_s^2}\right) dx + \int_{0}^{\delta_s} x^4 \left(\frac{x}{\delta_s^2}\right) dx$$

$$= -\frac{1}{\delta_s^2}\int_{-\delta_s}^{0} x^5 dx + \frac{1}{\delta_s^2}\int_{0}^{\delta_s} x^5 dx$$

$$= \frac{-1}{\delta_s^2}\left[\frac{x^6}{6}\right]_{-\delta_s}^{0} + \frac{1}{\delta_s^2}\left[\frac{x^6}{6}\right]_{0}^{\delta_s}$$

$$= \frac{\delta_s^6}{6\delta_s^2} + \frac{\delta_s^6}{6\delta_s^2}$$

Therefore

$$E(x^4) = \frac{\delta_s^4}{3} \qquad \text{(B-10)}$$

APPENDIX C

TRIANGLE PROBABILITY DENSITY FUNCTION

C-1 The Mean value of X

Figure (C.1) shows the probability density function (pdf) and cumulative distribution function (cdf) of a triangle distributed random variable x.

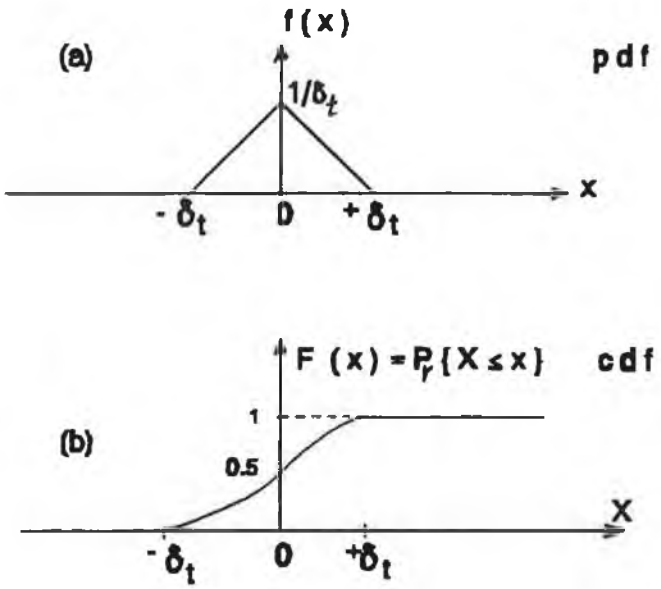

Figure (C.1): (a) probability density function (pdf). (b) cumulative distribution function (cdf).

From figure (C.1) The pdf is given by:

$$f_x(x) = \frac{1}{\delta_t}\left(1+\frac{x}{\delta_t}\right) \qquad -\delta_t \le x \le 0 \quad \text{(C-1)}$$

$$f_x(x) = \frac{1}{\delta_t}\left(1-\frac{x}{\delta_t}\right) \qquad 0 \le x \le \delta_t \quad \text{(C-2)}$$

The mean value of x is given by:

$$E(x) = \bar{x} = \int_{-\delta_t}^{0} x\left[\frac{1}{\delta_t}\left(1+\frac{x}{\delta_t}\right)\right]dx + \int_{0}^{\delta_t} x\left[\frac{1}{\delta_t}\left(1-\frac{x}{\delta_t}\right)\right]dx$$

$$= \frac{1}{\delta_t}\int_{-\delta_t}^{0} x\,dx + \frac{1}{\delta_t}\int_{-\delta_t}^{0}\frac{x^2}{\delta_t}dx + \frac{1}{\delta_t}\int_{0}^{\delta_t} x\,dx - \frac{1}{\delta_t}\int_{0}^{\delta_t}\frac{x^2}{\delta_t}dx$$

$$= \frac{-\delta_t^2}{2\delta_t} + \frac{\delta_t^3}{3\delta_t^2} + \frac{\delta_t^2}{2\delta_t} - \frac{\delta_t^3}{3\delta_t^2} = 0$$

Therefore $E(x) = \bar{x} = 0$

C-2 The Variance of x

The variance of x is given by:

$$\sigma_x^2 = \int_{-\delta_t}^{0} x^2\left[\frac{1}{\delta_t}\left(1+\frac{x}{\delta_t}\right)\right]dx + \int_{0}^{\delta_t} x^2\left[\frac{1}{\delta_t}\left(1-\frac{x}{\delta_t}\right)\right]dx$$

$$= \frac{1}{\delta_t}\left(\frac{\delta_t^3}{3}\right) - \frac{1}{\delta_t}\left(\frac{\delta_t^4}{4\delta_t}\right) + \frac{\delta_t^3}{3\delta_t} - \frac{\delta_t^4}{4\delta_t^2}$$

$$\sigma_x^2 = \frac{\delta_t^2}{6} \qquad \text{(C-3)}$$

C-3 Cumulative Distribution Function (cdf)

For $-\delta_t \le x \le 0$ the pdf is given by:

$$f_x(x) = \frac{1}{\delta_t}\left(1+\frac{x}{\delta_t}\right)$$

Therefore the cdf is

$$y = F_X(x) = P_r\{X \le x\} = \int_{-\delta_t}^{x} \frac{1}{\delta_t}\left(1+\frac{\tau}{\delta_t}\right) d\tau$$

$$y = \frac{1}{\delta_t}[\tau]_{-\delta_t}^{X} + \frac{1}{\delta_t^2}\left[\frac{\tau^2}{2}\right]_{-\delta_t}^{X}$$

$$y = \frac{X^2+2\delta_t X + \delta_t^2}{2\delta_t^2} = \frac{(X+\delta_t)^2}{2\delta_t^2}$$

$$y = \frac{(X+\delta_t)^2}{2\delta_t^2} \quad if \quad -\delta_t \le x \le 0 \qquad (C\text{-}4)$$

For $0 \le x \le \delta_t$ the pdf is given by:

$$f_x(x) = \frac{1}{\delta_t}\left(1-\frac{x}{\delta_t}\right)$$

Therefore the cdf is

$$y = F_X(x) = \int_{0}^{x} \frac{1}{\delta_t}\left(1-\frac{\tau}{\delta_t}\right) d\tau + 0.5$$

$$= \frac{1}{\delta_t}[\tau]_0^X - \frac{1}{\delta_t^2}\left[\frac{\tau^2}{2}\right]_0^X + 0.5$$

Therefore

$$y = \frac{2\delta_t X - X^2 + \delta_t^2}{2\delta_t^2} \qquad \text{(C-5)}$$

In summary, the cdf for a triangle pdf is given by:

$$y = \frac{(X+\delta_t)^2}{2\delta_t^2} \quad \text{if } -\delta_t \le x \le 0 \qquad \text{(C-6)}$$

$$= 0 \qquad x \le -\delta_t$$

$$= 0.5 \qquad x = 0$$

$$y = \frac{2\delta_t X - X^2 + \delta_t^2}{2\delta_t^2} \quad \text{if} \quad 0 \le x \le \delta_t \qquad \text{(C-7)}$$

$$= 0.5 \qquad x = 0$$

$$= 1 \qquad x \ge \delta_t$$

Equation (C-6) and (C-7) summarize the cdf function for a sawtooth. To generate a random draw from the pdf a number y is generate with a U(0,1) pdf.

C-4 Use of Probability Integral Transform to Generate Random Draw of Triangle pdf.

As discussed in section (A-4) of appendix A if y a random number y is U(0,1), then a random draw for X

is obtained from $X = F_X^{-1}(y)$ where $F_X(x)$ = cdf of X. if $0 \leq y \leq 0.5$ and from the equation (C-6) we get

$$(X + \delta_t)^2 = 2\delta_t^2 y$$

Solving for x we get two roots for X, the first one X_1 is given by:

$$X_1 = -\delta_t + \delta_t \sqrt{2y} = \delta_t(\sqrt{2y}-1)$$

the second root X_2 is given by:

$$X_2 = -\delta_t - \delta_t \sqrt{2y} = -\delta_t(1+\sqrt{2y})$$

The second root X_2 is refused because when $y = 0.5$, X_2 must be 0, and therefore the first root is the correct one.

$$X = \delta_t(\sqrt{2y}-1) \text{ if } 0 \leq y \leq 0.5 \quad \text{(C-8)}$$

From the equation (C-7) the random draw y must be inverse mapped through the cdf function onto the x axis, this is accomplished as follows: If $0.5 \leq y \leq 1$ the cdf is given by:

$$y = \frac{2\delta_t X - X^2 + \delta_t^2}{2\delta_t^2}$$

$$X^2 - 2\,\delta_t X - \delta_t^2 + 2\,\delta_t^2\, y = 0$$

$$(X - \delta_t)^2 - 2\,\delta_t^2 + 2\delta_t^2\, y = 0$$

$$(X - \delta_t)^2 = 2\,\delta_t^2\,(1-y)$$

Solving for X, we get two roots for X , X_1, and X_2.

The first root X_1 is given by:

$$X_1 = \delta_t + \delta_t\sqrt{2(1-y)}$$

and the second root X_2 is given by:

$$X_2 = \delta_t - \delta_t\sqrt{2(1-y)} = \delta_t[1-\sqrt{2(1-y)}]$$

The first root X_1 is refused because when y = 0.5 X must be 0

Therefore, the second root is the correct one.

$$X_2 = \delta_t - \delta_t\sqrt{2(1-y)} = \delta_t[1-\sqrt{2(1-y)}] \qquad \text{(C-9)}$$

if $0.5 \leq y \leq 1$

Therefore, for a given draw for y there are two equations needed (C-8), and (c-9) to generate random angle-of-arrival errors in S3 measurement data.
This technique is used to generate random angle-of-arrival errors in S3 measurement data.

C-5 The Expected Value of x^4

We need the $E\{x^4\}$, when we discus high-order terms in the covariance matrices in chapter (VI)

For $-\delta_t \leq x \leq 0$ the pdf is given by:

$$f_x(x) = \frac{1}{\delta_t}(1+\frac{x}{\delta_t})$$

For $0 \leq x \leq \delta_t$ the pdf is given by:

$$f_x(x) = \frac{1}{\delta_t}\left(1-\frac{x}{\delta_t}\right)$$

$$E(x^4) = \int_{-\delta_t}^{\delta_t} (x-\overline{x})^4 f_x(x)\,dx$$

Therefor the expected value of x^4 is given by:

$$E(x^4) = \int_{-\delta_t}^{0} x^4\left[\frac{1}{\delta_t}\left(1+\frac{x}{\delta_t}\right)\right]dx + \int_{0}^{\delta_t} x^4\left[\frac{1}{\delta_t}\left(1-\frac{x}{\delta_t}\right)\right]dx$$

$$= \frac{1}{\delta_t}\int_{-\delta_t}^{0} x^4 dx + \frac{1}{\delta_t^2}\int_{-\delta_t}^{0} x^5 dx + \frac{1}{\delta_t}\int_{0}^{\delta_t} x^4 dx - \frac{1}{\delta_t^2}\int_{0}^{\delta_t} x^5 dx$$

$$= \frac{1}{\delta_t}\left[\frac{x^5}{5}\right]_{-\delta_t}^{0} + \frac{1}{\delta_t^2}\left[\frac{x^6}{6}\right]_{-\delta_t}^{0} + \frac{1}{\delta_t}\left[\frac{x^5}{5}\right]_{0}^{\delta_t} - \frac{1}{\delta_t^2}\left[\frac{x^6}{6}\right]_{0}^{\delta_t}$$

$$= \frac{\delta_t^2}{5\delta_t} - \frac{\delta_t^6}{6\delta_t^2} + \frac{\delta_t^5}{5\delta_t} - \frac{\delta_t^6}{6\delta_t^2}$$

Therefore

$$E(x^4) = \frac{\delta_t^4}{15} \qquad \text{(C-10)}$$

APPENDIX D

If $f(-x) = f(x)$ then $E(x^3) = 0$

The proof:

$$E(x^{2n+1}) = \int_{-\delta}^{\delta} x^{2n+1} f(x)\, dx = \int_{-\delta}^{0} x^{2n+1} f(x)\, dx + \int_{0}^{\delta} x^{2n+1} f(x)\, dx$$

let $y = -x \Rightarrow$

$$E(x^{2n+1}) = \int_{y=\delta}^{0} (-y)^{2n+1} f(-y)\, (-dy) + \int_{0}^{\delta} y^{2n+1} f(y)\, dy$$

$$= -\int_{0}^{y=\delta} (y)^{2n+1} f(y)\, dy + \int_{0}^{\delta} y^{2n+1} f(y)\, dy$$

$$= 0$$

Therefore

$$E(x^{2n+1}) = 0 \text{ for all integers } n \qquad \text{(D-1)}$$